PRENTICE-HALL INTERNATIONAL SERIES IN OPTOELECTRONICS

Series Editor: P.J. Dean

Optical Fiber Communications

Principles and Practice

JOHN SENIOR

Nokia of America Corporation
IPR2023-00681, Ex. 1017
Ex. 1017.1

OPTICAL FIBER COMMUNICATIONS

Principles and Practice

John M. Senior

Dept. of Electrical and Electronic Engineering
Manchester Polytechnic

Prentice/Hall PHI International

Englewood Cliffs, NJ London New Delhi Rio de Janeiro
Singapore Sydney Tokyo Toronto Wellington

Ex. 1017.2

Library of Congress Cataloging in Publication Data

Senior, John, M., 1951–
Optical fiber communications.

Bibliography: p.
Includes index.
1. Optical communications. 2. Fiber optics. I. Title.
TK5103.59.S46 1984 621.38'0414 84–8315
ISBN 0–13–638248–7 (case)
ISBN 0–13–638222–3 (pbk.)

British Library Cataloging in Publication Data

Senior, John M.
Optical fiber communications.
1. Optical communications 2. Fiber optics
I. Title
621.38'0414 TK5103.59

ISBN 0–13–638248–7
ISBN 0–13–638222–3 Pbk

© 1985 by Prentice-Hall International, Inc., London

All rights reserved. No part of this publication may be reproduced, stored in a retrieval system, or transmitted, in any form or by any means, electronic, mechanical, photocopying, recording or otherwise, without the prior permission of Prentice-Hall International, Inc., London.
For permission within the United States contact Prentice-Hall Inc., Englewood Cliffs, NJ 07632.

ISBN 0-13-638248 7

ISBN 0-13-638222 3 {PBK}

Prentice-Hall International, Inc., *London*
Prentice-Hall of Australia Pty. Ltd., *Sydney*
Prentice-Hall Canada, Inc., *Toronto*
Prentice-Hall of India Private Ltd., *New Delhi*
Prentice-Hall of Southeast Asia Pte., Ltd., *Singapore*
Prentice-Hall Inc., *Englewood Cliffs, New Jersey*
Prentice-Hall do Brasil Ltda., *Rio de Janeiro*
Whitehall Books Ltd., *Wellington, New Zealand*

10 9 8 7 6 5 4 3 2 1

Typeset by Pintail Studios Ltd., Ringwood, Hants., UK.
Printed in the United States of America

Contents

Preface ix

Glossary of Symbols and Abbreviations xi

1 INTRODUCTION 1

1.1 Historical Development 1
1.2 The General System 4
1.3 Advantages of Optical Fiber Communication 7
References 10

2 OPTICAL FIBER WAVEGUIDES 11

2.1 Introduction 11
2.2 Ray Theory Transmission 12
2.2.1 Total internal reflection 12
2.2.2 Acceptance angle 14
2.2.3 Numerical aperture 15
2.2.4 Skew rays 19
2.3 Electromagnetic Mode Theory For Optical Propagation 22
2.3.1 Electromagnetic waves 22
2.3.2 Modes in a planar guide 24
2.3.3 Phase and group velocity 27
2.3.4 Phase shift with total internal reflection and the evanescent field 29
2.3.5 Goos–Haenchen shift 34
2.3.6 Cylindrical fiber 34
2.3.7 Mode coupling 41
2.4 Step Index Fibers 43
2.4.1 Multimode step index fibers 44
2.4.2 Single mode step index fibers 45
2.5 Graded Index Fibers 48
Problems 57
References 59

3 TRANSMISSION CHARACTERISTICS OF OPTICAL FIBERS 62

3.1 Introduction 62
3.2 Attenuation 63
3.3 Material Absorption Losses 65
3.3.1 Intrinsic absorption 65
3.3.2 Extrinsic absorption 66
3.4 Linear Scattering Losses 68
3.4.1 Rayleigh scattering 69
3.4.2 Mie scattering 71

Ex. 1017.4

3.5 Nonlinear Scattering Losses 71
3.5.1 Stimulated Brillouin scattering 72
3.5.2 Stimulated Raman scattering 72
3.6 Fiber Bend Loss 73
3.7 Dispersion 76
3.8 Intramodal Dispersion 80
3.8.1 Material dispersion 81
3.8.2 Waveguide dispersion 84
3.9 Intermodal Dispersion 84
3.9.1 Multimode step index fiber 85
3.9.2 Multimode graded index fiber 90
3.10 Overall Fiber Dispersion 93
3.10.1 Multimode fibers 93
3.10.2 Single mode fibers 94
3.11 Modal Noise 98
3.12 Polarization 100
3.12.1 Modal birefringence 100
Problems 104
References 108

4 OPTICAL FIBERS, CABLES AND CONNECTIONS 111

4.1 Introduction 111
4.2 Preparation of Optical Fibers 112
4.3 Liquid Phase (Melting) Techniques 113
4.31 Fiber drawing 114
4.4 Vapor Phase Deposition Techniques 118
4.4.1 Outside vapor phase oxidation (OVPO) process 120
4.4.2 Vapor axial deposition (VAD) 121
4.4.3 Modified chemical vapor deposition (MCVD) 123
4.4.4 Plasma-activated chemical vapor deposition (PCVD) 125
4.4.5 Summary of vapor phase deposition techniques 126
4.5 Optical Fibers 126
4.5.1 Multimode step index fibers 127
4.5.2 Multimode graded index fibers 128
4.5.3 Single mode fibers 130
4.5.4 Plastic-clad fibers 131
4.5.5 All-plastic fibers 132
4.6 Optical Fiber Cables 133
4.6.1 Fiber strength and durability 134
4.6.2 Stability of the fiber transmission characteristics 138
4.7 Cable Design 138
4.7.1 Fiber buffering 138
4.7.2 Cable structural and strength members 139
4.7.3 Cable sheath and water barrier 140
4.7.4 Examples of fiber cables 141
4.8 Optical Fiber Connection 144
4.8.1 Fiber alignment and joint loss 146
4.9 Fiber Splices 156
4.9.1 Fusion splices 157
4.9.2 Mechanical splices 159
4.9.3 Multiple splices 163
4.10 Fiber Connectors 164
4.11 Butt Jointed Connectors 165
4.11.1 Ferrule connector 166
4.11.2 Biconical connector 167

4.11.3 Ceramic capillary connector 168
4.11.4 Double eccentric connector 168
4.11.5 Triple ball connector 169
4.11.6 Single mode fiber connector 170
4.11.7 Multiple connectors 170
4.12 Expanded Beam Connectors 172
Problems 173
References 177

5 OPTICAL FIBER MEASUREMENTS 183

5.1 Introduction 183
5.2 Fiber Attenuation Measurements 186
5.2.1 Total fiber attenuation 186
5.2.2 Fiber absorption loss measurement 190
5.2.3 Fiber scattering loss measurement 194
5.3 Fiber Dispersion Measurements 196
5.3.1 Time domain measurement 197
5.3.2 Frequency domain measurement 200
5.4 Fiber Refractive Index Profile Measurements 202
5.4.1 Interferometric methods 202
5.4.2 Near field scanning method 204
5.4.3 End reflection method 206
5.5 Fiber Numerical Aperture Measurements 209
5.6 Fiber Diameter Measurements 212
5.6.1 Outer diameter 212
5.6.2 Core diameter 214
5.7 Field Measurements 215
5.7.1 Optical time domain reflectometry (OTDR) 219
Problems 224
References 228

6 OPTICAL SOURCES 1: THE LASER 231

6.1 Introduction 231
6.2 Basic Concepts 233
6.2.1 Absorption and emission of radiation 234
6.2.2 The Einstein relations 236
6.2.3 Population inversion 238
6.2.4 Optical feedback and laser oscillation 240
6.2.5 Threshold condition for laser oscillation 244
6.3 Optical Emission From Semiconductors 245
6.3.1 The *p–n* junction 245
6.3.2 Spontaneous emission 248
6.3.3 Carrier recombination 250
6.3.4 Stimulated emission and lasing 253
6.3.5 Heterojunctions 258
6.3.6 Semiconductor materials 260
6.4 The Semiconductor Injection Laser 262
6.4.1 Efficiency 264
6.4.2 Stripe geometry 265
6.5 Multimode Injection Lasers 267
6.5.1 Laser modes 267
6.5.2 Structures 268
6.5.3 Optical output power 269
6.5.4 Recent developments 270

6.6 Single Mode Injection Lasers 271
6.6.1 Single mode operation 272
6.7 Single Mode Structures 273
6.7.1 Buried heterostructure (BH) laser 273
6.7.2 Transverse junction stripe (TJS) laser 274
6.7.3 Channelled substrate lasers 274
6.7.4 Distributed feedback (DFB) lasers 276
6.7.5 Large optical cavity (LOC) lasers 277
6.8 Longer Wavelength Injection Lasers 278
6.9 Injection Laser Characteristics 281
6.9.1 Threshold current temperature dependence 281
6.9.2 Dynamic response 283
6.9.3 Self pulsations 284
6.9.4 Noise 285
6.9.5 Mode hopping 286
6.9.6 Reliability 287
6.10 Injection Laser Coupling and Packaging 288
6.11 Nonsemiconductor Lasers 289
Problems 290
References 292

7 OPTICAL SOURCES 2: THE LIGHT EMITTING DIODE 296

7.1 Introduction 296
7.2 LED Efficiency 298
7.2.1 The double heterojunction LED 302
7.3 LED Structures 303
7.3.1 Planar LED 303
7.3.2 Dome LED 304
7.3.3 Surface emitter (Burrus type) LED 304
7.3.4 Lens coupling 306
7.3.5 Edge emitter LED 308
7.4 LED Characteristics 310
7.4.1 Optical output power 310
7.4.2 Output spectrum 311
7.4.3 Modulation bandwidth 313
7.4.4 Reliability 318
7.5 Modulation 320
Problems 321
References 323

8 OPTICAL DETECTORS 326

8.1 Introduction 326
8.2 Device Types 327
8.3 Optical Detection Principles 328
8.4 Absorption 329
8.4.1 Absorption coeffecient 329
8.4.2 Direct and indirect absorption: silicon and germanium 331
8.4.3 III–V alloys 331
8.5 Quantum Efficiency 332
8.6 Responsivity 333
8.7 Long Wavelength Cutoff 335

8.8 Semiconductor Photodiodes Without Internal Gain 336
8.8.1 *p–n* photodiode 336
8.8.2 *p–i–n* photodiode 338
8.9 Semiconductor Photodiodes With Internal Gain 340
8.9.1 Avalanche photodiodes 340
8.9.2 Silicon reach-through avalanche photodiodes 342
8.9.3 Germanium avalanche photodiodes 343
8.9.4 III–V alloy avalanche photodiodes 343
8.9.5 Drawbacks with the avalanche photodiode 344
8.9.6 Multiplication factor 345
8.10 Phototransistors 345
Problems 348
References 350

9 RECEIVER NOISE CONSIDERATIONS 352

9.1 Introduction 352
9.2 Noise 353
9.2.1 Thermal noise 353
9.2.2 Dark current noise 353
9.2.3 Quantum noise 354
9.2.4 Digital signalling quantum noise 355
9.2.5 Analog transmission quantum noise 357
9.3 Receiver Noise 359
9.3.1 *p–n* and *p–i–n* photodiode receiver 360
9.3.2 Receiver capacitance 364
9.3.3 Avalanche photodiode (APD) receiver 366
9.3.4 Excess avalanche noise factor 371
9.4 Receiver Structures 372
9.4.1 Low impedance front end 372
9.4.2 High impedance (integrating) front end 373
9.4.3 The transimpedence front end 374
9.5 FET Preamplifiers 377
9.5.1 Gallium arsenide MESFETs 379
9.5.2 PIN–FET hybrids 379
Problems 381
References 384

10 OPTICAL FIBER SYSTEMS 386

10.1 Introduction 386
10.2 The Optical Transmitter Circuit 388
10.2.1 Source limitations 388
10.2.2 LED drive circuits 391
10.2.3 Laser drive circuits 399
10.3 The Optical Receiver Circuits 403
10.3.1 The preamplifier 404
10.3.2 Automatic gain control (AGC) 409
10.3.3 Equalization 412
10.4 System Design Considerations 415
10.4.1 Component choice 416
10.4.2 Multiplexing 417
10.5 Digital Systems 418

10.6 Digital System Planning Considerations 423
10.6.1 The regenerative repeater 424
10.6.2 The optical transmitter 426
10.6.3 The optical receiver 427
10.6.4 Channel losses 438
10.6.5 Temporal response 439
10.6.6 Optical power budgeting 444
10.6.7 Line coding 446
10.7 Analog Systems 449
10.7.1 Direct intensity modulation (D–IM) 451
10.7.2 System planning 457
10.7.3 Subcarrier intensity modulation 460
10.7.4 Subcarrier double sideband modulation (DSB–IM) 462
10.7.5 Subcarrier frequency modulation (FM–IM) 463
10.7.6 Subcarrier phase modulation (PM–IM) 466
10.7.7 Pulse analog techniques 467
10.8 Coherent Systems 470
Problems 473
References 479

11 APPLICATIONS AND FUTURE DEVELOPMENTS 484

11.1 Introduction 484
11.2 Public Network Applications 486
11.2.1 Trunk network 486
11.2.2 Junction network 489
11.2.3 Local and rural networks 491
11.2.4 Submerged systems 493
11.3 Military Applications 494
11.3.1 Mobiles 494
11.3.2 Communication links 495
11.4 Civil and Consumer Applications 497
11.4.1 Civil 497
11.4.2 Consumer 499
11.5 Industrial Applications 500
11.5.1 Sensor systems 501
11.6 Computer Applications 506
11.6.1 Local area networks 508
11.7 Integrated Optics 512
11.7.1 Planar waveguides 513
11.8 Integrated Optical Devices 517
11.8.1 Beam splitters and switches 517
11.8.2 Modulators 521
11.8.3 Periodic structures for filters and injection lasers 524
11.8.4 Bistable optical devices 526
11.8.5 Optoelectronic integration 530
11.8.6 Summary 532
References 533

Appendix A The Field Relations in a Planar Guide 539
Appendix B Variance of a Random Variable 540
Appendix C Variance of the Sum of Independent Random Variables 541
Appendix D Speed of Response of a Photodiode 542
Appendix E Closed Loop Transfer Function for the Transimpedance Amplifier 543
Appendix F Gaussian Pulse Response 544
Index 546

Preface

The concept of guided lightwave communication along optical fibers has stimulated a major new technology which has come to maturity over the last fifteen years. During this period tremendous advances have been achieved with optical fibers and components as well as with the associated optoelectronics. As a result this new technology has now reached the threshold of large scale commercial exploitation. Installation of optical fiber communication systems is progressing within both national telecommunication networks and more localized data communication and telemetry environments. Furthermore, optical fiber communication has become synonymous with the current worldwide revolution in information technology. The relentless onslaught will undoubtedly continue over the next decade and the further predicted developments will ensure even wider application of optical fiber communication technology in this 'information age'.

The practical realization of wide-scale optical fiber communications requires suitable education and training for engineers and scientists within the technology. In this context the book has been developed from both teaching the subject to final year undergraduates and from a successful series of short courses on optical fiber communications conducted for professional engineers at Manchester Polytechnic. This book has therefore been written as a comprehensive introductory textbook for use by undergraduate and postgraduate engineers and scientists to provide them with a firm grounding in the major aspects of this new technology whilst giving an insight into the possible future developments within the field. The reader should therefore be in a position to appreciate developments as they occur. With these aims in mind the book has been produced in the form of a teaching text enabling the reader to progress onto the growing number of specialist texts concerned with optical fiber waveguides, optoelectronics, integrated optics, etc.

In keeping with the status of an introductory text the fundamentals are included where necessary and there has been no attempt to cover the entire field in full mathematical rigor. However, selected proofs are developed in important areas throughout the text. It is assumed that the reader is conversant with differential and integral calculus and differential equations. In addition, the reader will find it useful to have a grounding in optics as well as a reasonable familiarity with the fundamentals of solid state physics.

Chapter 1 gives a short introduction to optical fiber communications by considering the historical development, the general system and the major advantages provided by this new technology. In Chapter 2 the concept of the optical fiber as a transmission medium is introduced using a simple ray theory approach. This is followed by discussion of electromagnetic wave theory applied to optical fibers prior to consideration of lightwave transmission within the various fiber types. The major transmission characteristics of optical fibers are then discussed in some detail in Chapter 3.

Chapters 4 and 5 deal with the more practical aspects of optical fiber communications and therefore could be omitted from an initial teaching program. In Chapter 4 the

Ex. 1017.10

manufacture and cabling of the various fiber types are described, together with fiber to fiber connection or jointing. Chapter 5 gives a general treatment of the major measurements which may be undertaken on optical fibers in both the laboratory and the field. This chapter is intended to provide sufficient background for the reader to pursue useful laboratory work with optical fibers.

Chapters 6 and 7 discuss the light sources employed in optical fiber communications. In Chapter 6 the fundamental physical principles of photoemission and laser action are covered prior to consideration of the various types of semiconductor and nonsemiconductor laser currently in use, or under investigation, for optical fiber communications. The other important semiconductor optical source, namely the light emitting diode, is dealt with in Chapter 7.

The next two chapters are devoted to the detection of the optical signal and the amplification of the electrical signal obtained. Chapter 8 discusses the basic principles of optical detection in semiconductors; this is followed by a description of the various types of photodetector currently utilized. The optical fiber receiver is considered in Chapter 9 with particular emphasis on its performance in noise.

Chapter 10 draws together the preceding material in a detailed discussion of optical fiber communication systems, aiming to provide an insight into the design criteria and practices for all the main aspects of both digital and analog fiber systems. A brief account of coherent optical fiber systems is also included to give an appreciation of this area of future development. Finally, Chapter 11 describes the many current and predicted application areas for optical fiber communications by drawing on examples from research and development work which has already been undertaken. This discussion is expanded into consideration of other likely future developments with a brief account of the current technology involved in integrated optics and optoelectronic integration.

Worked examples are interspersed throughout the text to assist the learning process by illustrating the use of equations and by providing realistic values for the various parameters encountered. In addition, problems have been provided at the end of relevant chapters (Chapters 2 to 10 inclusive) to examine the reader's understanding of the text and to assist tutorial work. A Teacher's Manual containing the solutions to these problems may be obtained from the publisher. Extensive end-of-chapter references provide a guide for further reading and indicate a source for those equations which have been quoted without derivation. A complete glossary of symbols, together with a list of common abbreviations employed in the text, is provided. SI units are used throughout the text.

I am very grateful for the many useful comments and suggestions provided by reviewers which have resulted in significant improvements to this text. Thanks must also be given to the authors of numerous papers, articles and books which I have referenced whilst preparing the text, and especially to those authors, publishers and companies who have kindly granted permission for the reproduction of diagrams and photographs. Further, I would like to thank my colleagues in the Dept. of Electrical and Electronic Engineering at Manchester Polytechnic for their many helpful comments on the text; in particular Dr. Norman Burrow, Dr. John Edwards and Stewart Cusworth for the time spent checking the manuscript. I am also grateful to my family and friends for tolerating my infrequent appearances over the period of the writing of this book. Finally, words cannot express my thanks to my wife, Marion, for her patience and encouragement with this project and for her skilful typing of the manuscript.

J. M. Senior
Manchester Polytechnic

Ex. 1017.11

Glossary of Symbols and Abbreviations

A	constant, area (cross-section, emission), far field pattern size, mode amplitude, wave amplitude (A_o)
A_{21}	Einstein coefficient of spontaneous emission
A_c	peak amplitude of the subcarrier waveform (analog transmission)
a	fiber core radius, parameter defining the asymmetry of a planar guide (eqn. 11.6), baseband message signal ($a(t)$)
a_k	integer 1 or 0
B	constant, electrical bandwidth (post detection), magnetic flux density, mode amplitude, wave amplitude (B_0)
B_{12}, B_{21}	Einstein coefficients of absorption, stimulated emission
B_F	modal birefringence
B_m	bandwidth of an intensity modulated optical signal $m(t)$
B_{opt}	optical bandwidth
B_r	recombination coefficient for electrons and holes
B_T	bit rate, when the system becomes dispersion limited (B_T (DL))
b	normalized propagation constant for a fiber, ratio of luminance to composite video
C	constant, capacitance, crack depth (fiber), wave coupling coefficient per unit length
C_a	effective input capacitance of an optical fiber receiver amplifier
C_d	optical detector capacitance
C_f	capacitance associated with the feedback resistor of a transimpedance optical fiber receiver amplifier
C_L	total optical fiber channel loss in decibels, including the dispersion–equalization penalty (C_{LD})
C_0	wave amplitude
C_T	total capacitance
c	velocity of light in a vacuum, constant (c_1, c_2)
c_i	tap coefficients for a transversal equalizer
D	amplitude coefficient, electric flux density, distance, corrugation period, decision threshold in digital optical fiber transmission
D_f	frequency deviation ratio (subcarrier FM)
D_L	dispersion–equalization penalty in decibels
D_p	frequency deviation ratio (subcarrier PM)
d	fiber core diameter, distance, width of the absorption region (photodetector), pin diameter (mode scrambler)
d_o	fiber outer (cladding) diameter
E	electric field, energy, Youngs modulus, expected value of a random variable

Ex. 1017.12

E_a	activation energy of homogeneous degradation for an LED
E_F	Fermi level (energy), quasi-Fermi level located in the conduction band (E_{Fc}), valence band (E_{Fv}) of a semiconductor
E_g	separation energy between the valence and conduction bands in a semiconductor (bandgap energy)
$E_m(t)$	subcarrier electric field (analog transmission)
E_o	optical energy
E_q	separation energy of the quasi-Fermi levels
e	electronic charge, base for natural logarithms
F	probability of failure, transmission factor of a semiconductor–external interface, excess avalanche noise factor ($F(M)$)
$\mathcal{F}$	Fourier transformation
F_n	noise figure (amplifier)
f	frequency
f_D	peak to peak frequency deviation (PFM–IM)
f_d	peak frequency deviation (subcarrier FM and PM)
f_o	pulse rate (PFM–IM)
G	open loop gain of an optical fiber receiver amplifier
$G_i(r)$	amplitude function in the WKB method
G_o	optical gain (phototransistor)
Gsn	Gaussian (distribution)
g	degeneracy parameter
g	gain coefficient per unit length (laser cavity)
g_m	transconductance of a field effect transistor
g_{th}	threshold gain per unit length (laser cavity)
H	magnetic field
$H_{(\omega)}$	optical power transfer function (fiber), circuit transfer function
$H_A(\omega)$	optical fiber receiver amplifier frequency response (including any equalization)
$H_{CL}(\omega)$	closed loop current to voltage transfer function (receiver amplifier)
$H_{eq}(\omega)$	equalizer transfer function (frequency response)
$H_{OL}(\omega)$	open loop current to voltage transfer function (receiver amplifier)
$H_{out}(\omega)$	output pulse spectrum from an optical fiber receiver
h	Planck's constant, thickness of a planar waveguide, power impulse response for an optical fiber ($h(t)$)
$h_A(t)$	optical fiber receiver amplifier impulse response (including any equalization)
h_{eff}	effective thickness of a planar waveguide
h_{FE}	common emitter current gain for a bipolar transistor
$h_f(t)$	optical fiber impulse response
$h_{out}(t)$	output pulse shape from an optical fiber receiver
$h_p(t)$	input pulse shape to an optical fiber receiver
$h_t(t)$	transmitted pulse shape on an optical fiber link
I	electrical current, optical intensity
I_b	background radiation induced photocurrent (optical receiver)
I_{bias}	bias current for an optical detector
I_c	collector current (phototransistor)
I_d	dark current (optical detector)
I_o	maximum optical intensity
I_p	photocurrent generated in an optical detector
I_{th}	threshold current (injection laser)
i	electrical current

Ex. 1017.13

i_a	optical receiver preamplifier shunt noise current
i_{amp}	optical receiver preamplifier total noise current
i_D	decision threshold current (digital transmission)
i_d	photodiode dark noise current
i_{det}	output current from an optical detector
i_f	noise current generated in the feedback resistor of an optical fiber receiver transimpedance preamplifier
i_N	total noise current at a digital optical fiber receiver
i_n	multiplied shot noise current at the output of an APD excluding dark noise current
i_s	shot noise current on the photocurrent for a photodiode
i_{SA}	multiplied shot noise current at the output of an APD including the dark noise current
i_{sig}	signal current obtained in an optical fiber receiver
i_t	thermal noise current generated in a resistor
i_{TS}	total shot noise current for a photodiode without internal gain
J	Bessel function, current density
J_{th}	threshold current density (injection laser)
j	$\sqrt{-1}$
K	Boltzmann's constant, constant dependent on the optical fiber properties, modified Bessel function
K_1	stress intensity factor, for an elliptical crack (K_{IC})
k	wave propagation constant in a vacuum (free space wave number), wave vector for an electron in a crystal, ratio of ionization rates for holes and electrons, integer
k_f	angular frequency deviation (subcarrier FM)
k_p	phase deviation constant (subcarrier PM)
L	length (fiber), distance between mirrors (laser)
L_B	beat length in a single mode optical fiber
L_{bc}	coherence length in a single mode optical fiber
L_c	characteristic length (fiber)
L_o	constant with dimensions of length
L_t	lateral misalignment loss at an optical fiber joint
$\mathcal{L}$	transmission loss factor (transmissivity) of an optical fiber
l	azimuthal mode number, distance, length
l_a	atomic spacing (bond distance)
l_o	wave coupling length
M	avalanche multiplication factor, material dispersion parameter, total number of guided modes or mode volume; for a multimode step index fiber (M_s); for multimode graded index fiber (M_g), mean value (M_1) and mean square value (M_2) of a random variable
M_a	safety margin in an optical power budget
M_{op}	optimum avalanche multiplication factor
M^x	excess avalanche noise factor, (also denoted as $F(M)$)
m	radial mode number, Weibull distribution parameter, intensity modulated optical signal ($m(t)$), mean value of a random variable, integer
m_a	modulation index
N	integer, density of atoms in a particular energy level (e.g. N_1, N_2, N_3), minority carrier concentration in n type semiconductor material, group index of an optical waveguide (N_1)
NA	numerical aperture of an optical fiber
NEP	noise equivalent power

N_o	defined by equation 10.80
n	refractive index (e.g. n_1, n_2, n_3), stress corrosion susceptibility, negative type semiconductor material
n_e	effective refractive index of a planar waveguide
n_o	refractive index of air
P	electrical power, minority carrier concentration in p type semiconductor material, probability, of error ($P(e)$), of detecting a zero level ($P(0)$), of detecting a one level ($P(1)$), of detecting z photons in a particular time period ($P(z)$), conditional probability, of detecting a zero when a one is transmitted ($P(0/1)$), of detecting a one when a zero is transmitted ($P(1/0)$)
P_a	total power in a baseband message signal $a(t)$
P_B	threshold optical power for Brillouin scattering
P_c	optical power coupled into a step index fiber
P_D	optical power density
P_{dc}	d.c. optical output power
P_e	optical power emitted from an optical source
P_G	optical power in a guided mode
P_i	mean input (transmitted) optical power launched into a fiber
P_{int}	internally generated optical power (optical source)
P_m	total power in an intensity modulated optical signal $m(t)$
P_o	mean output (received) optical power from a fiber
P_{opt}	mean optical power travelling in a fiber
P_{out}	initial output optical power (prior to degradation) from an optical source
P_{po}	peak received optical power
P_r	reference optical power level
P_R	threshold optical power for Raman scattering
$P_{Ra}(t)$	backscattered optical power (Rayleigh) within a fiber
P_{sc}	optical power scattered from a fiber
$P_i(\omega)$	frequency spectrum of the mean input optical power launched into a fiber
$P_o(\omega)$	frequency spectrum of the mean output optical power received from a fiber
p	crystal momentum, average photoelastic coefficient, positive type semiconductor material, probability density function ($p(x)$)
q	integer, fringe shift
R	photodiode responsivity, radius of curvature of a fiber bend, electrical resistance (e.g. R_{in}, R_{out})
R_{12}	upward transition rate for electrons from energy level 1 to level 2
R_{21}	downward transition rate for electrons from energy level 2 to level 1
R_a	effective input resistance of an optical fiber receiver preamplifier
R_b	bias resistance, for optical fiber receiver preamplifier (R_{ba})
R_c	critical radius of an optical fiber
R_D	radiance of an optical source
RE_{dB}	ratio of electrical input power in decibels for an optical fiber system
R_f	feedback resistance in an optical fiber receiver transimpedance pre-amplifier
R_L	load resistance associated with an optical fiber detector
RO_{dB}	ratio of optical output power to optical input power in decibels for an optical fiber system
R_{TL}	total load resistance within an optical fiber receiver
r	radial distance from the fiber axis, Fresnel reflection coefficient, mirror reflectivity, electro-optic coefficient

Ex. 1017.15

r_e	generated electron rate in an optical detector
r_{ER}, r_{ET}	reflection and transmission coefficients respectively for the electric field at a planar, guide-cladding interface
r_{HR}, r_{HT}	reflection and transmission coefficients respectively for the magnetic field at a planar guide-cladding interface
r_p	incident photon rate at an optical detector
S	fraction of captured optical power, macroscopic stress
S_f	fracture stress
$S_i(r)$	phase function in the WKB method
$S_m(\omega)$	spectral density of the intensity modulated optical signal $m(t)$
S/N	peak signal power to rms noise power ratio, with peak to peak signal power $[(S/N)_{p-p}]$, with rms signal power $[(S/N)$ rms$]$
S_t	theoretical cohesive strength
s	pin spacing (mode scrambler)
T	temperature, time
T_a	insertion loss resulting from an angular offset between jointed optical fibers
T_c	10–90% rise time arising from intramodal dispersion on an optical fiber link
T_D	10–90% rise time for an optical detector
T_F	fictive temperature
T_l	insertion loss resulting from a lateral offset between jointed optical fibers
T_n	10–90% rise time arising from intermodal dispersion on an optical fiber link
T_o	threshold temperature (injection laser), nominal pulse period (PFM–IM)
T_R	10–90% rise time at the regenerator circuit input (PFM–IM)
T_S	10–90% rise time for an optical source
T_{syst}	total 10–90% rise time for an optical fiber system
T_T	total insertion loss at an optical fiber joint
T_t	temperature rise at time t
T_∞	maximum temperature rise
t	time
t_c	time constant
t_d	switch on delay (laser)
t_e	1/e pulse width from the center
t_r	10–90% rise time
U	eigenvalue of the fiber core
V	electrical voltage, nomalized frequency for an optical fiber or planar waveguide
V_{bias}	bias voltage for a photodiode
V_c	cutoff value of normalized frequency
V_{CC}	collector supply voltage
V_{CE}	collector–emitter voltage (bipolar transistor)
V_{EE}	emitter supply voltage
V_{opt}	voltage reading corresponding to the total optical power in a fiber
V_{sc}	voltage reading corresponding to the scattered optical power in a fiber
v	electrical voltage
v_a	amplifier series noise voltage
$v_A(t)$	receiver amplifier output voltage
v_c	crack velocity
v_g	group velocity
$v_{out}(t)$	output voltage from an RC filter circuit

v_p	phase velocity
W	eigenvalue of the fiber cladding, random variable
W_e	electric pulse width
W_o	optical pulse width
X	random variable
x	coordinate, distance, constant, evanescent field penetration depth, slab thickness
Y	constant, shunt admittance, random variable
y	coordinate, lateral offset at a fiber joint
Z	random variable
Z_0	electrical impedance
z	coordinate, number of photons
z_m	average or mean number of photons arriving at a detector in a time period τ
z_{md}	average number of photons detected in a time period τ
α	characteristic refractive index profile for fiber (profile parameter), optimum profile parameter (α_{op})
$\bar{\alpha}$	loss coefficient per unit length (laser cavity)
α_{cr}	connector loss at transmitter and receiver in decibels
α_{dB}	signal attenuation in decibels per unit length
α_{fc}	fiber cable loss in decibels per kilometer
α_j	fiber joint loss in decibels per kilometer
α_N	signal attenuation in nepers
α_o	absorption coefficient
α_r	radiation attenuation coefficient
β	wave propagation constant
β	gain factor (injection laser cavity)
β_c	isothermal compressibility
β_o	proportionality constant
β_r	degradation rate
γ	angle, attenuation coefficient per unit length for a fiber
γ_p	surface energy of a material
γ_R	Rayleigh scattering coefficient for a fiber
Δ	relative refractive index difference between the fiber core and cladding
δ_E	phase shift associated with transverse electric waves
δ_f	uncorrected source frequency width
δ_H	phase shift associated with transverse magnetic waves
$\delta\lambda$	optical source spectral width (linewidth)
δT	intermodal dispersion time in an optical fiber
δT_g	delay difference between an extreme meridional ray and an axial ray for a graded index fiber
δT_s	delay difference between an extreme meridional ray and an axial ray for a step index fiber, with mode coupling (δT_{sc})
ε	electrical permittivity, of free space (ε_o), relative (ε_r)
ζ	solid acceptance angle
η	quantum efficiency (optical detector)
η_{ang}	angular coupling efficiency (fiber joint)
η_c	coupling efficiency (optical source to fiber)
η_D	differential external quantum efficiency (optical source)
η_{ep}	external power efficiency (optical source)
η_i	internal quantum efficiency (optical source)
η_{lat}	lateral coupling efficiency (fiber joint)
η_{pc}	overall power conversion efficiency (optical source)
η_T	total external quantum efficiency (optical source)

θ	angle, fiber acceptance angle (θ_a), Bragg diffraction angle (θ_B)
Λ	acoustic wavelength, period for perturbations in a fiber
Λ_c	cutoff period for perturbations in a fiber
λ	optical wavelength
λ_c	long wavelength cutoff (photodiode)
λ_o	wavelength at which first order dispersion is zero
μ	magnetic permeability, relative permeability (μ_r), permeability of free space (μ_o)
ν	optical source bandwidth in gigahertz
ρ	polarization rotation in a single mode optical fiber
ρ_f	spectral density of the radiation energy at a transition frequency f
σ	standard deviation, (rms pulse width), variance (σ^2)
σ_c	rms pulse broadening resulting from intramodal dispersion in a fiber
σ_m	rms pulse broadening resulting from material dispersion in a fiber
σ_n	rms pulse broadening resulting from intermodal disperion, in a graded index fiber (σ_g), in a step index fiber (σ_s)
σ_T	total rms pulse broadening in a fiber or fiber link
σ_λ	rms spectral width of emission from optical source
τ	time period, bit period, pulse duration 3 dB pulse width (τ(3 dB))
τ_{21}	spontaneous transition lifetime between energy levels 2 and 1
τ_E	time delay in a transversal equalizer
τ_e	$1/e$ full width pulse broadening due to dispersion on an optical fiber link
τ_g	group delay
τ_i	injected (minority) carrier lifetime
τ_r	radiative minority carrier lifetime
Φ	linear retardation
ϕ	angle, critical angle (ϕ_c)
ψ	scalar quantity representing E or H field
ω	angular frequency, of the subcarrier waveform in analog transmission (ω_c), of the modulating signal in analog transmission (ω_m)
ω_o	spot size of the fundamental mode
∇	vector operator, Laplacian operator (∇^2)

A–D	analog to digital
a.c.	alternating current
AGC	automatic gain control
AM	amplitude modulation
APD	avalanche photodiode
ASK	amplitude shift keying
BER	bit error rate
BH	buried heterostructure (injection laser)
BOD	bistable optical device
CAM	computer aided manufacture
CATV	common antenna television
CCTV	close circuit television
CDH	constricted double heterojunction (injection laser)
CMI	coded mark inversion
CMOS	complementary metal oxide silicon
CNR	carrier to noise ratio
CPU	central processing unit
CSP	channelled substrate planar (injection laser)
CW	continuous wave or operation
D–A	digital to analog
dB	decibel
D–IM	direct intensity modulation
DBF	distributed feedback (injection laser)
DBR	distributed Bragg reflector (injection laser)
d.c.	direct current
DH	double heterostructure or heterojunction (injection laser or LED)

DSB	double sideband (amplitude modulation)
EH	traditional mode designation
EMI	electromagnetic interference
EMP	electromagnetic pulse
erf	error function
erfc	complementary error function
FDM	frequency division multiplexing
FET	field effect transistor
FM	frequency modulation
FSK	frequency shift keying
FWHP	full width half power
HDB	high density bipolar
HE	traditional mode designation
He–Ne	helium–neon (laser)
HF	high frequency
HV	high voltage
IF	intermediate frequency
ILD	injection laser diode
IM	intensity modulation
IO	integrated optics
I/O	input/output
ISI	intersymbol interference
LAN	local area network
LED	light emitting diode
LOC	large optical cavity (injection laser)
LP	linearly polarized (mode notation)
LPE	liquid phase epitaxy
MCVD	modified chemical vapor deposition
MESFET	metal Schottky field effect transistor
MISFET	metal integrated-semiconductor field effect transistor
Nd:YAG	neodymium-doped yttrium–aluminum–garnet (laser)
NRZ	nonreturn to zero
OTDR	optical time domain reflectometry
OVPO	outside vapor phase oxidation
PAM	pulse amplitude modulation
PCM	pulse code modulation
PCS	plastic-clad silica (fiber)
PCVD	plasma-activated chemical vapor deposition
PCW	plano-convex waveguide (injection laser)
PDF	probability density function
PFM	pulse frequency modulation
PIN–FET	*p–i–n* photodiode followed by a field effect transistor
PM	phase modulation
PPM	pulse position modulation
PSK	phase shift keying
PTT	Post, Telegraph and Telecommunications
PWM	pulse width modulation
RAPD	reach-through avalanche photodiode
RFI	radio frequency interference
rms	root mean square
RO	relaxation oscillation
RZ	return to zero
SAW	surface acoustic wave
SDM	space division multiplexing
SHF	super high frequency
SML	separated multiclad layer (injection laser)
SNR	signal to noise ratio
TDM	time division multiplexing
TE	transverse electric
TEM	transverse electromagnetic
TJS	transverse junction stripe (injection laser)
TM	transverse magnetic
TTL	transistor–transistor logic
UHF	ultra high frequency
VAD	vapor axial deposition
VCO	voltage controlled oscillator
VHF	very high frequency
VPE	vapor phase epitaxy
WDM	wavelength division multiplexing
WKB	Wentzel, Kramers, Brillouin (analysis technique) for graded fiber
WPS	wideband switch point
ZD	zenner diode

10

Optical Fiber Systems

10.1 INTRODUCTION

The transfer of information in the form of light propagating within an optical fiber requires the successful implementation of an optical fiber communication system. This system, in common with all systems, is composed of a number of discrete components which are connected together in a manner that enables them to perform a desired task. Hence, to achieve reliable and secure communication using optical fibers it is essential that all the components within the transmission system are compatible so that their individual performances, as far as possible, enhance rather than degrade the overall system performance.

The principal components of a general optical fiber communication system for either digital or analog transmission are shown in the system block schematic of Fig. 10.1. The transmit terminal equipment consists of an information encoder or signal shaping circuit preceding a modulation or electronic driver stage which operates the optical source. Light emitted from the source is launched into an optical fiber incorporated within a cable which constitutes the transmission medium. The light emerging from the far end of the transmission medium is converted back into an electrical signal by an optical detector positioned at the input of the receive terminal equipment. This electrical signal is then amplified prior to decoding or demodulation in order to obtain the information originally transmitted.

The operation and characteristics of the optical components of this general system have been discussed in some detail within the previous chapters. However, to enable the successful incorporation of these components into an optical fiber communication system it is necessary to consider the interaction of one component with another, and then to evaluate the overall performance of the system. Furthermore, to optimize the system performance for a given application it is often helpful to offset a particular component characteristic by trading it off against the performance of another component, in order to provide a net gain within the overall system. The electronic components play an important role in this context, allowing the system designer further choices which, depending on the optical components utilized, can improve the system performance.

Ex. 1017.20

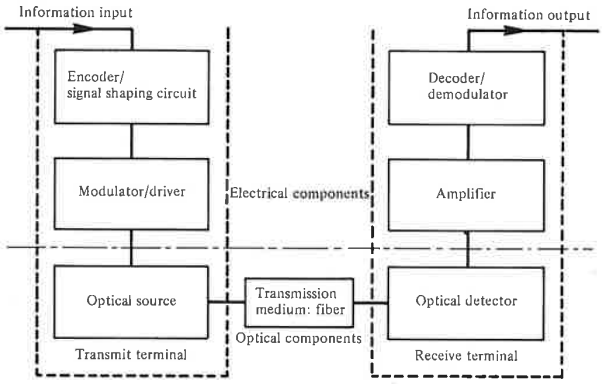

Fig. 10.1 The principal components of an optical fiber communication system.

The purpose of this chapter is to bring together the important performance characteristics of the individual system elements, and to consider their interaction within optical fiber communication systems. It is intended that this will provide guidance in relation to the various possible component configurations which may be utilized for different system applications, whilst also giving an insight into system design and optimization. Hence the optical components and the associated electronic circuits will be discussed prior to consideration of general system design procedures. Although the treatment is by no means exhaustive, it will indicate the various problems involved in system design and provide a description of the basic techniques and practices which may be adopted to enable successful system implementation.

We commence in Section 10.2 with a discussion of the optical transmitter circuit. This includes consideration of the source limitations prior to description of various LED and laser drive circuits for both digital and analog transmission. In Section 10.3 we present a similar discussion for the optical receiver including examples of preamplifier and main amplifier circuits. General system design considerations are then dealt with in Section 10.4. This is followed by a detailed discussion of digital systems commencing with an outline of the operating principles of pulse code modulated (PCM) systems in Section 10.5 before continuing to consider the various aspects of digital optical fiber systems in Section 10.6. Analog optical fiber systems are then dealt with in Section 10.7 where the various possible analog modulation techniques are described and analyzed. Finally, we conclude in Section 10.8 with a brief account of coherent optical fiber systems which are currently attracting much interest.

10.2 THE OPTICAL TRANSMITTER CIRCUIT

The unique properties and characteristics of the injection laser and the light emitting diode (LED) which make them attractive sources for optical fiber communications were discussed in Chapters 6 and 7.

Although both device types exhibit a number of similarities in terms of their general performance and compatibility with optical fibers, striking differences exist between them in relation to both system application and transmitter design. It is useful to consider these differences, as well as the limitations of the two source types, prior to discussion of transmitter circuits for various applications.

10.2.1 Source Limitations

10.2.1.1 *Power*

The electrical power required to operate both injection lasers and LEDs is generally similar with typical current levels of between 20 and 300 mA (certain laser thresholds may be substantially higher than this—of the order of 1–2 A), and voltage drops across the terminals of 1.5–2.5 V. However, the optical output power against current characteristic for the two devices varies considerably, as indicated in Fig. 10.2. The injection laser is a threshold device which must be operated in the region of stimulated emission (i.e. above the threshold) where continuous optical output power levels are typically in the range 1–10 mW.

Much of this light output may be coupled into an optical fiber because the isotropic distribution of the narrow linewidth, coherent radiation is relatively directional. In addition the spatial coherence of the laser emission allows it to be readily focused by appropriate lenses within the numerical aperture of the

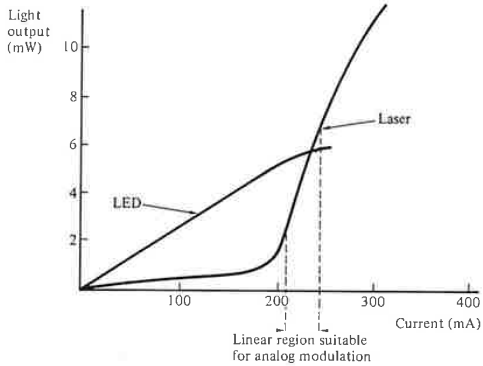

Fig. 10.2 Light output (power) emitted into air as a function of d.c. drive current for a typical high radiance LED and for a typical injection laser. The curves exhibit nonlinearity at high currents due to junction heating.

fiber. Coupling efficiencies near 30% may be obtained by placing a fiber close to a laser mirror, and these can approach 80% with a suitable lens arrangement [Refs. 1 and 2]. Therefore injection lasers are capable of launching between 0.5 and several milliwatts of optical power into a fiber.

LEDs are capable of similar optical output power levels to injection lasers depending on their structure and quantum efficiency as indicated by the typical characteristic for a surface emitter shown in Fig. 10.2. However, the spontaneous emission of radiation over a wide linewidth from the LED generally exhibits a Lambertian intensity distribution which gives poor coupling into optical fibers. Consequently only between 1 and perhaps 10% (using a good edge emitter) of the emitted optical power from an LED may be launched into a multimode fiber, even with appropriate lens coupling (see Section 7.3.4). These considerations translate into optical power levels from a few to several hundred microwatts launched into individual multimode fibers. Thus the optical power coupled into a fiber from an LED can be 10–20 dB below that obtained with a typical injection laser. The power advantage gained with the injection laser is a major factor in the choice of source, especially when considering a long-haul optical fiber link.

10.2.1.2 *Linearity*

Linearity of the optical output power against current characteristic is an important consideration with both the injection laser and LED. It is especially pertinent to the design of analog optical fiber communication systems where source nonlinearities may cause severe distortion of the transmitted signal. At first sight the LED may appear to be ideally suited to analog transmission as its output is approximately proportional to the drive current. However, most LEDs display some degree of nonlinearity in their optical output against current characteristic because of junction heating effects which may either prohibit their use, or necessitate the incorporation of a linearizing circuit within the optical transmitter. Certain LEDs (e.g. etched well surface emitters) do display good linearity, with distortion products (harmonic and intermodulation) between 35 and 45 dB below the signal level [Refs. 3 and 4].

An alternative approach to obtaining a linear source characteristic is to operate an injection laser in the light-generating region above its threshold, as indicated in Fig. 10.2. This may prove more suitable for analog transmission than would the use of certain LEDs. However, gross nonlinearities due to mode instabilities may occur in this region. These are exhibited as kinks in the laser output characteristic (see Section 6.5.3). Therefore many of the multimode injection lasers have a limited use for analog transmission without additional linearizing circuits within the transmitter, although some of the single mode structures have demonstrated linearity suitable for most analog applications. Alternatively, digital transmission, especially utilizing a binary (2 level) format, is far less sensitive to source nonlinearities and is therefore often preferred when using both injection lasers and LEDs.

10.2.1.3 *Thermal*

The thermal behavior of both injection lasers and LEDs can limit their operation within the optical transmitter. However, as indicated in Section 6.9.1 the variation of injection laser threshold current with the device junction temperature can cause a major operating problem. Threshold currents of typical AlGaAs devices increase by approximately 1% per degree centigrade increase in junction temperature. Hence any significant increase in the junction temperature may cause loss of lasing and a subsequent dramatic reduction in the optical output power. This limitation cannot usually be overcome by simply cooling the device on a heat sink, but must be taken into account within the transmitter design, through the incorporation of optical feedback, in order to obtain a constant optical output power level from the device.

The optical output from an LED is also dependent on the device junction temperature as indicated in Section 7.4.2. Most LEDs exhibit a decrease in optical output power following an increase in junction temperature, which is typically around −1% per degree centigrade. This thermal behavior, however, although significant is not critical to the operation of the device due to its lack of threshold. Nevertheless this temperature dependence can result in a variation in optical output power of several decibels over the temperature range 0–70 °C. It is therefore a factor within system design considerations which, if not tolerated, may be overcome by providing a circuit within the transmitter which adjusts the LED drive current with temperature.

10.2.1.4 *Response*

The speed of response of the two types of optical source is largely dictated by their respective radiative emission mechanisms. Spontaneous emission from the LED is dependent on the effective minority carrier lifetime in the semiconductor material (see Section 7.4.3). In heavily doped (10^{18}–10^{19} per cm^3) gallium arsenide this is typically between 1 and 10 nanoseconds. However, the response of an optical fiber source to a current step input is often specified in terms of the 10–90% rise time, a parameter which is reciprocally related to the device frequency response (see Section 10.6.5). The rise time of the LED is at least twice the effective minority carrier lifetime, and often much longer because of junction and stray capacitance. Hence, the rise times for currently available LEDs lie between 2 and 50 nanoseconds, give 3 dB bandwidths of around 7 to at best 175 MHz. Therefore LEDs are inherently restricted to lower bandwidth applications, although suitable drive circuits can maximize their bandwidth capabilities (i.e. reduce rise times).

Stimulated emission from injection lasers occurs over a much shorter period giving rise times of the order of 0.1–1 ns, thus allowing 3 dB bandwidths above 1 GHz. However, injection laser performance is limited by the device switch-on delay (see Section 6.9.2). To achieve the highest speeds it is therefore necessary to minimize the switch-on delay. Transmitter circuits which prebias the laser to just below or just above threshold in conjunction with high speed

Ex. 1017.24

drive currents which take the device well above threshold, prove useful in the reduction of this limitation.

10.2.1.5 *Spectral Width*

The finite spectral width of the optical source causes pulse broadening due to material dispersion on an optical fiber communication link. This results in a limitation on the bandwidth–length product which may be obtained using a particular source and fiber. The incoherent emission from an LED usually displays a spectral linewidth of between 20 and 50 nm (full width at half power (FWHP) points) when operating in the 0.8–0.9 μm wavelength range. This limits the bandwidth–length product with a silica fiber to around 100 and 160 MHz km at wavelengths of 0.8 and 0.9 μm respectively. Hence the overall system bandwidth for an optical fiber link over several kilometers may be restricted by material dispersion rather than the response time of the source.

The problem may be alleviated by working at a longer wavelength where the material dispersion in high silica fibers approaches zero (i.e. near 1.3 μm, see Section 3.8.1). In this region the source spectral width is far less critical and bandwidth–length products of 1 GHz km may be obtained using LEDs.

Alternatively, an optical source with a narrow spectral linewidth may be utilized in place of the LED. The coherent emission from an injection laser generally has a linewidth of 1 nm or less (FWHP). Use of the injection laser greatly reduces the effect of material dispersion within the fiber, giving bandwidth–length products of 1 GHz km at 0.8 μm, and far higher at longer wavelengths. Hence, the requirement for a system operating at a particular bandwidth over a specific distance will influence both the choice of source and operating wavelength.

10.2.2 LED Drive Circuits

Although the LED is somewhat restricted in its range of possible applications in comparison with the more powerful, higher speed injection laser, it is generally far easier to operate. Therefore in this section we consider some of the circuit configurations that may be used to convert the information voltage signal at the transmitter into a modulation current suitable for an LED source. In this context it is useful to discuss circuits for digital and analog transmission independently.

10.2.2.1 *Digital Transmission*

The operation of the LED for binary digital transmission requires the switching on and off of a current in the range of several tens to several hundreds of milliamperes. This must be performed at high speed in response to logic voltage levels at the driving circuit input. A common method of achieving this current switching operation for an LED is shown in Fig. 10.3. The circuit illustrated uses a bipolar transistor switch operated in the common emitter

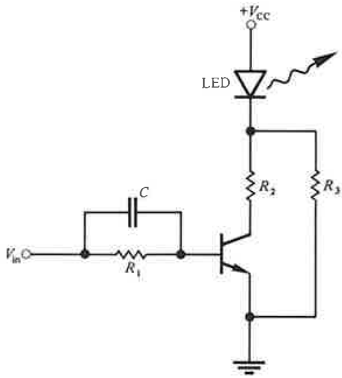

Fig. 10.3 A simple drive circuit for binary digital transmission consisting of a common emitter saturating switch.

mode. This single stage circuit provides current gain as well as giving only a small voltage drop across the switch when the transmitter is in saturation (i.e. when the collector–base junction is forward biassed, the emitter to collector voltage V_{CE} (sat) is around 0.3 V).

The maximum current flow through the LED is limited by the resistor R_2 whilst independent bias to the device may be provided by the incorporation of resistor R_3. However, the switching speed of the common emitter configuration is limited by space charge and diffusion capacitance; thus bandwidth is

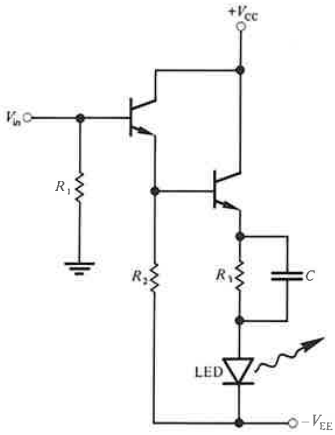

Fig. 10.4 Low impedance drive circuit consisting of an emitter follower with compensating matching network [Ref. 5].

traded for current gain. This may, to a certain extent, be compensated by overdriving (pre-emphasizing) the base current during the switch-on period. In the circuit shown in Fig. 10.3 pre-emphasis is accomplished by use of the speed up capacitor C.

Increased switching speed may be obtained from an LED without a pulse shaping or speed up element by use of a low impedance driving circuit, whereby charging of the space charge and diffusion capacitance occurs as rapidly as possible. This may be achieved with the emitter follower drive circuit shown in Fig. 10.4 [Ref. 5]. The use of this configuration with a compensating matching network (R_3C) provides fast direct modulation of LEDs with relatively low drive power. A circuit, with optimum values for the matching network, is capable of giving optical rise times of 2.5 ns for LEDs with capacitance of 180 pF, thus allowing 100 Mbits s^{-1} operation [Ref. 6].

Another type of low impedance driver is the shunt configuration shown in Fig. 10.5. The switching transistor in this circuit is placed in parallel with the LED providing a low impedance path for switching off the LED by shunting current around it. The switch-on performance of the circuit is determined by the combination of resistor R and the LED capacitance. Stored space charge may be removed by slightly reverse biassing the LED when the device is switched off. This may be achieved by placing the transistor emitter potential V_{EE} below ground. In this case a Schottky clamp (shown dotted) may be incorporated to limit the extent of the reverse bias without introducing any extra minority carrier stored charge into the circuit.

A frequent requirement for digital transmission is the interfacing of the LED drive circuit with a common logic family as illustrated in the block schematic of Fig. 10.6(a). In this case the logic interface must be considered along with possible drive circuits. Compatibility with TTL may be achieved by use of commercial integrated circuits as shown in Figs. 10.6(b) and (c). The configuration shown in Fig. 10.6(b) uses a Texas Instruments' 74S140 line driver

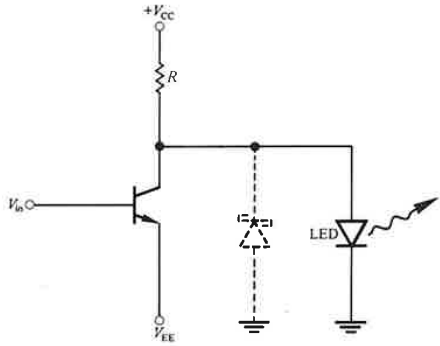

Fig. 10.5 Low impedance drive circuit consisting of a simple shunt configuration.

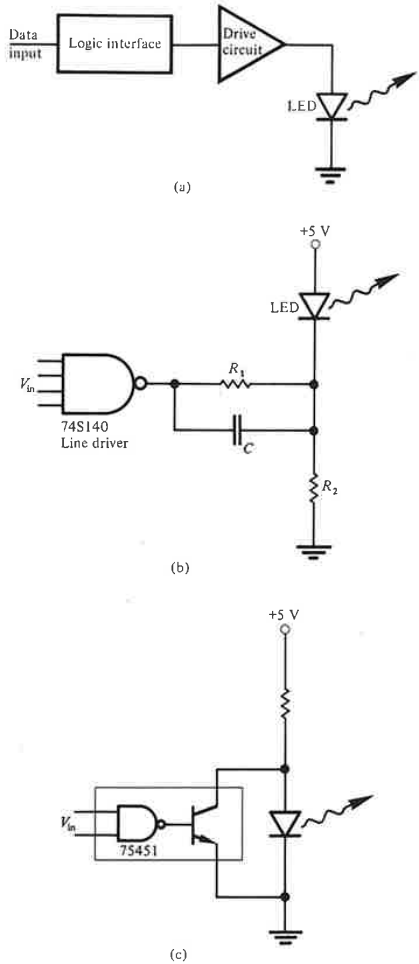

Fig. 10.6 Logic interfacing for digital transmission: (a) block schematic showing the interfacing of the LED drive circuit with logic input levels; (b) a simple TTL compatible LED drive circuit employing a Texas Instruments' 74S140 line driver [Ref. 7]; (c) a TTL compatible shunt drive circuit using a commercially available integrated circuit [Ref. 7].

which provides a drive current of around 60 mA to the LED when R_1 is 50 Ω. Moreover, the package contains two sections which may be connected in parallel in order to obtain a drive current of 120 mA. The incorporation of a suitable speed up capacitor (e.g. $C = 47$ pF) gives optical rise times of around 5 ns when using LEDs with between 150 and 200 pF capacitance [Ref. 7].

Figure 10.6(c) illustrates the shunt configuration using a standard TTL 75451 integrated circuit. The rise time of this shunt circuit may be improved through maintenance of charge on the LED capacitance by placing a resistor between the shunt switch collector and the LED [Ref. 7].

An alternative important drive circuit configuration is the emitter coupled circuit shown in Fig. 10.7 [Ref. 7]. The LED acts as a load in one collector so that the circuit provides current gain and hence a drive current for the device. Thus the circuit resembles a linear differential amplifier, but it is operated outside the linear range and in the switching mode. Fast switching speeds may be obtained due to the configuration's nonsaturating characteristic which avoids switch-off time degradations caused by stored charge accumulation on the transistor base region. The lack of saturation also minimizes the base drive requirements for the transistors thus preserving their small signal current gain. The emitter coupled driver configuration shown in Fig. 10.7 is compatible with commercial emitter coupled logic (ECL). However, to achieve this compatibility the circuit includes two level shifting transistors which give ECL levels (high –0.8 V, low –1.8 V) when the positive terminal of the LED is at earth potential. The response of this circuit is specified [Ref. 7] at up to 50 Mbit s^{-1}, with a possible extension to 300 Mbit s^{-1} when using a faster ECL logic family and high speed transistors. The emitter coupled drive circuit configuration may also be interfaced with other logic families, and a TTL compatible design is discussed in Ref. 8.

10.2.2.2 *Analog Transmission*

For analog transmission the drive circuit must cause the light output from an LED source to follow accurately a time-varying input voltage waveform in

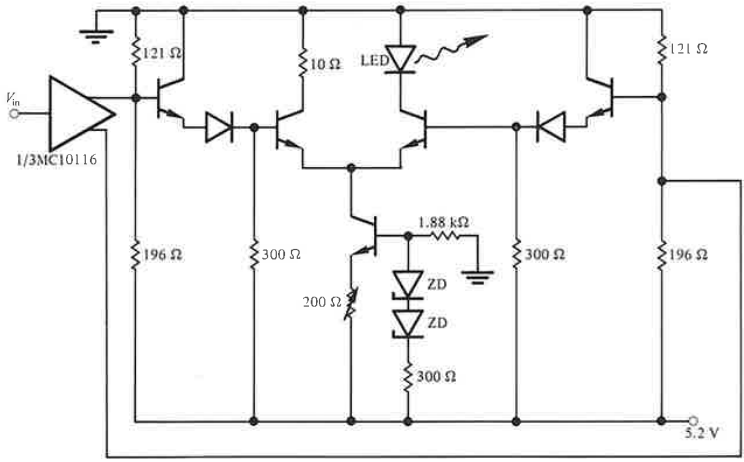

Fig. 10.7 An emitter coupled drive circuit which is compatible with ECL logic [Ref. 7].

both amplitude and phase. Therefore, as indicated previously, it is important that the LED output power responds linearly to the input voltage or current. Unfortunately, this is not always the case because of inherent nonlinearities within LEDs which create distortion products on the signal. Thus the LED itself tends to limit the performance of analog transmission systems unless suitable compensation is incorporated into the drive circuit. However, unless extremely low distortion levels are required, simple transistor drive circuits may be utilized.

Two possible high speed drive circuit configurations are illustrated in Fig. 10.8. Figure 10.8(a) shows a driver consisting of a common emitter transconductance amplifier which converts an input base voltage into a collector current. The circuit is biassed for a class A mode of operation with the quiescent collector current about half the peak value. A similar transconductance configuration which utilizes a Darlington transistor pair in order to reduce the impedance of the source is shown in Fig. 10.8(b). A circuit of this type has been used to drive high radiance LEDs at frequencies of 70 MHz [Ref. 9].

Another simple drive circuit configuration is shown in Fig. 10.9. It consists of a differential amplifier operated over its linear region which directly modulates the LED. The LED operating point is controlled by a reference voltage V_{ref} whilst the current generator provided by the transistor T_3 feeding the differential stage (T_1 and T_2) limits the maximum current through the device. The transimpedance of the driver is reduced through current series feedback provided by the two resistors R_1 and R_2 which are normally assigned equal values. Furthermore, variation between these feedback resistors can be used to compensate for the transfer function of both the drive circuit and the LED.

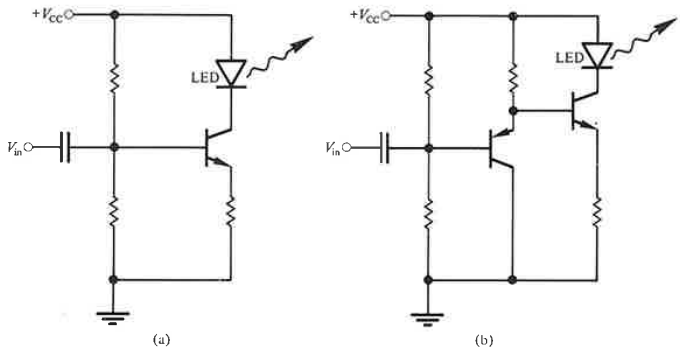

Fig. 10.8 Transconductance drive circuits for analog transmission: (a) common emitter configuration; (b) Darlington transistor pair.

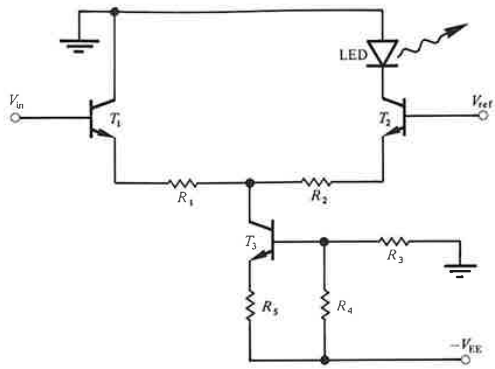

Fig. 10.9 A differential amplifier drive circuit.

Although in many communication applications where a single analog signal is transmitted certain levels of amplitude and phase distortion can be tolerated, this is not the case in frequency multiplexed systems (see Section 10.4.2) where a high degree of linearity is required in order to minimize interference between individual channels caused by the generation of intermodulation products. Also baseband video transmission of TV signals requires the maintenance of extremely low levels of amplitude and phase distortion. For such applications the simple drive circuits described previously are inadequate without some form of linearization to compensate for both LED and drive circuit nonlinearities. A number of techniques have been reported [Ref. 10], some of which are illustrated in Fig. 10.10. Figure 10.10(a) shows the complementary distortion technique [Ref. 11] where additional nonlinear devices are included in the system. It may take the form of predistortion compensation (before the source drive circuit) or postdistortion compensation (after the receiver). This approach has been shown [Ref. 12] to reduce harmonic distortion by up to 20 dB over a limited range of modulation amplitudes.

In the negative feedback compensation technique shown in Fig. 10.10(b), the LED is included in the linearization scheme. The optical output is detected and compared with the input waveform, the amount of compensation being dependent on the gain of the feedback loop. Although the technique is straightforward, large bandwidth requirements (i.e. video) can cause problems at high frequencies [Ref. 13].

The technique shown in Fig. 10.10(c) employs phase shift modulation for selective harmonic compensation using a pair of LEDs with similar characteristics [Ref. 14]. The input signal is divided into equal parts which are phase shifted with respect to each other. These signals then modulate the two LEDs giving a cancellation of the second and third harmonic with a 90° and 60°

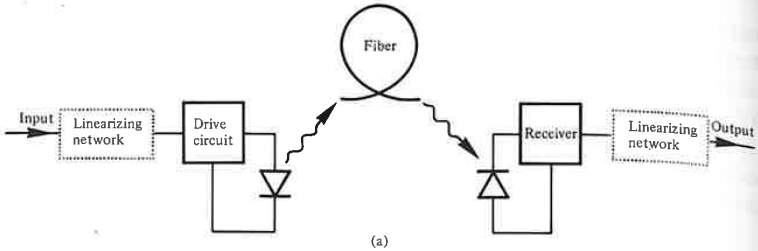

(a)

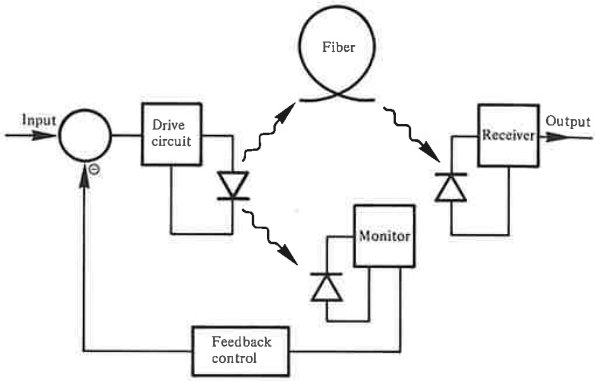

(b)

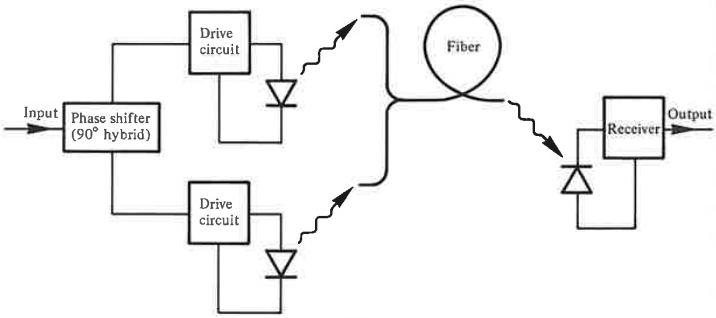

(c)

Fig. 10.10 Block schematics of some linearization methods for LED drive circuits: (a) complementary distortion technique; (b) negative feedback compensation technique; (c) selective harmonic compensation technique.

phase shift respectively. However, although there is a high degree of distortion cancellation, both harmonics cannot be reduced simultaneously.

Other linearization techniques include cascade compensation [Ref. 15], feedforward compensation [Ref. 16] and quasi-feedforward compensation [Refs. 17 and 18].

10.2.3 Laser Drive Circuits

A number of configurations described for use as LED drive circuits for both digital and analog transmission may be adapted for injection laser applications with only minor changes. The laser, being a threshold device, has somewhat different drive current requirements from the LED. For instance, when digital transmission is considered, the laser is usually given a substantial applied bias, often referred to as prebias, in the off state. Reasons for biassing the laser near but below threshold in the off state are:

(a) it reduces the switch-on delay and minimizes any relaxation oscillations;
(b) it allows easy compensation for changes in ambient temperature and device ageing;
(c) it reduces the junction heating caused by the digital drive current since the on and off currents are not widely different for most lasers.

Although biassing near threshold causes spontaneous emission of light in the off state, this is not normally a problem for digital transmission because the stimulated emission in the on state is generally greater by, at least, a factor of 10.

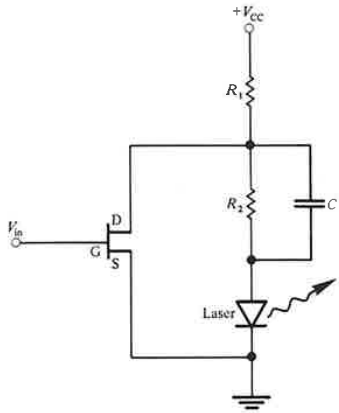

Fig. 10.11 A shunt drive circuit for use with an injection laser.

A simple laser drive circuit for digital transmission is shown in Fig. 10.11. This circuit is a shunt driver utilizing a field effect transistor (FET) to provide high speed laser operation. Sufficient voltage is maintained in series with the laser using the resistor R_2 and the compensating capacitor C such that the FET is biassed into its active or pinch-off region. Hence for a particular input voltage V_{in} (i.e. V_{GS}) a specific amount of the total current flowing through R_1 is diverted around the laser leaving the balance of the current to flow through R_2 and provide the off state for the device. Using suitable gallium arsenide MESFETs (see Section 9.5.1) the circuit shown in Fig. 10.11 has modulated lasers at rates in excess of 1 Gbit s^{-1} [Ref. 19].

An alternative high speed laser drive circuit employing bipolar transistors is shown in Fig. 10.12 [Ref. 20]. This circuit configuration, again for digital transmission, consists of two differential amplifiers connected in parallel. The input stage, which is ECL compatible, exhibits a 50 Ω input impedance by use of an emitter follower T_1 and a 50 Ω resistor in parallel with the input. The transistor T_2 acts as a current source with the zener diode ZD adjusting the signal level for ECL operation. The two differential amplifiers provide sufficient modulation current amplitude for the laser under the control of a d.c. control current I_E through the two emitter resistors R_{E1} and R_{E2}. I_E is provided by an optical feedback control circuit to be discussed shortly. Finally, a prebias current is applied to the laser from a separate current source. This circuit when utilizing microwave transistors was operated with a return to zero digital format (see Section 3.7) at 1 Gbit s^{-1} [Ref. 20].

A major difference between the drive circuits of Figs. 10.11 and 10.12 is the absence and use respectively of feedback control for adjustment of the laser

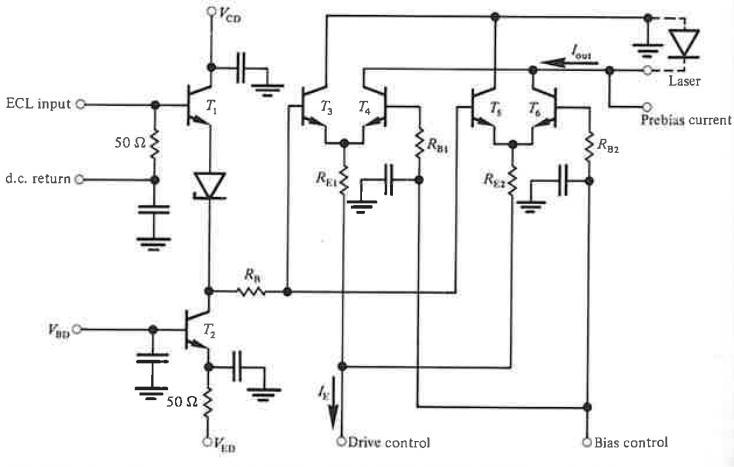

Fig. 10.12 An ECL compatible high speed laser drive circuit [Ref. 20].

output level. For this reason it is unlikely that the shunt drive circuit of Fig. 10.11 would be used for a system application. Some form of feedback control is generally required to ensure continuous laser operation because the device lasing threshold is a sensitive function of temperature. Also the threshold level tends to increase as the laser ages following an increase in internal device losses. Although lasers may be cooled to compensate for temperature variations, ageing is not so easily accommodated by the same process. However, both problems may be overcome through control of the laser bias using a feedback technique. This may be achieved using low speed feedback circuits which adjust the generally static bias current when necessary. For this purpose it is usually found necessary to monitor the light output from the laser in order to keep some aspect constant.

Several strategies of varying complexity are available to provide automatic output level control for the laser. The simplest and perhaps most common form of laser drive circuit incorporating optical feedback is the mean power control circuit shown in Fig. 10.13. Often the monitor detector consists of a cheap, slow photodiode positioned next to the rear face of the laser package as indicated in Fig. 10.13. Alternatively, an optical coupler at the fiber input can be used to direct some of the radiation emitted from the laser into the monitor photodiode. The detected signal is integrated and compared with a reference by an operational amplifier which is used to servo-control the d.c. bias applied to the laser. Thus the mean optical power is maintained constant by varying the threshold current level. This technique is suitable for both digital and analog transmission.

An alternative control method for digital systems which offers accurate threshold tracking and very little device dependence is the switch-on delay technique illustrated in Fig. 10.14 [Ref. 24]. This circuit monitors the switch-on delay of an optical pulse in order to control the laser bias current. The switch-on delay is measured for a zero level set below threshold and the feed-

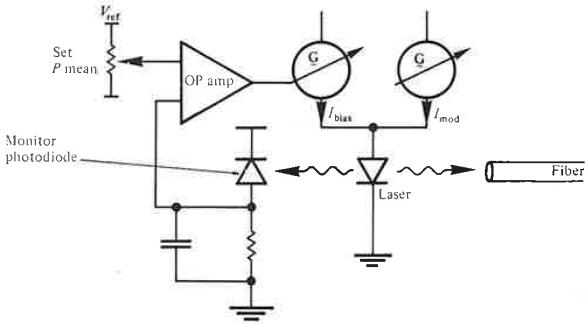

Fig. 10.13 Mean power feedback circuit for control of the laser bias current.

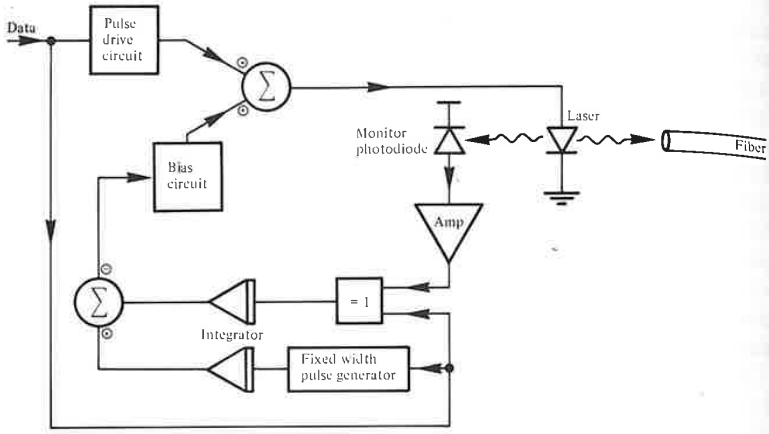

Fig. 10.14 Switch-on delay feedback laser control circuit [Ref. 24].

back is set to a constant fixed delay to control it. Hence, the circuit provides a reference signal proportional to the delay period. This signal is used to control the bias level. The technique requires a fast monitor photodiode as well as a wideband amplifier to allow measurement of the small delay periods. It is also essential that the zero level is set below the lasing threshold because the feedback loop will only stabilize for a finite delay (i.e. the delay falls to zero at the threshold).

A major disadvantage, however, with just controlling the laser bias current is that it does not compensate for variations in the laser slope efficiency. The modulation current for the device is preset and does not take into account any slope changes with temperature and ageing. In order to compensate for such changes, the a.c. and d.c. components of the monitored light output must be processed independently. This is especially important in the case of high bit rate digital systems where control of the on and off levels as well as the light level is required. A circuit which utilizes both a.c. and d.c. information in the laser output to control the device drive current and bias independently is shown in Fig. 10.15 [Ref. 20]. The electrical output from the monitor photodiode is fed into a low drift d.c. amplifier *A1* and into a wideband amplifier *A2*. Therefore the mean value of the laser output power P_e(ave) is proportional to the output from *A1* whilst the a.c. content of the monitoring signal is peak detected after the amplifier *A2*. The peak signals correspond to the maximum P_e(max) and the minimum P_e(min) laser output powers within a certain time interval. The difference signal proportional to (P_e(max) – P_e(min)) is acquired in *A3* and compared with a drive reference voltage in order to control the current output from *A4* and consequently the laser drive current. In this way the modulation amplitude of the laser is controlled. Control of the

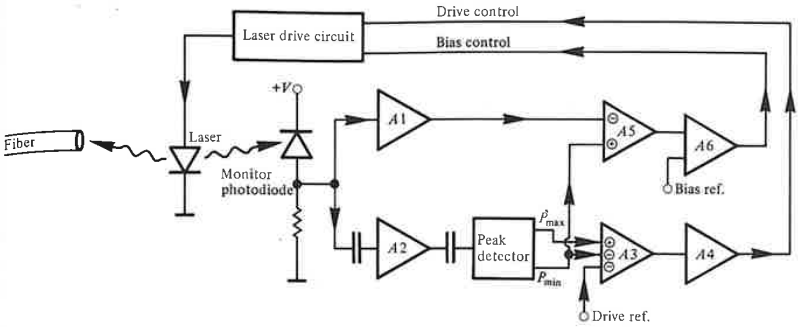

Fig. 10.15 A laser feedback control circuit which uses a.c. and d.c. information in the monitored light output to control the laser drive and bias currents independently [Ref. 20].

laser bias current is achieved from the difference between the output signal of *A1* (P_e(ave)) and P_e(min) which is acquired in *A5*. The output voltage of *A5* which is proportional to P_e(min) is compared with a bias reference voltage in *A6* which supplies a current output to control the laser d.c. bias. This feedback control circuit was designed for use with the laser drive circuit shown in Fig. 10.12 to give digital operation at bit rates in the gigahertz range.

10.3 THE OPTICAL RECEIVER CIRCUIT

The noise performance for optical fiber receivers incorporating both major detector types (the *p–i–n* and avalanche photodiode) was discussed in Chapter 9. Receiver noise is of great importance within optical fiber communications as it is the factor which limits receiver sensitivity and therefore can dictate the overall system design. It was necessary within the analysis given in Chapter 9 to consider noise generated by electronic amplification (i.e. within the pre-amplifier) of the low level signal as well as the noise sources associated with the optical detector. Also the possible strategies for the configuration of the pre-amplifier were considered (see Section 9.4) as a guide to optimization of the receiver noise performance for a particular application. In this section we extend the discussion to consider different possible circuit arrangements which may be implemented to achieve low noise preamplification as well as further amplification (main amplification) and processing of the detected optical signal.

A block schematic of an optical fiber receiver is shown in Fig. 10.16. Following the linear conversion of the received optical signal into an electrical current at the detector, it is amplified to obtain a suitable signal level. Initial amplification is performed in the preamplifier circuit where it is essential that additional noise is kept to a minimum in order to avoid corruption of the

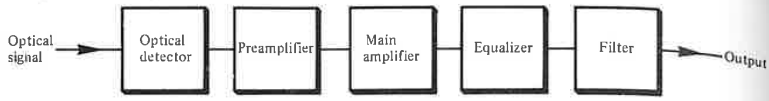

Fig. 10.16 Block schematic showing the major elements of an optical fiber receiver.

received signal. As noise sources within the preamplifier may be dominant, its configuration and design are major factors in determining the receiver sensitivity. The main amplifier provides additional low noise amplification of the signal to give an increased signal level for the following circuits.

Although optical detectors are very linear devices and do not themselves introduce significant distortion onto the signal, other components within the optical fiber communication system may exhibit nonlinear behavior. For instance, the received optical signal may be distorted due to the dispersive mechanisms within the optical fiber. Alternatively the transfer function of the preamplifier–main amplifier combination may be such that the input signal becomes distorted (especially the case with the high impedance front end preamplifier). Hence, to compensate for this distortion and to provide a suitable signal shape for the filter, an equalizer is often included in the receiver. It may precede or follow the main amplifier, or may be incorporated in the functions of the amplifier and filter. In Fig. 10.16 the equalizer is shown as a separate element following the amplifier and preceding the filter.

The function of the final element in the receiver, the filter, is to maximize the received signal to noise ratio whilst preserving the essential features of the signal. In digital systems the function of the filter is primarily to reduce intersymbol interference, whereas in analog systems it is generally required to hold the amplitude and phase response of the received signal within certain limits. The filter is also designed to reduce the noise bandwidth as well as in-band noise levels.

Finally, the general receiver consisting of the elements depicted in Fig. 10.16 is often referred to as a linear channel because all operations on the received optical signal may be considered to be mathematically linear.

10.3.1 The Preamplifier

The choice of circuit configuration for the preamplifier is largely dependent upon the system application. Bipolar or field effect transistors (FETs) can be operated in three useful connections. These are the common emitter or source, the common base or gate, and the emitter or source follower for the bipolar and field effect transistors respectively. Each connection has characteristics which will contribute to a particular preamplifier configuration. It is therefore useful to discuss the three basic preamplifier structures (low impedance, high impedance and transimpedance front end) and indicate possible choices of

transistor connection. In this context the discussion is independent of the type of optical detector utilized. However, it must be noted that there are a number of significant differences in the performance characteristics between the *p–i–n* and avalanche photodiode (see Chapter 8) which must be considered within the overall design of the receiver.

The simplest preamplifier structure is the low input impedance voltage amplifier. This design is usually implemented using a bipolar transistor configuration because of the high input impedance of FETs. The common emitter and the grounded emitter (without an emitter resistor) amplifier shown in Fig. 10.17 are favored connections, as they may be designed with reasonably low input impedance and therefore give operation over a moderate bandwidth without the need for equalization. However, this is achieved at the expense of increased thermal noise due to the low effective load resistance presented to the detector. Nevertheless it is possible to reduce the thermal noise contribution of this preamplifier by choosing a transistor with characteristics which give a high current gain at a low emitter current in order to maintain the bandwidth of the stage. Also an inductance may be inserted at the collector to provide partial equalization for any integration performed by the stage. The alternative connection giving very low input impedance is the common base circuit. Unfortunately this configuration has an input impedance which gives insufficient power gain when connected to the high impedance of the optical detector.

The preferred preamplifier configurations for low noise operation use either a high impedance integrating front end or a transimpedance amplifier (see Sections 9.4.2 and 9.4.3). Careful design employing these circuit structures can facilitate high gain coupled with low noise performance and therefore

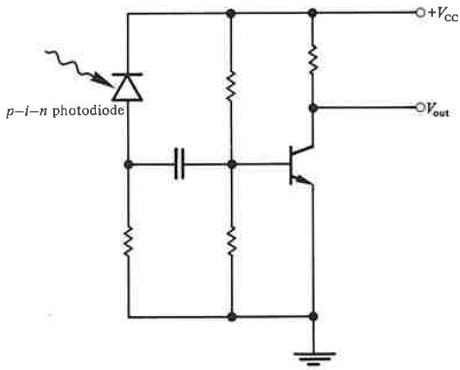

Fig. 10.17 A *p–i–n* photodiode with a grounded emitter, low input impedance voltage preamplifier.

enhanced receiver sensitivity. Although the bipolar transistor incorporated in the emitter follower circuit may be used to realize a high impedance front end amplifier, the FET is generally employed for this purpose because of its low noise operation. It was indicated in Section 9.5 that the grounded source FET connection was a useful circuit to provide a high impedance front end amplifier. The same configuration with a source resistor (common source connection) shown in Fig. 10.18 provides a similar high input impedance and may also be used (often both configurations are referred to as the common source connection). When operating in this mode the FET power gain and output impedance are both high, which tends to minimize any noise contributions from the following stages. It is especially the case when the voltage gain of the common source stage is minimized in order to reduce the Miller capacitance [Ref. 27] associated with the gate to drain capacitance of the FET. This may be achieved by following the common source stage with a stage having a low input impedance.

Two configurations which provide a low input impedance stage are shown in Fig. 10.19. Figure 10.19(a) shows the grounded source FET followed by a bipolar transistor in the common emitter connection with shunt feedback over the stage. Another favored configuration to reduce Miller capacitance in the first stage FET is shown in Fig. 10.19(b). In this case the second stage consists of a bipolar transistor in the common base configuration which, with the initial grounded source FET, forms the cascode configuration.

The high impedance front end structure provides a very low noise preamplifier design but suffers from two major drawbacks. The first is with regard to equalization which must generally be tailored to the amplifier in order to compensate for distortion introduced onto the signal. Secondly, the high input–impedance approach suffers from a lack of dynamic range which occurs

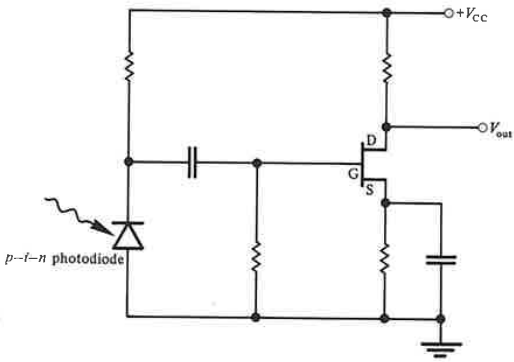

Fig. 10.18 An FET common source preamplifier configuration which provides high input impedance for the *p–i–n* photodiode.

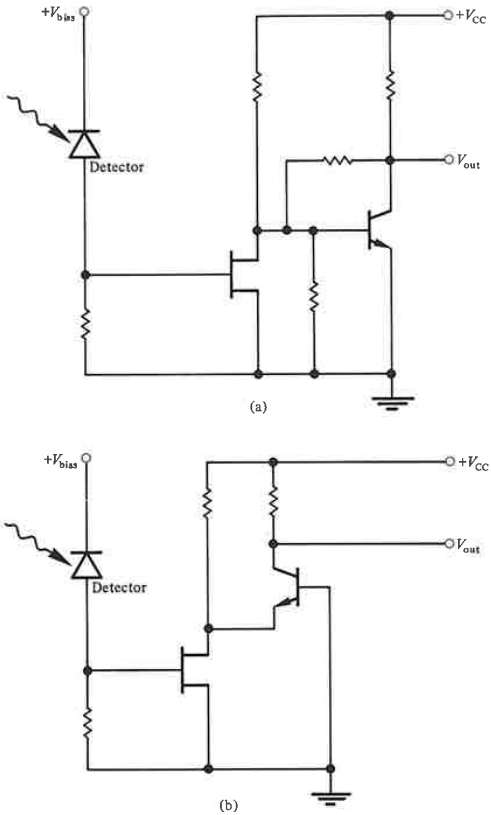

Fig. 10.19 High input impedance preamplifier configurations: (a) grounded source FET followed by common emitter connection with shunt feedback; (b) cascade connection. The separate bias voltage indicates the use of either *p–i–n* or avalanche photodiode.

because the charge on the input capacitance from the low frequency components in the signal builds up over a period of time, causing premature saturation of the amplifier at high input signal levels. Therefore although the circuits shown in Fig. 10.19 are examples of possible high impedance integrating front end amplifier configurations, similar connections may be employed with overall feedback (to the first stage) to obtain a transimpedance preamplifier.

The transimpedance or shunt feedback amplifier finds wide application in preamplifier design for optical fiber communications. This front end structure which acts as a current–voltage converter gives low noise performance without the severe limitations on bandwidth imposed by the high input impedance front

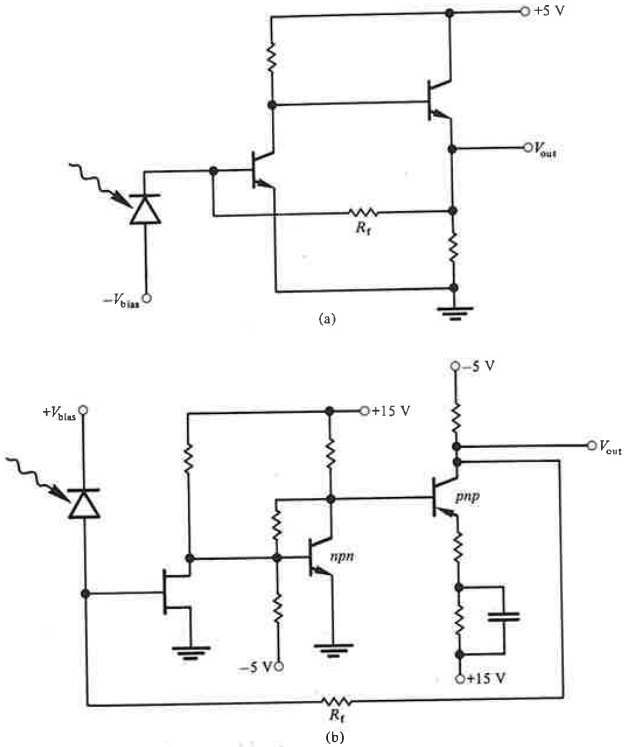

Fig. 10.20 Transimpedance front end configurations: (a) bipolar transistor design [Refs. 28 and 29]; (b) FET front end and bipolar transistor cascade structure [Ref. 32].

end design. It also provides greater dynamic range than the high input impedance structure. However, in practice the noise performance of the transimpedance amplifier is not quite as good as that achieved with the high impedance structure due to the noise contribution from the feedback resistor (see Section 9.4.3). Nevertheless the transimpedance design incorporating a large value of feedback resistor can achieve a noise performance which approaches that of the high impedance front end.

Two examples of transimpedance front end configurations are shown in Fig. 10.20. Figure 10.20(a) illustrates a bipolar transistor structure consisting of a common emitter stage followed by an emitter follower [Refs. 28 and 29] with overall feedback through resistor R_f. The output signal level from this transimpedance pair may be increased by the addition of a second common emitter stage [Ref. 30] after the emitter follower. This stage is not usually

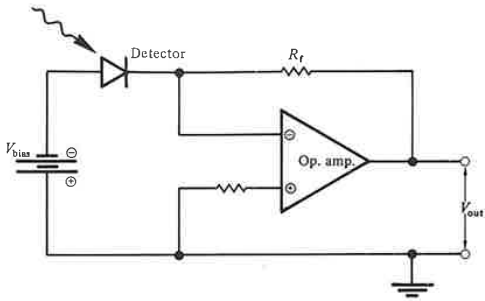

Fig. 10.21 A typical circuit for an operational amplifier transimpedance front end [Ref. 33].

included in the feedback loop. An FET front end transimpedance design is shown in Fig. 10.20(b) [Ref. 32].

The circuit consists of a grounded source configuration followed by a bipolar transistor cascade with feedback over the three stages. In this configuration the bias currents for the bipolar stages and the feedback resistance may be chosen to give good open loop bandwidth whilst making the noise contribution from these stages negligible.

Finally, for lower-bandwidth, shorter-haul applications an FET operational amplifier front end is often adequate [Ref. 33]. Such a transimpedance preamplifier circuit which is generally used with a *p–i–n* photodiode is shown in Fig. 10.21. The choice of the operational amplifier is dependent on the gain versus bandwidth product for the device. In a simple digital receiver design all that may be required in addition to the circuit shown in Fig. 10.21 is a logic (e.g. TTL) interface stage following the amplifier.

10.3.2 Automatic Gain Control (AGC)

It may be noted from the previous section that the receiver circuit must provide a steady reverse bias voltage for the optical detector. With a *p–i–n* photodiode this is not critical and a voltage of between 5 and 80 V supplying an extremely low current is sufficient. The avalanche photodiode requires a much larger bias voltage of between 100 and 400 V which defines the multiplication factor for the device. An optimum multiplication factor is usually chosen so that the receiver signal to noise ratio is maximized (see Section 9.3.3). The multiplication factor for the APD varies with the device temperature (see Section 8.9.5) making provision of fine control for the bias voltage necessary in order to maintain the optimum multiplication factor. However, the multiplication factor can be held constant by some form of automatic gain control (AGC). An additional advantage in the use of AGC is

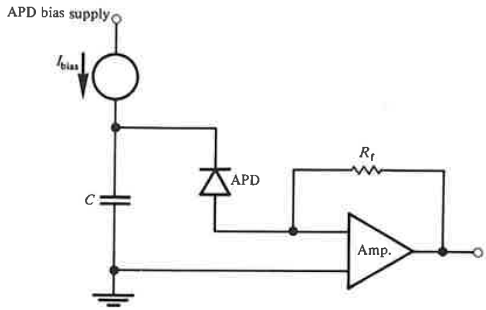

Fig. 10.22 Bias of an APD with a constant current source to provide simple AGC.

that it reduces the dynamic range of the signals applied to the preamplifier giving increased optical dynamic range at the receiver input.

One method of providing AGC is simply to bias the APD with a constant d.c. current source I_{bias} as illustrated in Fig. 10.22. The constant current source is decoupled by a capacitor C at all signal frequencies to prevent gain modulation. When the mean optical input power is known, the mean current to the APD is defined by the bias which gives a constant multiplication factor (gain) at all temperatures. Any variation in the multiplication factor will produce a variation in the charge on C, thus adjusting the biassing of the APD back to the required multiplication factor. Therefore the output current from the photodetector is only defined by the input current from the constant current source, giving full automatic gain control. However, this simple AGC technique is dependent on a constant, mean optical input power level, and takes no account of dark current generated within the detector.

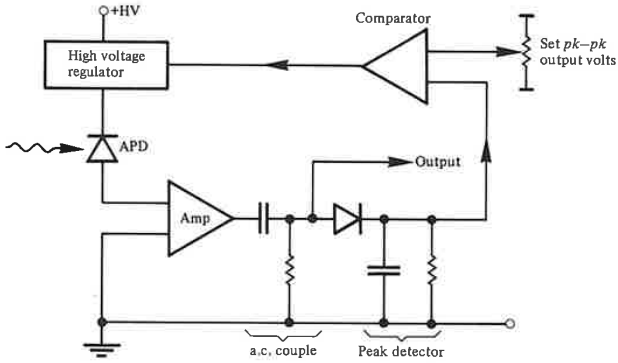

Fig. 10.23 Bias of an APD by peak detection and feedback to provide AGC.

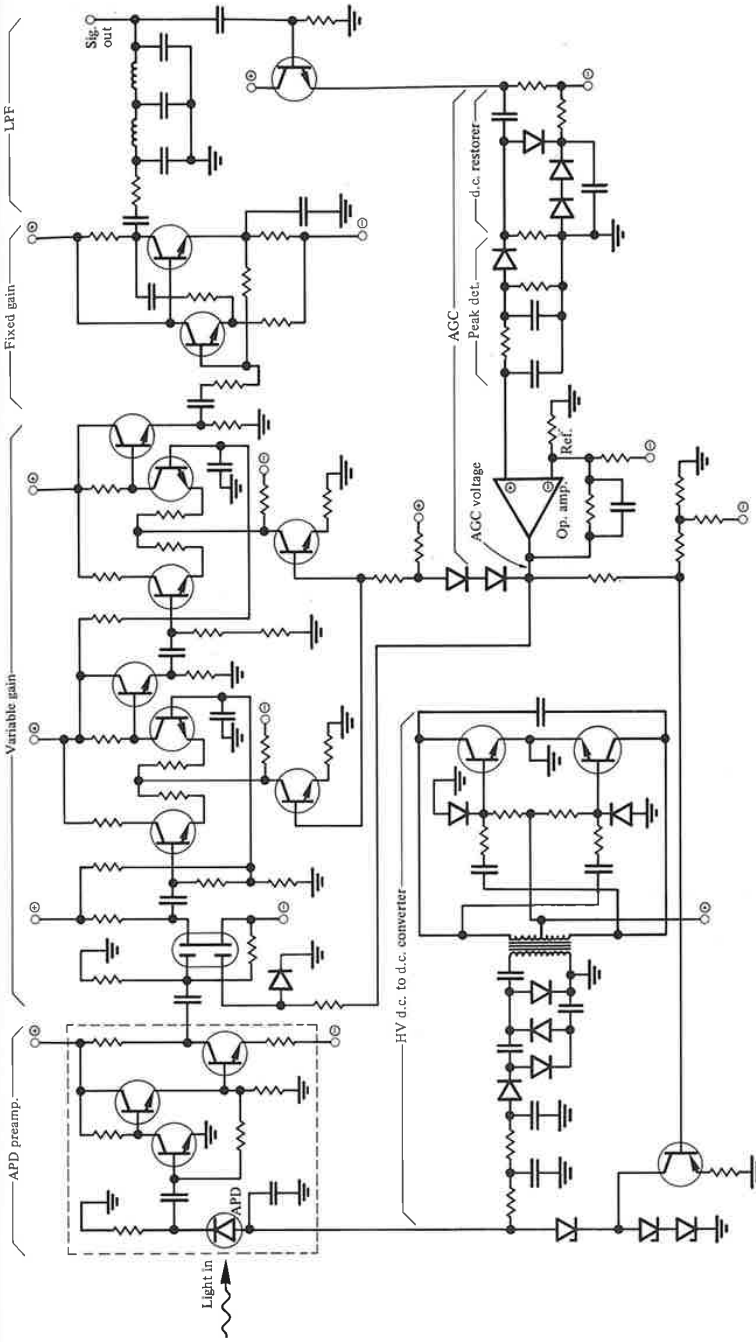

Fig. 10.24 An optical fiber receiver circuit for digital transmission with AGC provided by both control of the APD bias and the main amplifier gain [Ref. 34].

A more widely used method which allows for the effect of variations in the detector dark current whilst providing critical AGC is to peak detect the a.c. coupled signal after suitable low noise amplification as shown in Fig. 10.23. The signal from the final stage of the main amplifier is compared with a preset reference level and fed back to adjust the high voltage bias supply in order to maintain a constant signal level. This effectively creates a constant current source with the dark current subtracted.

A further advantage of this technique is that it may also be used to provide AGC for the main amplifier giving full control of the receiver gain.

A digital receiver circuit for an APD employing full AGC is shown in Fig. 10.24 [Ref. 34]. The APD is followed by a transimpedance preamplifier employing bipolar transistors, the output of which is connected into a main amplifier consisting of a variable gain amplifier followed by a fixed gain amplifier. The first stage of the main amplifier is provided by a dual gate FET which gives a variable gain over a range of 20 dB. This variable gain amplifier also incorporates two stages, each of which consist of an emitter coupled pair with a gain variation of 14 dB. The following fixed gain amplifier gives a 2 V peak to peak signal to the low pass filter, the output of which is maintained at 1 V peak to peak by the AGC. Peak detection is provided in the AGC where the signal level is compared with a preset reference prior to control of the gain for both the APD and the main amplifier. The gain of the APD is controlled via a simple d.c. to d.c. converter which supplies the bias from a low voltage input, whereas the gain of the main amplifier is controlled by an input on the dual gate FET front end. This circuit allows a gain variation of 26 and 47 dB for the APD and the main amplifier respectively. The APD bias circuit is designed to protect the device against possible excess power dissipation at very high optical input power levels as well as excess power dissipation when there is no optical input.

10.3.3 Equalization

The linear channel provided by the optical fiber receiver is often required to perform equalization as well as amplification of the detected optical signal. In order to discuss the function of the equalizer it is useful to assume the light falling on the detector to consist of a series of pulses given by:

$$P_o(t) = \sum_{k=-\infty}^{+\infty} a_k h_p(t - k\tau) \tag{10.1}$$

where $h_p(t)$ is the received pulse shape, $a_k = 0$ or 1 corresponding to the binary information transmitted and τ is the pulse repetition time or pulse spacing. In digital transmission τ corresponding to the bit period, although the pulse length does not necessarily fill the entire time period τ. For a typical optical fiber link,

the received pulse shape is dictated by the transmitted pulse shape $h_t(t)$ and the fiber impulse response $h_f(t)$ following:

$$h_p(t) = h_t(t) * h_f(t) \tag{10.2}$$

where * denotes convolution. Hence determination of the received pulse shape requires knowledge of the fiber impulse response which is generally difficult to characterize. However, it can be shown [Ref. 37] for fiber which exhibits mode coupling, that the impulse response is close to a Gaussian shape in both the time and frequency domain.

It is likely that the pulses given by Eq. (10.1) will overlap due to pulse broadening caused by dispersion on the link giving intersymbol interference (ISI). Following detection and amplification Eq. (10.1) may be written in terms of a voltage $v_A(t)$ as:

$$v_A(t) = \sum_{k=-\infty}^{+\infty} a_k h_A(t - k\tau) \tag{10.3}$$

where the response $h_A(t)$ includes any equalization required to compensate for distortion (e.g. integration) introduced by the amplifier. Therefore, although there is equalization for degradations caused by the amplifier, distortion caused by the channel and the resulting intersymbol interference is still included in $h_A(t - k\tau)$. The pulse overlap causing this intersymbol interference may be reduced through the incorporation of a suitable equalizer with a frequency response $H_{eq}(\omega)$ such that:

$$H_{eq}(\omega) = \frac{\mathcal{F}\{h_{out}(t)\}}{\{h_A(t)\}} = \frac{H_{out}(\omega)}{H_A(\omega)} \tag{10.4}$$

where $h_{out}(t)$ is the desired output pulse shape and $\mathcal{F}$ indicates Fourier transformation. A block diagram indicating the pulse shapes in the time and frequency domains at the various points in an optical fiber system is shown in Fig. 10.25.

An equalizer characterized by Eq. (10.4) will provide high frequency enhancement in the linear channel to compensate for high frequency roll off in the received pulses, thus giving the desired pulse shape. However, in order to construct such an equalizer we require knowledge of $h_A(t)$ and therefore $h_p(t)$. In turn this needs information on the fiber impulse response $h_f(t)$ which may not be easily obtained.

Nevertheless the conventional transversal equalizer shown in Fig. 10.26 may be incorporated into the linear channel to keep ISI at tolerable levels, even if it is difficult to design a circuit which gives the optimum system response indicated in Eq. (10.4).

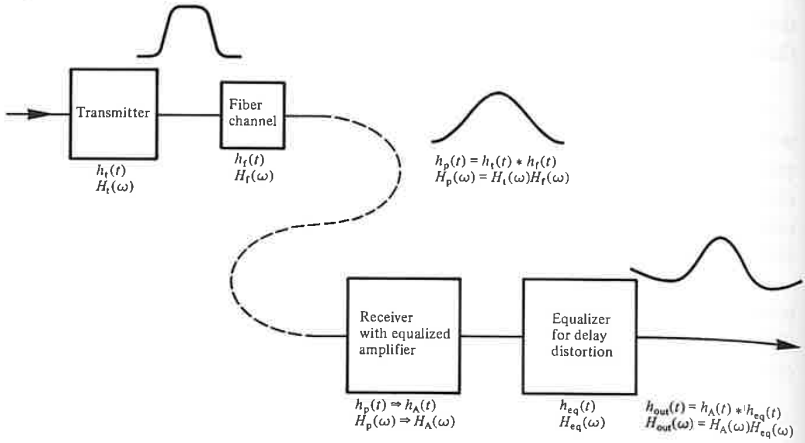

Fig. 10.25 Block schematic of an optical fiber system illustrating the transmitted and received optical pulse shapes together with electrical pulse shape at the linear channel output.

The transversal equalizer consists of a delay line tapped at τ_E second intervals. Each tap is connected through a variable gain device with tap coefficients c_i to a summing amplifier. Intersymbol interference is reduced by filtering the input signal and by the computing values for the tap coefficients which minimize the peak ISI. It is likely that further reduction in ISI will be accomplished using adaptive equalization which has yet to be rigorously applied to optical fiber communications. This topic is discussed further in Ref. 40.

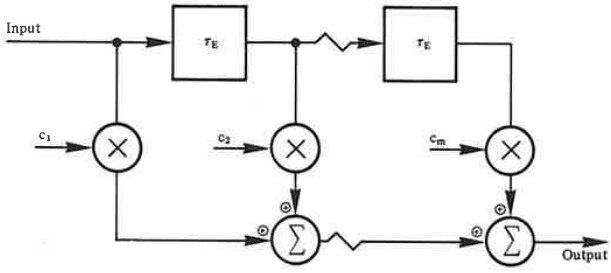

Fig. 10.26 The transversal equalizer employing a tapped delay line.

10.4 SYSTEM DESIGN CONSIDERATIONS

Many of the problems associated with the design of optical fiber communication systems occur as a result of the unique properties of the glass fiber as a transmission medium. However, in common with metallic line transmission systems, the dominant design criteria for a specific application using either digital or analog transmission techniques are the required transmission distance and the rate of information transfer.

Within optical fiber communications these criteria are directly related to the major transmission characteristics of the fiber, namely optical attenuation and dispersion. Unlike metallic conductors where the attenuation (which tends to be the dominant mechanism) can be adjusted by simply changing the conductor size, entirely different factors limit the information transfer capability of optical fibers (see Chapter 3). Nevertheless it is mainly these factors, together with the associated constraints within the terminal equipment, which finally limit the maximum distance that may be tolerated between the optical fiber transmitter and receiver. Where the terminal equipment is more widely spaced than this maximum distance, as in long-haul telecommunication applications, it is necessary to insert repeaters at regular intervals as shown in Fig. 10.27. The repeater incorporates a line receiver in order to convert the optical signal back into the electrical regime where, in the case of analog transmission, it is amplified and equalized (see Section 10.3.3) before it is retransmitted as an optical signal via a line transmitter. When digital transmission techniques are used the repeater also regenerates the original digital signal in the electrical regime (a regenerative repeater which is often simply called a regenerator) before it is retransmitted as a digital optical signal. In this case the repeater may additionally provide alarm, supervision and engineering order wire facilities.

The installation of repeaters substantially increases the cost and complexity of any line communication system. Hence a major design consideration for long-haul telecommunication systems is the maximum distance of unrepeatered transmission so that the number of intermediate repeaters may

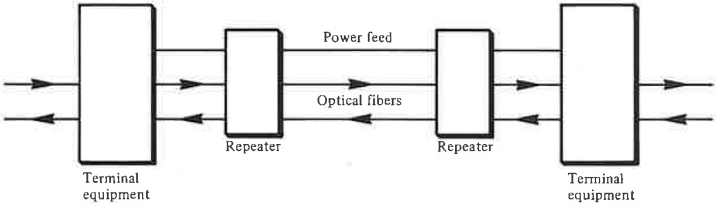

Fig. 10.27 The use of repeaters in a long-haul optical fiber communication system.

be reduced to a minimum. In this respect optical fiber systems display a marked improvement over alternative line transmission systems using metallic conductors. However, this major advantage of optical fiber communications is somewhat reduced due to the present requirement for electrical signal processing at the repeater. This necessitates the supply of electrical power to the intermediate repeaters via metallic conductors as may be observed in Fig. 10.27.

Before any system design procedures can be initiated it is essential that certain basic system requirements are specified. These specifications include:

(a) transmission type: digital or analog;
(b) acceptable system fidelity generally specified in terms of the received BER for digital systems or the received SNR and signal distortion for analog systems;
(c) required transmission bandwidth;
(d) acceptable spacing between the terminal equipment or intermediate repeaters;
(e) cost;
(f) reliability.

However, the exclusive use of the above specifications inherently assumes that system components are available which will allow any system, once specified, to be designed and implemented. Unfortunately this is not always the case, especially when the desired result is a wideband, long-haul system. In this instance it may be necessary to make choices by considering factors such as availability, reliability, cost and ease of installation and operation, before specifications (a)–(d) can be fully determined. A similar approach must be adopted in lower-bandwidth, shorter-haul applications where there is a requirement for the use of specific components which may restrict the system performance. Hence it is likely that the system designer will find it necessary to consider the possible component choices in conjunction with the basic system requirements.

10.4.1 Component Choice

The system designer has many choices when selecting components for an optical fiber communication system. In order to exclude certain components at the outset it is useful if the operating wavelength of the system is established (i.e. shorter wavelength region 0.8–0.9 μm or longer wavelength region 1.1–1.6 μm). This decision will largely be dictated by the overall requirements for the system performance, the ready availability of suitable reliable components, and cost. Hence the major component choices are:

(a) Optical fiber type and parameters. Multimode or single mode; size, refractive index profile, attenuation, dispersion, mode coupling, strength, cabling, jointing, etc.

(b) Source type and characteristics. Laser or LED; optical power launched into the fiber, rise and fall time, stability, etc.
(c) Transmitter configuration. Design for digital or analog transmission; input impedance, supply voltage, dynamic range, optical feedback, etc.
(d) Detector type and characteristics, *p–n*, *p–i–n*, or avalanche photodiode; responsivity, response time, active diameter, bias voltage, dark current, etc.
(e) Receiver configuration. Preamplifier design (low impedance, high impedance or transimpedance front end), BER or SNR, dynamic range, etc.
(f) Modulation and coding. Source intensity modulation; using pulse modulation techniques for either digital (e.g. pulse code modulation, adaptive delta modulation) or analog (pulse amplitude modulation, pulse frequency modulation, pulse width modulation, pulse position modulation) transmission. Also encoding schemes for digital transmission such as biphase (Manchester) and delay modulation (Miller) codes [Ref. 7]. Alternatively analog transmission using direct intensity modulation or frequency modulation of the electrical subcarrier (subcarrier FM). In the latter technique the frequency of an electrical subcarrier is modulated rather than the frequency of the optical source as would be the case with direct frequency modulation. The electrical subcarrier, in turn, intensity modulates the optical source (see Section 10.7.5).

Digital and analog modulation techniques which require coherent detection are under investigation but system components which will permit these modulation methods to be utilized are not widely available (see Section 10.8).

Decisions in the above areas are interdependent and may be directly related to the basic system requirements. The potential choices provide a wide variety of economic optical fiber communication systems. However, it is necessary that the choices are made in order to optimize the system performance for a particular application.

10.4.2 Multiplexing

In order to maximize the information transfer over an optical fiber communication link it is usual to multiplex several signals onto a single fiber. It is possible to convey these multichannel signals by multiplexing in the electrical time or frequency domain, as with conventional electrical line or radio communication, prior to intensity modulation of the optical source. Hence, digital pulse modulation schemes may be extended to multichannel operation by time division multiplexing (TDM) narrow pulses from multiple modulators under the control of a common clock. Pulses from the individual channels are interleaved and transmitted sequentially, thus enhancing the bandwidth utilization of a single fiber link.

Alternatively, a number of baseband channels may be combined by frequency division multiplexing (FDM). In FDM the optical channel bandwidth

is divided into a number of nonoverlapping frequency bands and each signal is assigned one of these bands of frequencies. The individual signals can be extracted from the combined FDM signal by appropriate electrical filtering at the receive terminal. Hence frequency division multiplexing is generally performed electrically at the transmit terminal prior to intensity modulation of a single optical source. However, it is possible to utilize a number of optical sources each operating at a different wavelength on the single fiber link. In this technique, often referred to as wavelength division multiplexing (WDM), the separation and extraction of the multiplexed signals (i.e. wavelength separation) is performed with optical filters (e.g. interference filters, diffraction grating filters, or prism filters) [Ref. 41].

Finally, a multiplexing technique which does not involve the application of several message signals onto a single fiber is known as space division multiplexing (SDM). In SDM each signal channel is carried on a separate fiber within a fiber bundle or multifiber cable form. The good optical isolation offered by fibers means that cross coupling between channels can be made negligible. However, this technique necessitates an increase in the number of optical components required (e.g. fiber, connectors, sources, detectors) within a particular system and therefore is not widely used.

10.5 DIGITAL SYSTEMS

Most of the future expansion of the telecommunication network is being planned around digital telephone exchanges linked by digital transmission systems. The shift towards digitizing the network followed the introduction of digital circuit techniques and, especially, integrated circuit technology which made the transmission of discrete time signals both advantageous and economic. Digital transmission systems generally give superior performance over their analog counterparts as well as providing an ideal channel for data communications and compatibility with digital computing techniques.

Optical fiber communication is well suited to baseband digital transmission in several important ways. For instance, it offers a tremendous advantage with regard to the acceptable signal to noise ratio (SNR) at the optical fiber receiver over analog transmission by some 20–30 dB (for practical systems) as indicated in the noise considerations of Section 9.2. Also the use of baseband digital signalling reduces problems involved with optical source (and sometimes detector) nonlinearities and temperature dependence which may severely affect analog transmission. Therefore, most high capacity optical fiber communication systems convey digital information in the baseband using intensity modulation (IM) of the optical source.

In common with electrical transmission systems, analog signals (e.g. speech) may be digitized for transmission utilizing pulse code modulation (PCM). Encoding the analog signal into a digital bit pattern is performed by initially

Ex. 1017.52

sampling the analog signal at a frequency in excess of the Nyquist rate (i.e. greater than twice the maximum signal frequency). Within the European telecommunication network where the 3 dB telephone bandwidth is defined as 3.4 kHz, the sampling rate is 8 kHz. Hence, the amplitude of the constant width sampling pulses varies in proportion to the sample values of the analog signal giving a discrete time signal known as pulse amplitude modulation (PAM) as indicated in Fig. 10.28. The sampled analog signal is then quantized into a number of discrete levels, each of which are designated by a binary code which provides the PCM signal. This process is also illustrated in Fig. 10.28 using a linear quantizer with eight levels (or seven steps) so that each PAM sample is encoded into three binary bits. The analog signal is thus digitized and may be transmitted as a baseband signal or alternatively be modulated by amplitude, frequency or phase shift keying [Ref. 43]. However, in practical PCM systems for speech transmission, nonlinear encoding (A law in Europe and μ law in North America) is generally employed over 128 levels (2^7) giving eight binary bits per sample (seven bits for code levels plus one polarity bit). Hence, the bandwidth requirement for PCM transmission is substantially greater (in this case by a factor of approximately 16) than the corresponding baseband analog transmission. This is not generally a problem with optical fiber communications because of the wideband nature of the optical channel.

Nonlinear encoding may be implemented via a mechanism known as companding where the input signal is compressed before transmission to give a nonlinear encoding characteristic and expanded again at the receive terminal after decoding. A typical nonlinear input–output characteristic giving compression is shown in Fig. 10.29. Companding is used to reduce the quantization error on small amplitude analog signal levels when they are encoded from PAM to PCM. The quantization error (i.e. the rounding off to the nearest

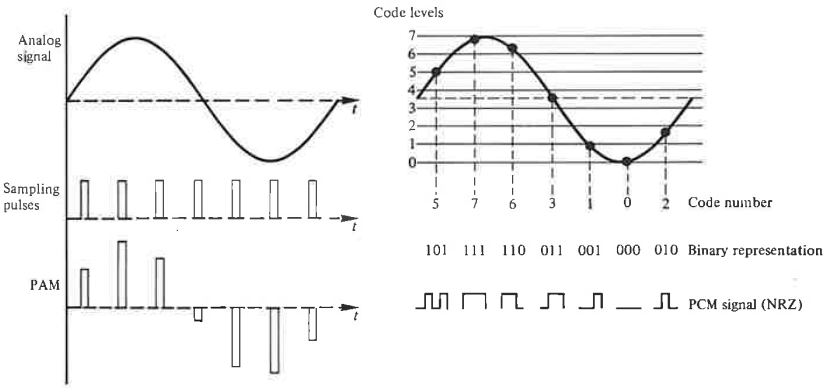

Fig. 10.28 The quantization and encoding of an analog signal into PCM using a linear quantizer with eight levels.

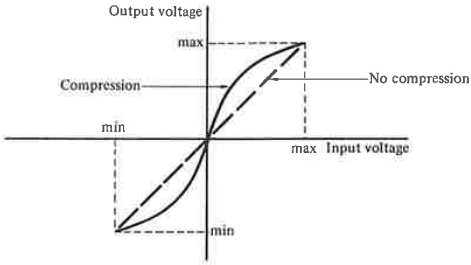

Fig. 10.29 A typical nonlinear input–output characteristic which provides compression.

discrete level) is exhibited as distortion or noise on the signal (often called quantization noise). Companding tapers the step size, thus reducing the distance between levels for small amplitude signals whilst increasing the distance between levels for higher amplitude signals. This substantially reduces the quantization noise on small amplitude signals at the expense of slightly increased quantization noise, in terms of signal amplitude, for the larger signal levels. The corresponding SNR improvement for small amplitude signals significantly reduces the overall signal degradation of the system due to the quantization process.

A block schematic of a simplex (one direction only) baseband PCM system is shown in Fig. 10.30(a). The optical interface is not shown but reference may be made to Fig. 10.1 which illustrates the general optical fiber communication system. It may be noted from Fig. 10.30(a) that the received PCM waveform is decoded back to PAM via the reverse process to encoding, and then simply passed through a low pass filter to recover the original analog signal.

The conversion of a continuous analog waveform into a discrete PCM signal allows a number of analog channels to be time division multiplexed (TDM) for simultaneous transmission down one optical fiber link as illustrated in Fig. 10.30(b). The encoded samples from the different channels are interleaved within the multiplexer to give a single composite signal consisting of all the interleaved pulses. This signal is then transmitted over the optical channel. At the receive terminal the interleaved samples are separated by a synchronous switch or demultiplexer before each analog signal is reconstructed from the appropriate set of samples. Time division multiplexing a number of channels onto a single link can be used with any form of digital transmission and is frequently employed in the transmission of data as well as with the transmission of digitized analog signals. However, the telecommunication network is primarily designed for the transmission of analog speech signals although the compatibility of PCM with data signals has encouraged the adoption of digital transmission systems.

Ex. 1017.54

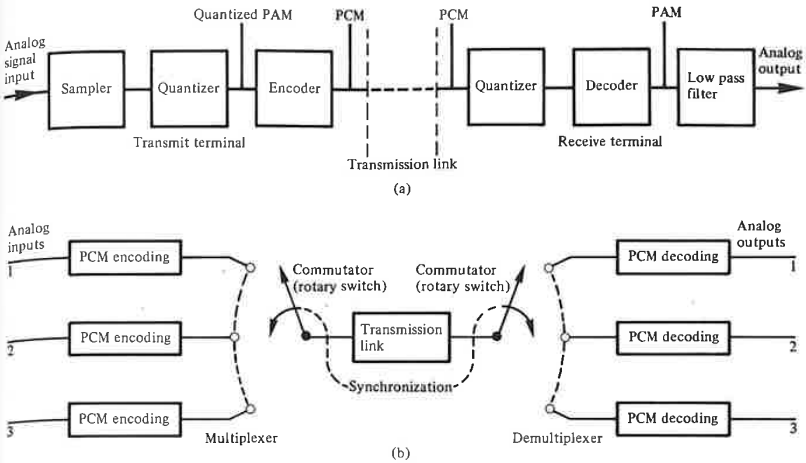

Fig. 10.30 PCM transmission: (a) block schematic of a baseband PCM transmission system for single channel transmission; (b) time division multiplexing of three PCM channels onto a single transmission link and subsequent demultiplexing at the link output.

A current European standard for speech transmission using PCM on metallic conductors (i.e. coaxial line) is the 30 channel system. In this system the PAM samples from each channel are encoded into eight binary bits which are incorporated into a single time slot. Time slots from respective channels are interleaved (multiplexed) into a frame consisting of 32 time slots. The two additional time slots do not carry encoded speech but signalling and synchronization information. Finally, 16 frames are incorporated into a multiframe which is a self-contained timing unit. The timing for this line signalling structure is shown in Fig. 10.31 and calculated in example 10.1.

Example 10.1

The sampling rate for each speech channel on the 30 channel PCM system is 8 kHz and each sample is encoded into eight bits. Determine:

(a) the transmission or bit rate for the system;
(b) the duration of a time slot;
(c) the duration of a frame and multiframe.

Solution: (a) The 30 channel PCM system has 32 time slots each eight bits wide which make up a frame. Therefore,

$$\text{number of bits in a frame} = 32 \times 8 = 256 \text{ bits}$$

This frame must be transmitted within the sampling period and thus 8×10^3 frames

are transmitted per second. Hence, the transmission rate for the system is:

$$8 \times 10^3 \times 256 = 2.048 \text{ Mbit s}^{-1}$$

(b) The bit duration is simply:

$$\frac{1}{2.048 \times 10^6} = 488 \text{ ns}$$

Therefore, the duration of a time slot is:

$$8 \times 488 \text{ ns} = 3.9 \ \mu\text{s}$$

(c) The duration of a frame is thus:

$$32 \times 3.9 \ \mu\text{s} = 125 \ \mu\text{s}$$

and the duration of a multiframe is:

$$16 \times 125 \ \mu\text{s} = 2 \text{ ms}$$

The signalling structure shown in Fig. 10.31 applies to 30 channel PCM systems which were originally designed to transmit over metallic conductors

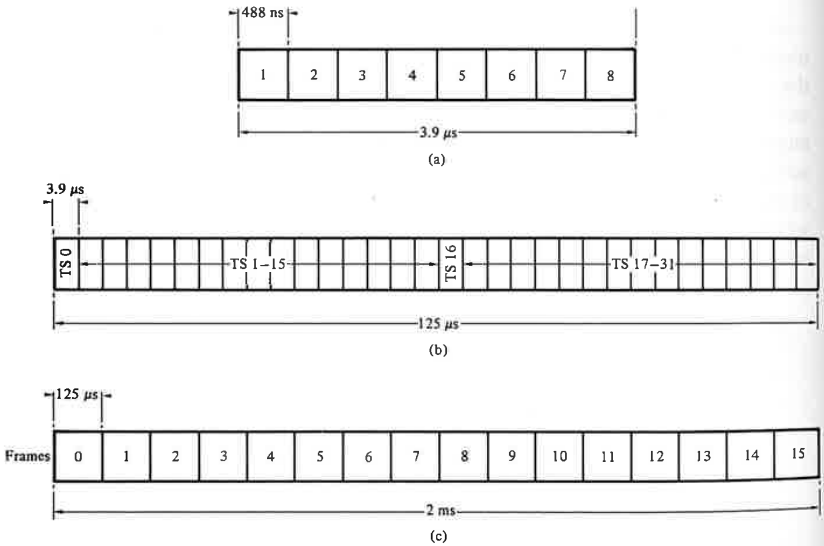

Fig. 10.31 The timing for the line signalling structure of the European standard 30 channel PCM system: (a) bits per time slot; (b) time slots per frame; (c) frames per multiframe.

Table 10.1 Digital bit rates for multichannel PCM transmission transmission in Europe and North America

Europe		North America	
Telephone channels	Bit rates Mbit s^{-1}	Telephone channels	Bit rates Mbit s^{-1}
30	2.048	24	1.544
120	8.448	48	3.152
480	34.368	96	6.312
1920	139.364	672	44.736
7680	565.000	4032	274.176

using a high density bipolar line code (HDB 3). The increased bandwidth with optical fiber communications allows transmission rates far in excess of 2.048 Mbit s^{-1}. Therefore an increased number of telephone channels may be sampled, encoded, multiplexed and transmitted on an optical fiber link. In Europe the increased bit rates were chosen as multiples of the 30 channel system, whereas in North America they tend to be multiples of a 24 channel system. These bit rates and the corresponding number of transmitted telephone channels are specified in Table 10.1.

It must be noted that a bipolar code with a zero mean level (i.e. with positive and negative going pulses in the electrical regime) such as HDB 3 cannot be transmitted directly over an optical fiber link unless the mean level is raised to allow both positive and negative going pulses to be transmitted by the intensity modulated optical source. The resultant ternary (three level) optical transmission is not always suitable for telecommunication applications and therefore binary coding after appropriate scrambling, biphase (Manchester encoding), delay modulation (Miller encoding), etc., is often employed. This involves additional complexity at the transmit and receive terminals as well as necessitating extra redundancy (i.e. bits which do not contain the transmitted information, thus giving a reduction in the information per transmitted symbol) in the line code. This topic is considered in greater detail in Section 10.6.7.

10.6 DIGITAL SYSTEM PLANNING CONSIDERATIONS

The majority of digital optical fiber communication systems for the telecommunication network or local data applications utilize binary intensity modulation of the optical source. Therefore we choose to illustrate the planning considerations for digital transmission based on this modulation technique. Baseband PCM transmission using source intensity modulation is usually designated as PCM-IM.

10.6.1 The Regenerative Repeater

In the case of the long-haul, high-capacity digital systems, the most important overall system performance parameter is the spacing of the regenerative repeaters. It is therefore useful to consider the performance of the digital repeater, especially as it is usually designed with the same optical components as the terminal equipment. Figure 10.32 shows the functional parts of a typical regenerative repeater for optical fiber communications. The attenuated and dispersed optical pulse train is detected and amplified in the receiver unit. This consists of a photodiode followed by a low noise preamplifier. The electrical signal thus acquired is given a further increase in power level in a main amplifier prior to reshaping in order to compensate for the transfer characteristic of the optical fiber (and the amplifier) using an equalizer. Depending on the photodiode utilized, automatic gain control may be provided at this stage for both the photodiode bias current and the main amplifier (see Section 10.3.2).

Accurate timing (clock) information is then obtained from the amplified and equalized waveform using a timing extraction circuit such as a ringing circuit or phase locked loop. This enables precise operation of the following regenerator circuit within the bit intervals of the original pulse train. The function of the regenerator circuit is to reconstitute the originally transmitted pulse train, ideally without error. This can be achieved by setting a threshold above which a binary one is registered, and below which a binary zero is recorded, as indicated in Fig. 10.32. The regenerator circuit makes these decisions at times corresponding to the center of the bit intervals based on the clock information provided by the timing circuit.

Hence the decision times are usually set at the mid-points between the decision level crossings of the pulse train. The pulse train is sampled at a regular frequency equal to the bit rate, and at each sample instant a decision is made of the most probable symbol being transmitted. The symbols are then regenerated in their original form (either a binary one or zero) before

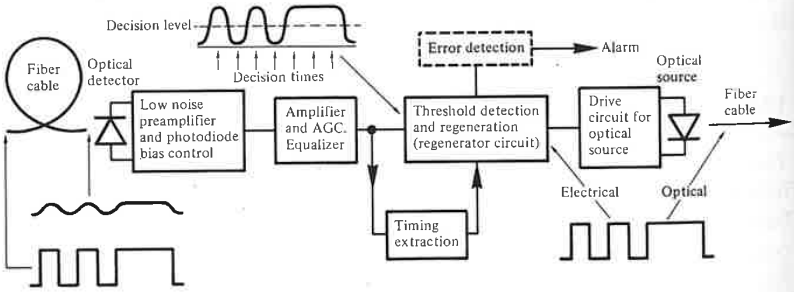

Fig. 10.32 Block schematic showing a typical regenerative repeater for digital optical fiber communications.

retransmission as an optical signal using a source operated by an electronic drive circuit. Hence the possible regeneration of an exact replica of the originally transmitted waveform is a major advantage of digital transmission over corresponding analog systems. Repeaters in analog systems filter, equalize and amplify the received waveform, but are unable to reconstitute the originally transmitted waveform entirely free from distortion and noise. Signal degradation in long-haul analog systems is therefore accumulative being a direct function of the number of repeater stages. In contrast the signal degradation encountered in PCM systems is purely a function of the quantization process and the system bit error rate.

Errors may occur in the regeneration process when:

(a) The signal to noise ratio at the decision instant is insufficient for an accurate decision to be made. For instance, with high noise levels, the binary zero may occur above the threshold and hence be registered as a binary one.
(b) There is intersymbol interference due to dispersion on the optical fiber link. This may be reduced by equalization which forces the transmitted binary one to pass through zero at all neighboring decision times.
(c) There is a variation in the clock rate and phase degradations (jitter) such as distortion of the zero crossings and static decision time misalignment.

A method which is often used to obtain a qualitative indication of the performance of a regenerative repeater or a PCM system is the examination of the received waveform on an oscilloscope using a sweep rate which is a fraction of the bit rate. The display obtained over two bit intervals duration, which is the result of superimposing all possible pulse sequences is called an eye pattern or diagram. An illustration of an eye pattern for a binary system with little distortion and no additive noise is shown in Fig. 10.33(a). It may be observed that the pattern has the shape of a human eye which is open and that the decision time corresponds to the center of the opening. To regenerate the pulse sequence without error the eye must be open thereby indicating a decision area exists, and the decision crosshair (provided by the decision time and the decision threshold) must be within this open area. The effect of practical degradations on the pulses (i.e. intersymbol interference and noise) is to reduce the size of, or close, the eye as shown in Fig. 10.33(b). Hence for reliable transmission it is essential that the eye is kept open, the margin against an error occurring being the minimum distance between the decision crosshair and the edge of the eye.

In practice, a low bit error rate (BER) in the region 10^{-7}–10^{-10} may be tolerated with PCM transmission. However, with data transmission (e.g. computer communications) any error can cause severe problems, and it is necessary to incorporate error detecting and possibly correcting circuits into the regenerator. This invariably requires the insertion of a small amount of redundancy into the transmitted pulse train (see Section 10.6.7).

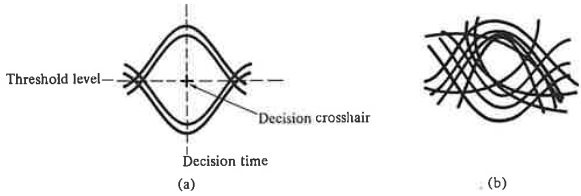

Fig. 10.33 Eye patterns in binary digital transmission: (a) the pattern obtained with a bandwidth limitation but no additive noise (open eye); (b) the pattern obtained with a bandwidth limitation and additive noise (partially closed eye).

Calculation of the possible repeater spacing must take account of the following system component performances:

(a) The average optical power launched into the fiber based on the end of life transmitter performance.
(b) The receiver input power required to achieve an acceptably low BER (e.g. 10^{-9}), taking into account component deterioration during the system's lifetime.
(c) The installed fiber cable loss, including jointing and coupling (to source and detector) losses as well as the effects of ageing and from anticipated environmental changes.
(d) The temporal response of the system including the effects of pulse dispersion on the channel. This becomes an important consideration with high bit rate multimode fiber systems which may be dispersion limited.

These considerations are discussed in detail in the following sections.

10.6.2 The Optical Transmitter

The average optical power launched into the fiber from the transmitter depends upon the type of source used and the required system bit rate as indicated in Section 10.2.1. These factors may be observed in Fig. 10.34 [Ref. 45] which compares the optical power available from an injection laser and an LED for transmission over a multimode fiber with a core diameter of 50 μm and a numerical aperture of 0.2. Typically the laser launches around 1 mW whereas usually the LED is limited to about 100 μW. It may also be noted that both device types emit less optical power at higher bit rates. However, the LED gives reduced output at modulation bandwidths in excess of 50 MHz whereas laser output is unaffected below 200 MHz. Also the fact that generally the optical power which may be launched into a fiber from an LED even at low bit rates is 10–15 dB down on that available from a laser is an important consideration, especially when receiver noise is a limiting factor within the system.

Ex. 1017.60

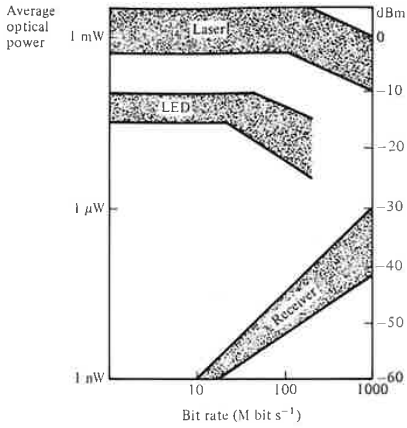

Fig. 10.34 The average power launched into multimode optical fiber from typical injection lasers and LEDs as a function of digital bit rate (upper bands). Also included in the lower band is the received optical power required for binary NRZ pulses transmitted with a BER of 10^{-9}. Reproduced with permission from D. C. Gloge and T. Li, 'Multimode-fiber technology for digital transmission', *Proc. IEEE*, **68**, p. 1269, 1980. Copyright © 1980 IEEE.

10.6.3 The Optical Receiver

The input optical power required at the receiver is a function of the detector combined with the electrical components within the receiver structure. It is strongly dependent upon the noise (i.e. quantum, dark current and thermal) associated with the optical fiber receiver. The theoretical minimum pulse energy or quantum limit required to maintain a given BER was discussed in Section 9.2.4.

It was predicted that approximately 21 incident photons were necessary at an ideal photodetector in order to register a binary one with a BER of 10^{-9}. However, this is a fundamental limit which cannot be achieved in practice and therefore it is essential that estimates of the minimum required optical input power are made in relation to practical devices and components.

Although the statistics of quantum noise follow a Poisson distribution, other important sources of noise within practical receivers (e.g. thermal) are characterized by a Gaussian probability distribution. Hence estimates of the required SNR to maintain particular bit error rates may be obtained using the procedure adopted for error performance of electrical digital systems where the noise distribution is considered to be white Gaussian. This Gaussian approximation [Ref. 46] is sufficiently accurate for design purposes and is far easier to evaluate than the more exact probability distribution within the receiver [Ref. 47]. The receiver sensitivities calculated by using the Gaussian

approximation are generally within 1 dB of those calculated by other methods [Ref. 29].

Although the transmitted signal consists of two well-defined light levels, in the presence of noise the signal at the receiver is not as well defined. This situation is shown in Fig. 10.35(a) which illustrates a binary signal in the presence of noise. The signal plus the additive noise at the detector may be defined in terms of the probability density functions (PDFs) shown in Fig. 10.35(b). These PDFs describe the probability that the input current (or output voltage) has a value i (or v) within the incremental range di (or dv). The expected values of the signal in the two transmitted states, namely 0 and 1, are indicated by $p_0(x)$ and $p_1(x)$ respectively. When the additive noise is assumed to have a Gaussian distribution, the PDFs of the two states will also be Gaussian. The Gaussian PDF which is continuous is defined by:

$$p(x) = \frac{1}{\sqrt{(2\pi)}} \exp -[(x-m)^2/2\sigma^2] \tag{10.5}$$

where m is the mean value and σ the standard deviation of the distribution. When $p(x)$ describes the probability of detecting a noise current or voltage, σ corresponds to the rms value of that current or voltage.

If a decision threshold D is set between the two signal states as indicated in Fig. 10.35, signals greater than D are registered as a one and those less than D as a zero. However, when the noise current (or voltage) is sufficiently large it can either decrease a binary one to a zero or increase a binary zero to a one. These error probabilities are given by the integral of the signal probabilities

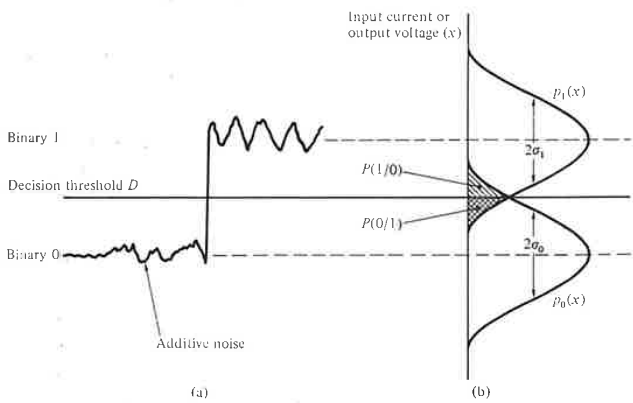

Fig. 10.35 Binary transmission: (a) the binary signal with additive noise; (b) probability density functions for the binary signal showing the decision case. $P(0/1)$ is the probability of falsely identifying a binary one and $P(1/0)$ is the probability of falsely identifying a binary zero.

outside the decision region. Hence the probability that a signal transmitted as a 1 is received as a 0, $P(0/1)$, is proportional to the shaded area indicated in Fig. 10.35(b). The probability that a signal transmitted as a 0 is received as a 1, $P(1/0)$, is similarly proportional to the other shaded area shown in the figure. If $P(1)$ and $P(0)$ are the probabilities of transmission for binary ones and zeros respectively, then the total probability of error $P(\mathrm{e})$ may be defined as:

$$P(\mathrm{e}) = P(1)P(0/1) + P(0)P(1/0) \tag{10.6}$$

Now let us consider a signal current i_{sig} together with an additive noise current i_{N} and a decision threshold set at $D = i_D$. If at any time when a binary 1 is transmitted the noise current is negative such that:

$$i_{\mathrm{N}} < -(i_{\mathrm{sig}} - i_D) \tag{10.7}$$

then the resulting current $i_{\mathrm{sig}} + i_{\mathrm{N}}$ will be less than i_D and an error will occur. The corresponding probability of the transmitted 1 being received as a 0 may be written as:

$$P(0/1) = \int_{-\infty}^{i_D} p(i, i_{\mathrm{sig}})\, \mathrm{d}i \tag{10.8}$$

and following Eq. (10.5):

$$p_1(x) = p(i, i_{\mathrm{sig}}) = \frac{1}{(\overline{i_{\mathrm{N}}^2})^{\frac{1}{2}}\sqrt{(2\pi)}} \exp - \left[\frac{(i - i_{\mathrm{sig}})^2}{2(\overline{i_{\mathrm{N}}^2})}\right] \tag{10.9}$$

$$= \mathrm{Gsn}\,[i, i_{\mathrm{sig}}, (\overline{i_{\mathrm{N}}^2})^{\frac{1}{2}}] \tag{10.10}$$

where i is the actual current, i_{sig} is the peak signal current during a binary 1 (this corresponds to the peak photocurrent I_{p} when only a signal component is present), and $\overline{i_{\mathrm{N}}^2}$ is the mean square noise current. Substituting Eq. (10.10) into Eq. (10.8) gives:

$$P(0/1) = \int_{-\infty}^{i_D} \mathrm{Gsn}\,[i, i_{\mathrm{sig}}, (\overline{i_{\mathrm{N}}^2})^{\frac{1}{2}}]\, \mathrm{d}i \tag{10.11}$$

Similarly, the probability that a binary 1 will be received when a 0 is transmitted is the probability that the received current will be greater than i_D at some time during the zero bit interval. It is given by:

$$P(1/0) = \int_{i_D}^{\infty} p(i, 0) \tag{10.12}$$

Assuming the mean square noise current in the zero state is equal to the mean square noise current in the one state ($\overline{i_{\mathrm{N}}^2}$) (this is an approximation if shot noise is dominant), and that for a zero bit $i_{\mathrm{sig}} = 0$, then following Eq. (10.5):

$$p_0(x) = p(i, 0) = \frac{1}{(\overline{i_N^2})^{\frac{1}{2}}\sqrt{(2\pi)}} \exp - \left[\frac{(i-0)^2}{2(\overline{i_N^2})}\right] \tag{10.13}$$

$$= \mathrm{Gsn}\,[i, 0, (\overline{i_N^2})^{\frac{1}{2}}] \tag{10.14}$$

Hence substituting Eq. (10.14) into Eq. (10.12) gives:

$$P(1/0) = \int_{i_D}^{\infty} \mathrm{Gsn}\,[i, 0, (\overline{i_N^2})^{\frac{1}{2}}]\,\mathrm{d}i \tag{10.15}$$

The integrals of Eqs. (10.11) and (10.15) are not readily evaluated but may be written in terms of the error function (erf)* where:

$$\mathrm{erf}\,(u) = \frac{2}{\sqrt{\pi}} \int_0^u \exp(-z^2)\,\mathrm{d}z \tag{10.16}$$

and the complementary error function is:

$$\mathrm{erfc}\,(u) = 1 - \mathrm{erf}\,(u) = \frac{2}{\sqrt{\pi}} \int_u^{\infty} \exp(-z^2)\,\mathrm{d}z \tag{10.17}$$

Hence

$$P(0/1) = \frac{1}{2}\left[1 - \mathrm{erfc}\left(\frac{|i_{sig} - i_D|}{(\overline{i_N^2})^{\frac{1}{2}}\sqrt{2}}\right)\right]$$

$$= \tfrac{1}{2}\,\mathrm{erfc}\left(\frac{|i_{sig} - i_D|}{(\overline{i_N^2})^{\frac{1}{2}}\sqrt{2}}\right) \tag{10.18}$$

and

$$P(1/0) = \tfrac{1}{2}\,\mathrm{erfc}\left(\frac{|0 - i_D|}{(\overline{i_N^2})^{\frac{1}{2}}\sqrt{2}}\right) = \tfrac{1}{2}\,\mathrm{erfc}\left(\frac{|-i_D|}{(\overline{i_N^2})^{\frac{1}{2}}\sqrt{2}}\right) \tag{10.19}$$

If we assume that a binary code is chosen such that the number of transmitted ones and zeros are equal, then $P(0) = P(1) = \frac{1}{2}$, and the net probability of error is one half the sum of the shaded areas in Fig. 10.35(b). Therefore Eq. (10.6) becomes:

$$P(\mathrm{e}) = \tfrac{1}{2}[P(0/1) + P(1/0)] \tag{10.20}$$

and substituting for $P(0/1)$ and $P(1/0)$ from Eqs. (10.18) and (10.19) gives:

* Another form of the error function denoted by Erf is defined in problem 10.10.

$$P(\mathrm{e}) = \frac{1}{2}\left[\tfrac{1}{2}\,\mathrm{erfc}\left(\frac{|i_{\mathrm{sig}} - i_D|}{(\overline{i_{\mathrm{N}}^2})^{\frac{1}{2}}\sqrt{2}}\right) + \tfrac{1}{2}\,\mathrm{erfc}\left(\frac{|-i_D|}{(\overline{i_{\mathrm{N}}^2})^{\frac{1}{2}}\sqrt{2}}\right)\right] \tag{10.21}$$

Equation (10.21) may be simplified by setting the threshold decision level at the mid-point between zero current and the peak signal current such that $i_D = i_{\mathrm{sig}}/2$. In electrical systems this situation corresponds to an equal minimum probability of error in both states due to the symmetrical nature of the PDFs. It must be noted that for optical fiber systems this is not generally the case since the noise in each signal state contains shot noise contributions proportional to the signal level. Nevertheless assuming a Gaussian distribution for the noise and substituting $i_D = i_{\mathrm{sig}}/2$ into Eq. (10.21) we obtain:

$$P(\mathrm{e}) = \frac{1}{2}\left(\frac{|i_{\mathrm{sig}}/2|}{(\overline{i_{\mathrm{N}}^2})^{\frac{1}{2}}\sqrt{2}}\right) + \tfrac{1}{2}\,\mathrm{erfc}\left(\frac{|-i_{\mathrm{sig}}/2|}{(\overline{i_{\mathrm{N}}^2})^{\frac{1}{2}}\sqrt{2}}\right)\Bigg]$$

$$= \tfrac{1}{2}\,\mathrm{erfc}\left(\frac{i_{\mathrm{sig}}}{2(\overline{i_{\mathrm{N}}^2})^{\frac{1}{2}}\sqrt{2}}\right) \tag{10.22}$$

The electrical SNR at the detector may be written in terms of the peak signal power to rms noise power (mean square noise current) as:

$$\frac{\mathrm{S}}{\mathrm{N}} = \frac{i_{\mathrm{sig}}^2}{\overline{i_{\mathrm{N}}^2}} \tag{10.23}$$

Comparison of Eq. (10.23) with Eq. (10.22) allows the probability of error to be expressed in terms of the analog SNR as:

$$P(\mathrm{e}) = \tfrac{1}{2}\,\mathrm{erfc}\left(\frac{(\mathrm{S/N})^{\frac{1}{2}}}{2\sqrt{2}}\right) \tag{10.24}$$

Estimates of the required SNR to maintain a given error rate may be obtained using the standard table for the complementary error function. A plot of $P(\mathrm{e})$ against $\frac{1}{2}\,\mathrm{erfc}\,(u)$ is shown in Fig. 10.36(a). This may be transposed into the characteristic illustrated in Fig. 10.36(b) where the bit error rate which is equivalent to the error probability $P(\mathrm{e})$ is shown as a function of the SNR following Eq. (10.24).

Example 10.2

Using the Gaussian approximation determine the required signal to noise ratios (optical and electrical) to maintain a BER of 10^{-9} on a baseband binary digital optical fiber link. It may be assumed that the decision threshold is set midway between the one and the zero level and that $2 \times 10^{-9} \simeq \mathrm{erfc}\ 4.24$.

Solution: Under the above conditions, the probability of error is given by

Eq. (10.24) where,

$$P(\mathrm{e}) = \tfrac{1}{2}\,\mathrm{erfc}\left(\frac{(\mathrm{S/N})^{\frac{1}{2}}}{2\sqrt{2}}\right) = 10^{-9}$$

Hence

$$\mathrm{erfc}\left(\frac{(\mathrm{S/N})^{\frac{1}{2}}}{2\sqrt{2}}\right) = 2 \times 10^{-9}$$

and

$$\frac{(\mathrm{S/N})^{\frac{1}{2}}}{2\sqrt{2}} = 4.24$$

giving

$$(\mathrm{S/N})^{\frac{1}{2}} = 4.24 \times 2\sqrt{2} \simeq 12$$

The optical SNR may be defined in terms of the peak signal current and rms noise current as $i_{\mathrm{sig}}/(\overline{i_{\mathrm{N}}^2})^{\frac{1}{2}}$. Therefore using Eq. (10.23):

$$\frac{i_{\mathrm{sig}}}{(\overline{i_{\mathrm{N}}^2})^{\frac{1}{2}}} = \left(\frac{\mathrm{S}}{\mathrm{N}}\right)^{\frac{1}{2}} = 12 \text{ or } 10.8 \text{ dB}$$

The electrical SNR is defined by Eq. (10.23) as:

$$\frac{i_{\mathrm{sig}}^2}{\overline{i_{\mathrm{N}}^2}} = \frac{\mathrm{S}}{\mathrm{N}} = 144 \text{ or } 21.6 \text{ dB}$$

These results for the SNRs may be seen to correspond to a bit error rate of 10^{-9} on the curve shown in Fig. 10.36(b).

However, the plot shown in Fig. 10.36(b) does not reflect the best possible results, or those which may be obtained with an optimized receiver design. In this case, if the system is to be designed with a particular BER, the appropriate value of the error function is established prior to adjustment of the parameter values (signal levels, decision threshold level, avalanche gain, component values, etc.) in order to obtain this BER [Ref. 48]. It is therefore necessary to use the generalized forms of Eqs. (10.18) and (10.19) where:

$$P(0/1) = \tfrac{1}{2}\,\mathrm{erfc}\left(\frac{|i_{\mathrm{sig1}} - i_D|}{(\overline{i_{\mathrm{N1}}^2})^{\frac{1}{2}}\sqrt{2}}\right) \tag{10.25}$$

$$P(1/0) = \tfrac{1}{2}\,\mathrm{erfc}\left(\frac{|i_D - i_{\mathrm{sig0}}|}{(\overline{i_{\mathrm{N0}}^2})^{\frac{1}{2}}\sqrt{2}}\right) \tag{10.26}$$

where i_{sig1} and i_{sig0} are the signal currents, in the 1 and 0 states respectively, and $\overline{i_{\mathrm{N1}}^2}$ and $\overline{i_{\mathrm{N0}}^2}$ are the corresponding mean square noise currents which may

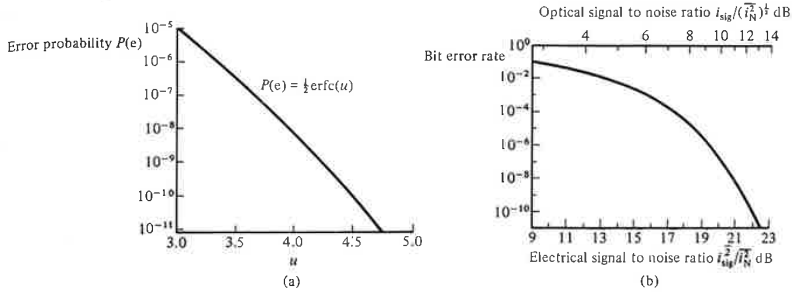

Fig. 10.36 (a) A plot of the probability of error $\frac{1}{2}\text{erfc}(u)$ against the argument of the error function u. (b) The bit error rate as a function of both the ratio of peak signal power to rms noise power (electrical SNR) and the ratio of peak signal current to rms noise current (optical SNR) for binary transmission.

include both shot and thermal noise terms. Equations (10.25) and (10.26) allow a more exact evaluation of the error performance of the digital optical fiber system under the Gaussian approximation [Refs. 48 and 49]. Unfortunately this approach does not give a simple direct relationship between the BER and the analog SNR the one shown in Eq. (10.24). Thus for estimates of SNR within this text we will make use of the slightly poorer approximation given by Eq. (10.24). Although this approximation does not give the correct decision threshold level or optimum avalanche gain it is reasonably successful at predicting bit error rate as a function of signal power and hence provides realistic estimates of the number of photons required at a practical detector in order to maintain given bit error rates.

For instance, let us consider a good avalanche photodiode receiver which we assume to be quantum noise limited. Hence we ignore the shot noise contribution from the dark current within the APD as well as the thermal noise generated by the electronic amplifier. In practice this assumption holds when the multiplication factor M is chosen to be sufficiently high to ensure that the SNR is determined by photon noise rather than by electronic amplifier noise, and the APD used has a low dark current. To determine the SNR for this ideal APD receiver it is useful to define the quantum noise on the primary photocurrent I_p within the device in terms of shot noise following Eq. (9.8). Therefore, the mean square shot noise current is given by:

$$\overline{i_s^2} = 2eBI_pM^2 \tag{10.27}$$

where e is the electronic charge and B is the post detection or effective noise bandwidth. It may be observed that the mean square shot noise current $\overline{i_s^2}$ given in Eq. (10.27) is increased by a factor M^2 due to avalanche gain in the APD. However, Eq. (10.27) does not give the total noise current at the output of the APD as there is an additional noise contribution from the random gain mechanism. The excess avalanche noise factor incurred $F(M)$ was discussed in

Section 9.3.4 and defined by Eqs. (9.27) and (9.28). Equation (9.27) may be simplified [Ref. 50] to give an expression for electron injection in the low frequency limit of:

$$F(M) = kM + \left(2 - \frac{1}{M}\right)(1-k) \tag{10.28}$$

where k is the ratio of the carrier ionization rates. Hence the excess avalanche noise factor may be combined into Eq. (10.27) to give a total mean square shot noise current $\overline{i_n^2}$

$$\overline{i_n^2} = 2eBI_pM^2F(M) \tag{10.29}$$

Furthermore, the avalanche multiplication mechanism raises the signal current to MI_p and therefore the SNR in terms of the peak signal power to rms noise power may be written as:

$$\frac{S}{N} = \frac{(MI_p)^2}{2eBI_pM^2F(M)} = \frac{I_p}{2eBF(M)} \tag{10.30}$$

Now, if we let z_{md} correspond to the average number of photons detected in a time period of duration τ,

$$I_p = \frac{z_{md}e}{\tau} = \frac{z_m e\eta}{\tau} \tag{10.31}$$

where z_m is the average number of photons incident on the APD and η is the quantum efficiency of the device. Substituting for I_p in Eq. (10.30) we have:

$$\frac{S}{N} = \frac{z_m\eta}{2B\tau F(M)} \tag{10.32}$$

Rearranging Eq. (10.32) gives an expression for the average number of photons required within the signalling interval τ to detect a binary one in terms of the received SNR for the good APD receiver as:

$$z_m = \frac{2B\tau F(M)}{\eta}\left(\frac{S}{N}\right) \tag{10.33}$$

A reasonable pulse shape obtained at the receiver in order to reduce intersymbol interference has the raised cosine spectrum shown in Fig. 10.37. The raised cosine spectrum for the received pulse gives a pulse response resulting in a binary pulse train passing through either full or zero amplitude at the centers of the pulse intervals and with transitions passing through half amplitude at points which are midway in time between pulse centers. For raised cosine pulse shaping the full τ signalling $B\tau$ is around 0.6. Hence the

Ex. 1017.68

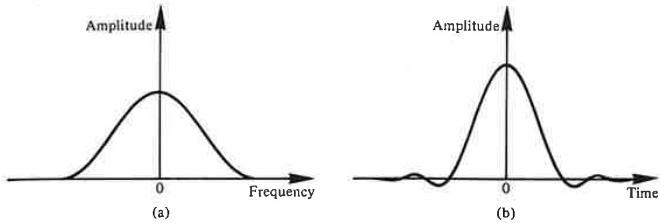

Fig. 10.37 (a) Raised cosine spectrum. (b) Output of a system with a raised cosine output spectrum for a single input pulse.

average number of photons required to detect a binary one using a good APD receiver at a specified BER may be estimated using Eq. (10.33) in conjunction with Eq. (10.24).

Example 10.3

A good APD is used as a detector in an optical fiber PCM receiver designed for baseband binary transmission with a decision threshold set midway between the zero and one signal levels. The APD has a quantum efficiency of 80%, a ratio of carrier ionization rates of 0.02 and is operated with a multiplication factor of 100. Assuming a raised cosine signal spectrum at the receiver, estimate the average number of photons which must be incident on the APD to register a binary one with a BER of 10^{-9}.

Solution: The electrical SNR required to obtain a BER of 10^{-9} at the receiver is given by the curve shown in Fig. 10.36(b), or the solution to example 10.2 as 21.6 dB or 144. Also the excess avalanche noise factor $F(M)$ may be determined using Eq. (10.28) where,

$$F(M) = kM + \left(2 - \frac{1}{M}\right)(1 - k)$$

$$= 2 + (2 - 0.01)(1 - 0.02)$$

$$= 3.95 \simeq 4$$

The average number of photons which must be incident at the receiver in order to maintain the BER can be estimated using Eq. (10.33) (assuming $B\tau = 0.6$ for the raised cosine pulse spectrum) as:

$$z_m = \frac{2B\tau F(M)}{\eta}\left(\frac{S}{N}\right)$$

$$= \frac{2 \times 0.6 \times 4 \times 144}{0.8}$$

$$= 864 \text{ photons}$$

The estimate in example 10.3 gives a more realistic value for the average number of incident photons required at a good APD receiver in order to register a binary one with a BER of 10^{-9} than the quantum limit of 21 photons determined for an ideal photodetector in example 9.1. However, it must be emphasized that the estimate in example 10.3 applies to a good silicon APD receiver (with high sensitivity and low dark current) which is quantum noise limited, and that no account has been taken of the effects of either dark current within the APD or thermal noise generated within the preamplifier. It is therefore likely that at least 1000 incident photons are required at a good APD receiver to register a binary one and provide a BER of 10^{-9} [Ref. 51]. Nevertheless somewhat lower values may be achieved by setting the decision threshold below the half amplitude level because the shot noise on the zero level is lower than the shot noise on the one level.

The optical power required at the receiver P_o is simply the optical energy divided by the time interval over which it is incident. The optical energy E_o may be obtained directly from the average number of photons required at the receiver in order to maintain a particular BER following:

$$E_o = z_m hf \tag{10.34}$$

where hf is the energy associated with a single photon which is given by Eq. (6.1). In order that a binary one is registered at the receiver, the optical energy E_o must be incident over the bit interval τ. For system calculations we can assume a zero disparity code which has an equal density of ones and zeros. In this case the optical power required to register a binary one may be considered to be incident over two bit intervals giving:

$$P_o = \frac{E_o}{2\tau} \tag{10.35}$$

Substituting for E_o from Eq. (10.34) we obtain:

$$P_o = \frac{z_m hf}{2\tau} \tag{10.36}$$

Also as the bit rate B_T for the channel is the reciprocal of the bit interval τ, Eq. (10.36) may be written as:

$$P_o = \frac{z_m hf B_T}{2} \tag{10.37}$$

Equation (10.37) allows estimates of the incident optical power required at a good APD receiver in order to maintain a particular BER, based on the average number of incident photons. In system calculations these optical power levels are usually expressed in dBm. It may also be observed that the required incident optical power is directly proportional to the bit rate B_T which typifies a shot noise limited receiver.

Ex. 1017.70

Example 10.4

The receiver of example 10.3 operates at a wavelength of 1 μm. Assuming a zero disparity binary code, estimate the incident optical power required at the receiver to register a binary one with a BER of 10^{-9} at bit rates of 10 Mbit s^{-1} and 140 Mbit s^{-1}.

Solution: Under the above conditions, the required incident optical power may be obtained using Eq. (10.37) where,

$$P_o = \frac{z_m h f B_T}{2} = \frac{z_m h c B_T}{2\lambda}$$

At 10 Mbit s^{-1},

$$P_o = \frac{864 \times 6.626 \times 10^{-34} \times 2.998 \times 10^8 \times 10^7}{2 \times 1 \times 10^{-6}}$$

$$= 858.2 \text{ pW}$$

$$= -60.7 \text{ dBm}$$

At 140 Mbit s^{-1},

$$P_o = \frac{864 \times 6.626 \times 10^{-34} \times 2.998 \times 10^8 \times 14 \times 10^7}{2 \times 1 \times 10^{-14}}$$

$$= 12.015 \text{ nW}$$

$$= -49.2 \text{ dBm}$$

Example 10.4 illustrates the effect of direct proportionality between the optical power required at the receiver and the system bit rate. In the case considered, the required incident optical power at the receiver to give a BER of 10^{-9} must be increased by around 11.5 dB (factor of 14) when the bit rate is increased from 10 to 140 Mbit s^{-1}. Also comparison with example 9.1 where a similar calculation was performed for an ideal photodetector operating at 10 Mbit s^{-1} emphasizes the necessity of performing the estimate for a practical photodiode. The good APD receiver considered in example 10.4 exhibits around 16 dB less sensitivity than the ideal photodetector (i.e. quantum limit).

The assumptions made in the evaluation of examples 10.3 and 10.4 are not generally valid when considering *p–i–n* photodiode receivers because these devices are seldom quantum noise limited due to the absence of internal gain within the photodetector. In this case thermal noise generated within the electronic amplifier is usually the dominating noise contribution and is typically 1×10^3 to 3×10^3 times larger than the peak response produced by the displacement current of a single electron–hole pair liberated in the detector. Hence, for reliable performance with a BER of 10^{-9}, between 1 and 3×10^4 photons must be detected when a binary one is incident on the receiver [Ref. 53].

This translates into sensitivities which are about 30 dB or more, less than

the quantum limit. Finally for a thermal noise limited receiver the input optical power is proportional to the square root of both the post detection or effective noise bandwidth and the SNR (i.e. $P_o \propto [(S/N)B]^{\frac{1}{2}}$). However, this result is best obtained from purely analog SNR considerations and therefore is dealt with in Section 10.7.1.

10.6.4 Channel Losses

Another important factor when estimating the permissible separation between regenerative repeaters or the overall link length is the total loss encountered between the transmitter(s) and receiver(s) within the system. Assuming there are no dispersion penalties on the link, the total channel loss may be obtained by simply summing in decibels the installed fiber cable loss, the fiber–fiber jointing losses and the coupling losses of the optical source and detector. The fiber cable loss in decibels per kilometer α_{fc} is normally specified by the manufacturer, or alternatively it may be obtained by measurement (see Sections 5.2 and 5.7). It must be noted that the cabled fiber loss is likely to be greater than the uncabled fiber loss usually measured in the laboratory due to possible microbending of the fiber within the cabling process (see Section 4.6.2).

Loss due to joints (generally splices) on the link may also, for simplicity, be specified in terms of an equivalent loss in decibels per kilometer α_j. In fact, it is more realistic to regard α_j as a distributed loss since the optical attenuation resulting from the disturbed mode distribution at a joint does not only occur in the vicinity of the joint. Finally the loss contribution attributed to the connectors α_{cr} (in decibels) used for coupling the optical source and detector to the fiber must be included in the overall channel loss. Hence the total channel loss C_L (in decibels) may be written as:

$$C_L = (\alpha_{fc} + \alpha_j)L + \alpha_{cr} \tag{10.38}$$

where L is the length of the fiber cable either between regenerative repeaters or between the transmit and receive terminals for a link without repeaters.

Example 10.5

An optical fiber link of length 4 km comprises a fiber cable with an attenuation of 5 dB km^{-1}. The splice losses for the link are estimated at 2 dB km^{-1}, and the connector losses at the source and detector are 3.5 and 2.5 dB respectively. Ignoring the effects of dispersion on the link determine the total channel loss.

Solution: The total channel loss may be simply obtained using Eq. (10.38) where:

$$\begin{aligned} C_L &= (\alpha_{fc} + \alpha_j)L + \alpha_{cr} \\ &= (5 + 2)4 + 3.5 + 2.5 \\ &= 34 \text{ dB} \end{aligned}$$

10.6.5 Temporal Response

The system design considerations must also take into account the temporal response of the system components. This is especially the case with regard to pulse dispersion on the optical fiber channel. The formula given in Eq. (10.38) allows determination of the overall channel loss in the absence of any pulse broadening due to the dispersion mechanisms within the transmission medium. However, the finite bandwidth of the optical system may result in overlapping of the received pulses or intersymbol interference, giving a reduction in sensitivity at the optical receiver. Therefore either a worse BER must be tolerated, or the ISI must be compensated by equalization within the receiver (see Section 10.3.3). The latter necessitates an increase in optical power at the receiver which may be considered as an additional loss penalty. This additional loss contribution is usually called the dispersion–equalization or ISI penalty. The dispersion–equalization penalty D_L becomes especially significant in high bit rate multimode fiber systems and has been determined analytically for Gaussian shaped pulses [Ref. 48]. In this case it is given by:

$$D_L = 2\left(\frac{\tau_e}{\tau}\right)^4 \text{ dB} \tag{10.39}$$

where τ_e is the $1/e$ full width pulse broadening due to dispersion on the link and τ is the bit interval or period. For Gaussian shaped pulses, τ_e may be written in terms of the rms pulse width σ as (see Appendix F):

$$\tau_e = 2\sigma\sqrt{2} \tag{10.40}$$

Hence, substituting into Eq. (10.39) for τ_e, and writing the bit rate B_T as the reciprocal of the bit interval τ gives:

$$D_L = 2(2\sigma B_T\sqrt{2})^4 \text{ dB} \tag{10.41}$$

Since the dispersion–equalization penalty as defined by Eq. (10.41) is measured in decibels, it may be included in the formula for the overall channel loss given by Eq. (10.38). Therefore the total channel loss including the dispersion–equalization penalty C_{LD} is given by:

$$C_{LD} = (\alpha_{fc} + \alpha_j)L + \alpha_{cr} + D_L \text{ dB} \tag{10.42}$$

The dispersion–equalization penalty is usually only significant in wideband multimode fiber systems which exhibit intermodal as well as intramodal dispersion. Single mode fiber systems which are increasingly being utilized for wideband long-haul applications are not generally limited by pulse broadening on the channel because of the absence of intermodal dispersion. However, it is often the case that intermodal dispersion is the dominant mechanism within multimode fibers. In Section 3.9.1 intermodal pulse broadening was considered to be a linear function of the fiber length L. Furthermore it was indicated that the presence of mode coupling within the fiber made the pulse broadening

increase at a slower rate proportional to $L^{\frac{1}{2}}$. Hence it is useful to consider the dispersion–equalization penalty in relation to fibers without and with mode coupling operating at various bit rates.

Example 10.6

The rms pulse broadening resulting from intermodal dispersion within a multimode optical fiber is 0.6 ns km^{-1}. Assuming this to be the dominant dispersion mechanism, estimate the dispersion–equalization penalty over an unrepeatered fiber link of length 8 km at bit rates of (a) 25 Mbit s^{-1} and (b) 150 Mbit s^{-1}. In both cases evaluate the penalty without and with mode coupling. The pulses may be assumed to have a Gaussian shape.

Solution: (a) *Without mode coupling.* The total rms pulse broadening over 8 km is given by:

$$\sigma_T = \sigma \times L = 0.6 \times 8 = 4.8 \text{ ns}$$

The dispersion–equalization penalty is given by Eq. (10.41) where:

$$D_L = 2(2\sigma_T B_T \sqrt{2})^4 = 2(2 \times 4.8 \times 10^{-9} \times 25 \times 10^6 \sqrt{2})^4$$
$$= 0.03 \text{ dB}$$

With mode coupling. The total rms pulse broadening is:

$$\sigma_T \simeq \sigma\sqrt{L} = 0.6 \times \sqrt{8} = 1.7 \text{ ns}$$

Hence the dispersion–equalization penalty is:

$$D_L = 2(2 \times 1.7 \times 10^{-9} \times 25 \times 10^6 \sqrt{2})^4$$
$$= 4.2 \times 10^{-4} \text{ dB (i.e. negligible)}$$

(b) *Without mode coupling.*

$$\sigma_T = 4.8 \text{ ns}$$
$$D_L = 2(2 \times 4.8 \times 10^{-9} \times 150 \times 10^6 \sqrt{2})^4 = 34.38 \text{ dB}$$

With mode coupling.

$$\sigma_T = 1.7 \text{ ns}$$
$$D_L = 2(2 \times 1.7 = 10^{-9} \times 150 \times 10^6 \sqrt{2})^4 = 0.54 \text{ dB}$$

Example 10.6(a) demonstrates that at low bit rates the dispersion–equalization penalty is very small if not negligible. In this case the slight advantage of the effect of mode coupling on the penalty is generally outweighed by increased attenuation on the link because of the mode coupling, which may be of the order of 1 dB km^{-1}. Example 10.6(b) indicates that at higher bit rates with no mode coupling the dispersion–equalization penalty dominates to the extent that it would be necessary to reduce the repeater spacing to between 4 and 5 km. However, it may be observed that encouragement of mode coupling on the link greatly reduces this penalty and outweighs any additional attenuation incurred through mode coupling within the fiber. In summary, it is clear

that the dispersion–equalization penalty need only be applied when considering wideband systems. Moreover it is frequently the case that lower bit rate systems may be up-graded at a later date to a higher capacity without incurring a penalty which might necessitate a reduction in repeater spacing.

An alternative approach involving the calculation of the system rise time can be employed to determine the possible limitation on the system bandwidth resulting from the temporal response of the system components. Therefore, if there is not a pressing need to obtain the maximum possible bit rate over the maximum possible distance, it is sufficient within the system design to establish that the total temporal response of the system is adequate for the desired system bandwidth. Nevertheless this approach does allow for a certain amount of optimization of the system components, but at the exclusion of considerations regarding equalization and the associated penalty.

The total system rise time may be determined from the rise times of the individual system components which include the source (or transmitter), the fiber cable, and the detector (or receiver). These times are defined in terms of a Gaussian response as the 10–90% rise (or fall) times of the individual components. The fiber cable 10–90% rise time may be separated into rise times arising from intermodal T_n and intramodal or chromatic dispersion T_c. The total system rise time is given by [Ref. 56]:

$$T_{syst} = 1.1(T_S^2 + T_n^2 + T_c^2 + T_D^2)^{\frac{1}{2}} \tag{10.43}$$

where T_S and T_D are the source and detector 10–90% rise times respectively, and all the rise times are measured in nanoseconds. Comparison of the rise time edge with the overall pulse dispersion results in the weighting factor of 1.1.

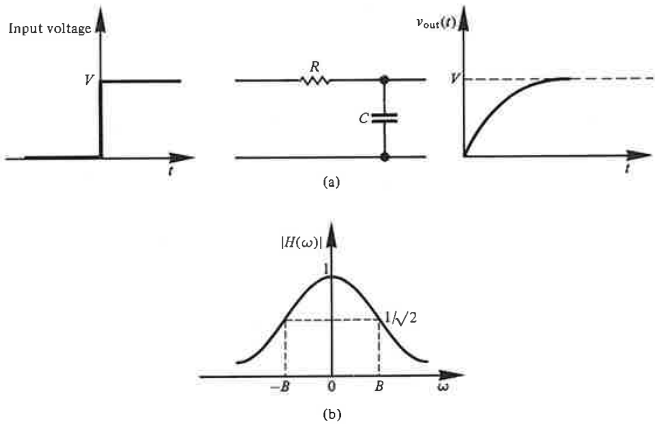

Fig. 10.38 (a) The response of a low pass RC filter circuit to a voltage step input. (b) The transfer function $H(\omega)$ for the circuit in (a).

The maximum system bit rate $B_T(\max)$ is usually defined in terms of T_{syst} by consideration of the rise time of the simple RC filter circuit shown in Fig. 10.38(a). For a voltage step input of amplitude V, the output voltage waveform $v_{out}(t)$ as a function of time t is:

$$v_{out}(t) = V(1 - e^{-t/RC}) \tag{10.44}$$

Hence the 10–90% rise time t_r for the circuit is given by:

$$t_r = \frac{2.2}{RC} \tag{10.45}$$

The transfer function for this circuit is shown in Fig. 10.38(b) and is given by:

$$|H(\omega)| = \frac{1}{(1 + \omega^2 C^2 R^2)^{\frac{1}{2}}} \tag{10.46}$$

Therefore the 3 dB bandwidth for the circuit is

$$B = \frac{1}{2\pi RC} \tag{10.47}$$

Combining Eqs. (10.45) and (10.47) gives,

$$t_r = \frac{2.2}{2\pi B} = \frac{0.35}{B} \tag{10.48}$$

The result for the 10–90% rise time indicated in Eq. (10.48) is of general validity, but a different constant term may be obtained with different filter circuits. However, for rise time calculations involving optical fiber systems the constant 0.35 is often utilized and hence in Eq. (10.48), $t_r = T_{syst}$. Alternatively, if an ideal (unrealizable) filter with an arbitrarily sharp cutoff is considered, the constant in Eq. (10.48) becomes 0.44. However, although this value for the constant is frequently employed when calculating the optical bandwidth of fiber from pulse dispersion measurements (see Section 5.3.1), the more conservative estimate obtained using a constant term of 0.35 is generally favored for use in system rise time calculations [Refs. 56 and 57]. Also, in both cases it is usually accepted [Ref. 43] that to conserve the shape of a pulse with a reasonable fidelity through the RC circuit then the 3 dB bandwidth must be at least large enough to satisfy the condition $B\tau = 1$, where τ is the pulse duration. Combining this relation with Eq. (10.48) gives:

$$T_{syst} = t_r = 0.35\tau \tag{10.49}$$

For an RZ pulse format, the bit rate $B_T = B = 1/\tau$ (see Section 3.7) and hence substituting into Eq. (10.49) gives:

$$B_T(\max) = \frac{0.35}{T_{\text{syst}}} \tag{10.50}$$

Alternatively for an NRZ pulse format $B_T = B/2 = 1/2\tau$ and therefore the maximum bit rate is given by:

$$B_T(\max) = \frac{0.7}{T_{\text{syst}}} \tag{10.51}$$

Thus the upper limit on T_{syst} should be less than 35% of the bit interval for an RZ pulse format and less than 70% of the bit interval for an NRZ pulse format.

The effects of mode coupling are usually neglected in calculations involving system rise time, and hence the pulse dispersion is assumed to be a linear function of the fiber length. This results in a pessimistic estimate for the system rise time and therefore provides a conservative value for the maximum possible bit rate.

Example 10.7

An optical fiber system is to be designed to operate over an 8 km length without repeaters. The rise times of the chosen components are:

Source (LED)	8 ns
Fiber: intermodal	5 ns km^{-1}
(pulse broadening) intramodal	1 ns km^{-1}
Detector (*p–i–n* photodiode)	6 ns

From system rise time considerations, estimate the maximum bit rate that may be achieved on the link when using an NRZ format.

Solution: The total system rise time is given by Eq. (10.43) as:

$$\begin{aligned} T_{\text{syst}} &= 1.1(T_S^2 + T_n^2 + T_c^2 + T_D^2)^{\frac{1}{2}} \\ &= 1.1(8^2 + (8 \times 5)^2 + (8 \times 1)^2 + 6^2)^{\frac{1}{2}} \\ &= 46.2 \text{ ns} \end{aligned}$$

Hence the maximum bit rate for the link using an NRZ format is given by Eq. (10.51) where:

$$B_T(\max) = \frac{0.7}{T_{\text{syst}}} = \frac{0.7}{46.2 \times 10^{-9}} \simeq 15.2 \text{ Mbit s}^{-1}$$

The rise time calculations indicate that the link will support a maximum bit rate of 15.2 Mbit s^{-1} which for an NRZ format is equivalent to a 3 dB optical bandwidth of 7.6 MHz (i.e. the NRZ format has two bit intervals per wavelength).

Once it is established that pulse dispersion is not a limiting factor, the major design exercise is the optical power budget for the system.

10.6.6 Optical Power Budgeting

Power budgeting for a digital optical fiber communication system is performed in a similar way to power budgeting within any communication system. When the transmitter characteristics, fiber cable losses and receiver sensitivity are known, the relatively simple process of power budgeting allows the repeater spacing or the maximum transmission distance for the system to be evaluated. However, it is necessary to incorporate a system margin into the optical power budget so that small variations in the system operating parameters do not lead to an unacceptable decrease in system performance. The operating margin is often included in a safety margin M_a which also takes into account possible source and modal noise together with receiver impairments such as equalization error, noise degradations and eye opening impairments. The safety margin depends to a large extent on the system components as well as the system design procedure and is typically in the range 5–10 dB. Systems using an injection laser transmitter generally require a larger safety margin (e.g. 9 dB) than those using an LED source (e.g. 7 dB) because the temperature variation and ageing of the LED are less pronounced.

The optical power budget for a system is given by the following expression:

$$P_i = P_o + C_L + M_a \text{ dB} \tag{10.52}$$

where P_i is the mean input optical power launched into the fiber, P_o is the mean incident optical power required at the receiver and C_L (or C_{LD} when there is a dispersion–equalization penalty) is the total channel loss given by Eq. (10.38) (or Eq. (10.42)). Therefore the expression given in Eq. (10.52) may be written as:

$$P_i = P_o + (\alpha_{fc} + \alpha_j)L + \alpha_{cr} + M_a \text{ dB} \tag{10.53}$$

Alternatively, when a dispersion–equalization penalty is included Eq. (10.52) becomes:

$$P_i = P_o + (\alpha_{fc} + \alpha_j)L + \alpha_{cr} + D_L + M_a \text{ dB} \tag{10.54}$$

Equations (10.53) and (10.54) allow the maximum link length without repeaters to be determined, as demonstrated in example 10.8.

Example 10.8

The following parameters are established for a long-haul single mode optical fiber system operating at a wavelength of 0.85 μm.

Mean power launched from the laser transmitter	−3 dBm
Cabled fiber loss	1.9 dB km^{-1}
Splice loss	0.3 dB km^{-1}
Connector losses at the transmitter and receiver	1 dB each
Mean power required at the APD receiver:	
when operating at 35 Mbit s^{-1} (BER 10^{-1})	−55 dBm
when operating at 500 Mbit s^{-1} (BER 10^{-9})	−44 dBm
Required safety margin	9 dB

Estimate:

(a) the maximum possible link length without repeaters when operating at 35 Mbit s^{-1} (BER 10^{-9}). It may be assumed that there is no dispersion–equalization penalty at this bit rate.
(b) the maximum possible link length without repeaters when operating at 500 Mbit s^{-1} (BER 10^{-9}) and assuming no dispersion–equalization penalty.
(c) the reduction in the maximum possible link length without repeaters of (b) when there is a dispersion–equalization penalty of 5 dB. It may be assumed for the purposes of this estimate that the reduced link length has the 5 dB penalty.

Solution: (a) When the system is operating at 35 Mbit s^{-1} an optical power budget may be performed using Eq. (10.53), where

$$P_i - P_o = (\alpha_{fc} + \alpha_j)L + \alpha_{cr} + M_a \text{ dB}$$

$$-3 \text{ dBm} - (-55 \text{ dBm}) = (\alpha_{fc} + \alpha_j)L + \alpha_{cr} + M_a$$

Hence,

$$(\alpha_{fc} + \alpha_j)L = 52 - \alpha_{cr} - M$$

$$2.1L = 52 - 2 - 9$$

$$L = \frac{41}{2.1} = 19.5 \text{ km}$$

(b) Again using Eq. (10.53) when the system is operating at 500 Mbit s^{-1}:

$$-3 \text{ dBm} - (-44 \text{ dBm}) = (\alpha_{fc} + \alpha_j)L + \alpha_{cr} + M$$

$$(\alpha_{fc} + \alpha_j)L = 41 - 2 - 9$$

$$L = \frac{30}{2.1} = 14.3 \text{ km}$$

(c) Performing the optical power budget using Eq. (10.54) gives:

$$P_i - P_o = (\alpha_{fc} + \alpha_j)L + \alpha_{cr} + D_L + M_a$$

Hence,

$$2.1L = 41 - 2 - 5 - 9$$

and

$$L = \frac{25}{2.1} = 11.9 \text{ km}$$

Thus there is a reduction of 2.4 km in the maximum possible link length without repeaters.

Although we have demonstrated in example 10.8 the use of the optical power budget to determine the maximum link length without repeaters, it is also frequently used to aid decisions with relation to the combination of components required for a particular optical fiber communication system. In this case the maximum transmission distance and the required bandwidth may already be known. Therefore the optical power budget is used to provide a

basis for optimization in the choice of the system components, whilst also establishing that a particular component configuration meets the system requirements.

Example 10.9

Components are chosen for a digital optical fiber link of overall length 7 km and operating at a 20 Mbit s^{-1} using an RZ code. It is decided that an LED emitting at 0.85 μm with graded index fiber to a *p–i–n* photodiode is a suitable choice for the system components, giving no dispersion–equalization penalty. An LED which is capable of launching an average of 100 μW of optical power (including the connector loss) into a 50 μm core diameter graded index fiber is chosen. The proposed fiber cable has an attenuation of 2.6 dB km^{-1} and requires splicing every kilometer with a loss of 0.5 dB per splice. There is also a connector loss at the receiver of 1.5 dB. The receiver requires mean incident optical power of −41 dBm in order to give the necessary BER of 10^{-10}, and it is predicted that a safety margin of 6 dB will be required.

Write down the optical power budget for the system and hence determine its viability.

Solution:

Mean optical power launched into the fiber from the transmitter (100 mW)	−10 dBm
Receiver sensitivity at 20 Mbit s^{-1} (BER 10^{-10})	−41 dBm
Total system margin	31 dB
Cabled fiber loss (7 × 2.6 dB km^{-1})	18.2 dB
Splice losses (6 × 0.5 dB)	3.0 dB
Connector loss (1 × 1.5 dB)	1.5 dB
Safety margin	6.0 dB
Total system loss	28.7 dB
Excess power margin	2.3 dB

Based on the figures given the system is viable and provides a 2.3 dB excess power margin. This could give an extra safety margin to allow for possible future splices if these were not taken into account within the original safety margin.

10.6.7 Line Coding

The previous discussions of digital system design have assumed that only information bits are transmitted, and that the 0 and 1 symbols are equally likely. However, within digital line transmission there is a requirement for redundancy in the line coding to provide efficient timing recovery and synchronization (frame alignment) as well as possible error detection and correction at the receiver. Line coding also provides suitable shaping of the transmitted signal power spectral density. Hence the choice of line code is an important consideration within digital optical fiber system design.

Binary line codes are generally preferred because of the large bandwidth available in optical fiber communications. In addition these codes are less

susceptible to any temperature dependence of optical sources and detectors. Under these conditions two level codes are more suitable than codes which utilize an increased number of levels (multilevel codes). Nevertheless, these factors do not entirely exclude the use of multilevel codes, and it is likely that ternary codes (three levels 0, $\frac{1}{2}$, 1) which give increased information transmission per symbol over binary codes will be considered for some system applications. The corresponding symbol transmission rate (i.e. bit rate) for a ternary code may be reduced by a factor of 1.58 ($\log_2 3$) whilst still providing the same information transmission rate as a similar system using a binary code. It must be noted that this gain in information capacity for a particular bit rate is obtained at the expense of the dynamic range between adjacent levels as there are three levels inserted in place of two. This is exhibited as a 3 dB SNR penalty at the receiver when compared with a binary system at a given BER. Therefore ternary codes (and higher multilevel codes) are not attractive for long-haul systems.

For the reasons described above most digital optical fiber communication systems currently in use employ binary codes. In practice, binary codes are designed which insert extra symbols into the information data stream on a regular and logical basis to minimize the number of consecutive identical received symbols, and to facilitate efficient timing extraction at the receiver by producing a high density of decision level crossings. The reduction in consecutive identical symbols also helps to minimize the variation in the mean signal level which provides a reduction in the low frequency response requirement of the receiver. This shapes the transmitted signal spectrum by reducing the d.c. component. However, this factor is less important for optical fiber systems where a.c. coupling is performed with capacitors unlike metallic cable systems where transformers are often used, and the avoidance of d.c. components is critical. A further advantage is apparent within the optical receiver with a line code which is free from long identical symbol sequences, and where the continuous presence of 0 and 1 levels aids decision level control and avoids gain instability effects.

Two level block codes of the *nBmB* type fulfil the above requirements through the addition of a limited amount of redundancy. These codes convert blocks of n bits into blocks of m bits where $m > n$ so that the difference between the number of transmitted ones and zeros is on average zero. A simple code of this type is the $1B2B$ code in which a 0 may be transmitted as 01, and a 1 as 10. This encoding format is shown in Fig. 10.39(b) and is commonly referred to as biphase or Manchester encoding. It may be observed that with this code there are never more than two consecutive identical symbols, and that two symbols must be transmitted for one information bit, giving 50% redundancy. Thus twice the transmission bandwidth is required for the $1B2B$ code which restricts its use to systems where pulse dispersion is not a limiting factor. Another example of a $1B2B$ code which is illustrated in Fig. 10.39(c) is the coded mark inversion (CMI) code. In this code a digit 0 is transmitted as 01 and the digit 1 alternately as 00 or 11.

Ex. 1017.81

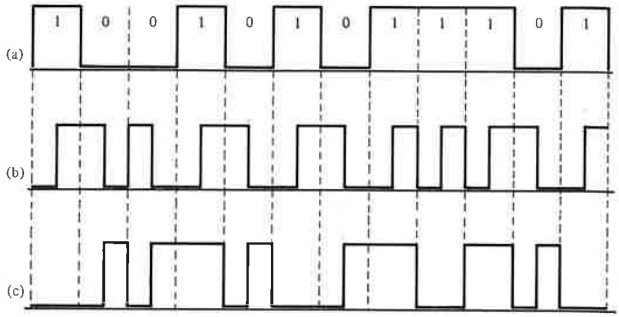

Fig. 10.39 Examples of binary 1*B*2*B* codes used in optical fiber communications: (a) unencoded NRZ data; (b) biphase or Manchester encoding; (c) coded mark inversion (CMI) encoding.

Timing information is obtained from the frequent positive to negative transitions, but once again the code is highly redundant requiring twice as many transmitted bits as input information bits.

More efficient codes of this type requiring less redundancy exist such as the 3*B*4*B*, 5*B*6*B* and the 7*B*8*B* codes. There is a trade-off within this class of code between the complexity of balancing the number of zeros and ones, and the added redundancy. The increase in line symbol rate (bit rate) and the corresponding power penalty over uncoded binary transmission is given by the ratio $m:n$. Hence, considering the widely favored 5*B*6*B* code, the symbol rate is increased by a factor of 1.2 whilst the power penalty is also equal to 1.2 or about 0.8 dB. It is therefore necessary to take into account the increased bandwidth requirement and the power penalty resulting from coding within the optical fiber system design.

Simple error monitoring may be provided with block codes, at the expense of a small amount of additional redundancy, by parity checking. Each block of N bits can be made to have an even (even parity) or odd (odd parity) number of ones so that any single error in a block can be identified. More extensive error detection and error correction may be provided with increased redundancy and equipment complexity. This is generally not considered worthwhile unless it is essential that the digital transmission system is totally secure (e.g. data transmission applications). Alternatively, error monitoring when using block codes may be performed by measuring the variation in disparity between the numbers of ones and zeros within the received bit pattern. Any variation in the accumulated disparity above an upper limit or below a lower limit allowed by a particular code is indicated as an error. Further discussion of error correction with relation to disparity may be found in Ref. 65.

Ex. 1017.82

10.7 ANALOG SYSTEMS

In Section 10.5 we indicated that the vast majority of optical fiber communication systems are designed to convey digital information (e.g. analog speech encoded as PCM). However, in certain areas of the telecommunication network or for particular applications, information transfer in analog form is still likely to remain for some time to come, or be advantageous. Therefore, analog optical fiber transmission will undoubtedly have a part to play in future communication networks, especially in situations where the optical fiber link is part of a larger analog network (e.g. microwave relay network). Use of analog transmission in these areas avoids the cost and complexity of digital terminal equipment, as well as degradation due to quantization noise. This is especially the case with the transmission of video signals over short distances where the cost of high speed analog to digital (A–D) and D–A converters is not generally justified. Hence, there are many applications such as direct cable television and common antenna television (CATV) where analog optical fiber systems may be utilized.

There are limitations, however, inherent to analog optical fiber transmission, some of which have been mentioned previously. For instance, the unique requirements of analog transmission over digital are for high signal to noise ratios at the receiver output which necessitates high optical input power (see Section 9.2.5), and high end to end linearity to avoid distortion and prevent cross talk between different channels of a multiplexed signal (see Section 10.4.2). Furthermore, it is instructive to compare the SNR constraints for typical analog optical fiber and coaxial cable systems.

In a coaxial cable system the fundamental limiting noise is $4KTB$, where K is Boltzmann's constant, T is the absolute temperature, and B is the effective noise bandwidth for the channel. If we assume for simplicity that the coaxial cable loss is constant and independent of frequency, the SNR for a coaxial system is

$$\left(\frac{\mathrm{S}}{\mathrm{N}}\right)_{\mathrm{coax}} = \frac{V^2 \exp(-\alpha_{\mathrm{N}})}{Z_0 4KTB} \tag{10.55}$$

where α_{N} is the attenuation in nepers between the transmitter and receiver, V is the peak output voltage, and Z_0 is the impedance of the coaxial cable.

The SNR for an analog optical fiber system may be obtained by referring to Eq. (9.11) where

$$\left(\frac{\mathrm{S}}{\mathrm{N}}\right)_{\mathrm{fiber}} = \frac{\eta P_0}{2hfB} \tag{10.56}$$

The expression given in Eq. (10.56) includes the fundamental limiting noise for

optical fiber systems which is $2hfB$. Although Eq. (10.56) is sufficiently accurate for the purpose of comparison it applies to an unmodulated optical carrier. A more accurate expression would take into account the depth of modulation for the analog optical fiber system which cannot be unity [Ref. 53].* The average received optical power P_o may be expressed in terms of the average input (transmitted) optical power P_i as

$$P_o = P_i \exp(-\alpha_N) \tag{10.57}$$

Substituting for P_o into Eq. (10.56) gives

$$\left(\frac{S}{N}\right)_{fiber} = \frac{P_i \exp(-\alpha_N)}{2hfB} \tag{10.58}$$

Equations (10.55) and (10.58) allow a simple comparison to be made of available SNR (or CNR) between analog coaxial and optical fiber systems as demonstrated in example 10.10.

Example 10.10

A coaxial cable system operating at a temperature of 17 °C has a transmitter peak output voltage of 5 V with a cable impedance of 100 Ω. An analog optical fiber system uses an injection laser source emitting at 0.85 μm and launches an average of 1 mW of optical power into the fiber cable. The optical receiver comprises a photodiode with a quantum efficiency of 70%. Assuming the effective noise bandwidth and the attenuation between the transmitter and receiver for the two systems is identical, estimate in decibels the ratio of the SNR of the coaxial system to the SNR of the fiber system.

Solution: Using Eqs. (10.55) and (10.58) for the SNRs of the coaxial and fiber systems respectively:

$$\text{Ratio} = \frac{\left(\frac{S}{N}\right)_{coax}}{\left(\frac{S}{N}\right)_{fiber}} = \frac{\dfrac{V^2 \exp(-\alpha_N)}{Z_0 4KTB}}{\dfrac{\eta P_i \exp(-\alpha_N)}{2hfB}} = \frac{V^2 hf}{2KTZ_0 \eta P_i}$$

$$= \frac{V^2 hc}{2KTZ_0 \eta P_i \lambda}$$

Hence,

$$\text{Ratio} = \frac{25 \times 6.626 \times 10^{-34} \times 2.998 \times 10^8}{2 \times 1.385 \times 10^{-23} \times 290 \times 100 \times 0.7 \times 1 \times 10^{-3} \times 0.85 \times 10^{-6}}$$

$$= 1.04 \times 10^4 \simeq 40 \text{ dB}$$

---

* Strictly speaking Eq. (10.56) depicts the optical carrier to noise ratio (CNR).

The optical fiber channel in example 10.10 has around 40 dB less SNR available than the alternative coaxial channel exhibiting similar channel losses. This results both from $2hfB$ being larger than $4KTB$ and from the far smaller transmitted power with the optical system. Furthermore it must be noted that the comparison was made using an injection laser transmitter. If an LED transmitter with 10–20 dB less optical output power was compared, the coaxial system would display an advantage in the region 50–60 dB. For this reason it is difficult to match with fiber systems the SNR requirements of some analog coaxial links, even though the fiber cable attenuation may be substantially lower than that of the coaxial cable.

The analog signal can be transmitted within an optical fiber communication system using one of several modulation techniques. The simplest form of analog modulation for optical fiber communications is direct intensity modulation (D–IM) of the optical source. In this technique the optical output from the source is modulated simply by varying the current flowing in the device around a suitable bias or mean level in proportion to the message. Hence the information signal is transmitted directly in the baseband.

Alternatively the baseband signal can be translated onto an electrical subcarrier by means of amplitude, phase or frequency modulation using standard techniques, prior to intensity modulation of the optical source. Pulse analog techniques where a sequence of pulses are used for the carrier may also be utilized. In this case a suitable parameter such as the pulse amplitude, pulse width, pulse position or pulse frequency is electrically modulated by the baseband signal. Again the modulated electrical carrier is transmitted optically by intensity modulation of the optical source.

Direct modulation of the optical source in frequency, phase or polarization rather than by intensity requires these parameters to be well defined throughout the optical fiber system. Although there is much interest in this area (see Section 10.8) present optical component technology does not as yet completely provide for practical system implementation.

10.7.1 Direct Intensity Modulation (D–IM)

A block schematic for an analog optical fiber system which uses direct modulation of the optical source intensity with the baseband signal is shown in Fig. 10.40(a). Obviously no electrical modulation or demodulation is required with this technique, making it both inexpensive and easy to implement.

The transmitted optical power waveform as a function of time $P_{opt}(t)$, an example of which is illustrated in Fig. 10.40(b), may written as:

$$P_{opt}(t) = P_i(1 + m(t)) \tag{10.59}$$

where P_i is the average transmitted optical power (i.e. the unmodulated carrier power) and $m(t)$ is the intensity modulating signal which is proportional to the source message $a(t)$. For a cosinusoidal modulating signal:

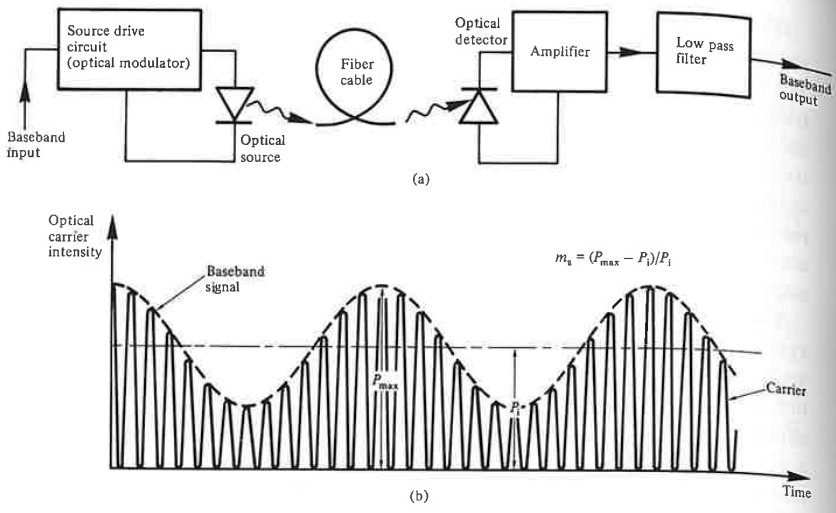

Fig. 10.40 (a) Analog optical fiber system employing direct intensity modulation. (b) Time domain representation showing direct intensity modulation of the optical carrier with a baseband analog signal.

$$m(t) = m_a \cos \omega_m t \tag{10.60}$$

where m_a is the modulation index or the ratio of the peak excursion from the average to the average power as shown in Fig. 10.40(b), and ω_m is the angular frequency of the modulating signal. Combining Eqs. (10.59) and (10.60) we get:

$$P_{opt}(t) = P_i(1 + m_a \cos \omega_m t) \tag{10.61}$$

Furthermore, assuming the transmission medium has zero dispersion, the received optical power will be of the same form as Eq. (10.61), but with an average received optical power P_o. Hence the secondary photocurrent $I(t)$ generated at an APD receiver with a multiplication factor M is given by:

$$I(t) = I_p M(1 + m_a \cos \omega_m t) \tag{10.62}$$

where the primary photocurrent obtained with an unmodulated carrier I_p is given by Eq. (8.8) as,

$$I_p = \frac{\eta e}{hf} P_o \tag{10.63}$$

The mean square signal current $\overline{i_{sig}^2}$ which is obtained from Eq. (10.62) is given by:

$$\overline{i_{\text{sig}}^2} = \tfrac{1}{2}(m_a M I_p)^2 \tag{10.64}$$

The total average noise in the system is composed of quantum, dark current, and thermal (circuit) noise components. The noise contribution from quantum effects and detector dark current may be expressed as the mean square total shot noise current for the APD receiver $\overline{i_{\text{SA}}^2}$ given by Eq. (9.21) where the excess avalanche noise factor is written following Eq. (9.26) as $F(M)$ such that:

$$\overline{i_{\text{SA}}^2} = 2eB(I_p + I_d)M^2F(M) \tag{10.65}$$

where B is the effective noise or post detection bandwidth.

Thermal noise generated by the load resistance R_L and the electronic amplifier noise can be expressed in terms of the amplifier noise figure F_n referred to R_L as given by Eq. (9.17). Thus the total mean square noise current $\overline{i_N^2}$ may be written as:

$$\overline{i_N^2} = 2eB(I_p + I_d)M^2F(M) + \frac{4KTBF_n}{R_L} \tag{10.66}$$

The SNR defined in terms of the ratio of the mean square signal current to the mean square noise current (rms signal power to rms noise power) for the APD receiver is therefore given by:

$$\left(\frac{S}{N}\right)_{\text{rms}} = \frac{\overline{i_{\text{sig}}^2}}{\overline{i_N^2}} = \frac{\tfrac{1}{2}(m_a M I_p)^2}{2eB(I_p + I_d)M^2F(M) + (4KTBF_n/R_L)} \quad \text{(APD)} \tag{10.67}$$

It must be emphasized that the SNR given in Eq. (10.67) is defined in terms of rms signal power rather than peak signal power used previously. When a unity gain photodetector is utilized in the receiver (i.e. *p–i–n* photodiode) Eq. (10.67) reduces to:

$$\left(\frac{S}{N}\right)_{\text{rms}} = \frac{\tfrac{1}{2}(m_a I_p)^2}{2eB(I_p + I_d) + (4KTBF_n/R_L)} \quad (p\text{–}i\text{–}n) \tag{10.68}$$

Moreover, the SNR for video transmission is often defined in terms of the peak to peak picture signal power to the rms noise power and may include the ratio of luminance to composite video b. Using this definition in the case of the unity gain detector gives:

$$\left(\frac{S}{N}\right)_{\text{p–p}} = \frac{(2m_a I_p b)^2}{2eB(I_p + I_d) + (4KTBF_n/R_L)} \quad (p\text{–}i\text{–}n) \tag{10.69}$$

It may be observed that, excluding b, the SNR defined in terms of the peak signal power given in Eq. (10.69) is a factor of 8 (or 9 dB) greater than that defined in Eq. (10.68).

Example 10.11

A single TV channel is transmitted over an analog optical fiber link using direct intensity modulation. The video signal which has a bandwidth of 5 MHz and a ratio of luminance to composite video of 0.7 is transmitted with a modulation index of 0.8. The receiver contains a *p–i–n* photodiode with a responsivity of 0.5 A W^{-1} and a preamplifier with an effective input impedance of 1 MΩ together with a noise figure of 1.5 dB. Assuming the receiver is operating at a temperature of 20 °C and neglecting the dark current in the photodiode, determine the average incident optical power required at the receiver (i.e. receiver sensitivity) in order to maintain a peak to peak signal power to rms noise power ratio of 55 dB.

Solution: Neglecting the photodiode dark current, the peak to peak signal power to rms noise power ratio is given following Eq. (10.69) as:

$$\left(\frac{S}{N}\right)_{p-p} = \frac{(2m_a I_p b)^2}{2eBI_p + (4KTBF_n/R_L)}$$

The photocurrent I_p may be expressed in terms of the average incident optical power at the receiver P_o using Eq. (8.4) as:

$$I_p = RP_o$$

where R is the responsivity of the photodiode. Hence,

$$\left(\frac{S}{N}\right)_{p-p} = \frac{(2m_a RP_o b)^2}{2eBRP_o + (4KTBF_n/R_L)}$$

and

$$\left(\frac{S}{N}\right)_{p-p}\left(2eBRP_o + \frac{4KTBF_n}{R_L}\right) = (2m_a RP_o b)^2$$

Rearranging,

$$(2m_a Rb)^2 P_o^2 - \left(\frac{S}{N}\right)_{p-p} 2eBRP_o - \left(\frac{S}{N}\right)_{p-p} \frac{4KTBF_n}{R_L} = 0$$

where

$$(2m_a Rb)^2 = 4 \times 0.64 \times 0.25 \times 0.49$$
$$= 0.314$$

$$\left(\frac{S}{N}\right)_{p-p} 2eBR = 3.162 \times 10^5 \times 2 \times 1.602 \times 10^{-19} \times 5 \times 10^6 \times 0.5$$
$$= 2.533 \times 10^{-7}$$

$$\left(\frac{S}{N}\right)_{p-p} \frac{4KTBF_n}{R_L} = \frac{3.162 \times 10^5 \times 4 \times 1.381 \times 10^{-23} \times 293 \times 5 \times 10^6 \times 1.413}{10^6}$$
$$= 3.616 \times 10^{-14}$$

Therefore,

$$0.314P_o^2 - 2.533 \times 10^{-7}P_o - 3.616 \times 10^{-14} = 0$$

and

$$P_o = \frac{2.533 \times 10^{-7} \pm \sqrt{[(2.533 \times 10^{-7})^2 - (-4 \times 0.314 \times 3.616 \times 10^{-14})]}}{0.628}$$

$$= 0.93\ \mu\text{W}$$

$$= -30.3\ \text{dBm}$$

It must be noted that the low noise preamplification depicted in example 10.11 may not always be obtained, and that higher thermal noise levels will adversely affect the receiver sensitivity for a given SNR. This is especially the case with lower SNRs as illustrated in the peak to peak signal power to rms noise power ratio against average received optical power characteristics for a video system shown in Fig. 10.41. The performance of the system for various values of mean square thermal noise current $\overline{i_t^2} = 4KTBF_n/R_L$, where $\overline{i_t^2}$ is expressed as a spectral density in $A^2\ Hz^{-1}$, is indicated. The value for the receiver sensitivity obtained in example 10.11 is approaching the quantum limit, also illustrated in Fig. 10.41, which is the best that could possibly be achieved with a noiseless amplifier.

The quantum or shot noise (when ignoring the photodetector dark current) limit occurs with large values of signal current (i.e. primary photocurrent) at the receiver. Considering a *p–i–n* photodiode receiver, this limiting case which

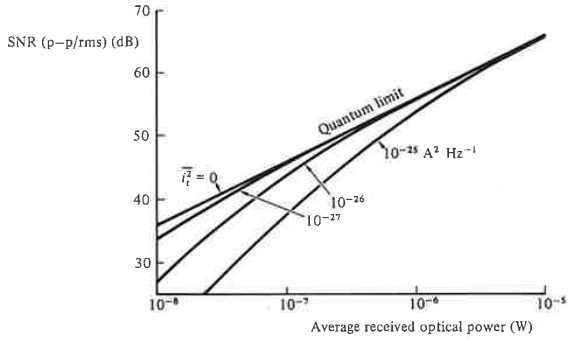

Fig. 10.41 Peak to peak signal power to rms noise power ratio against the average received optical power for a direct intensity modulated video system and various levels of thermal noise given by $\overline{i_t^2}$. Reproduced with permission from G. G. Windus, *Marconi Rev.*, **XLIV**, p. 77, 1981.

corresponds to large SNR is given by Eq. (10.68) when neglecting the device dark current as:

$$\left(\frac{S}{N}\right)_{rms} \simeq \frac{m_a^2 I_p}{4eB} \quad \text{(quantum noise limit)} \tag{10.70}$$

Using the relationship between the average received optical power P_o and the primary photocurrent given in Eq. (10.63) allows Eq. (10.70) to be expressed as:

$$P_o \simeq \frac{4hf}{m_a^2 \eta} \left(\frac{S}{N}\right)_{rms} B \tag{10.71}$$

Equation (10.71) indicates that for a quantum noise limited analog receiver, the optical input power is directly proportional to the effective noise or post detection bandwidth B. A similar result was obtained in Eq. (10.37) for the digital receiver.

Alternatively at low SNRs thermal noise is dominant, and the thermal noise limit when I_p is small, which may also be obtained from Eq. (10.68), is given by:

$$\left(\frac{S}{N}\right)_{rms} \simeq \frac{(m_a I_p)^2 R_L}{8KTBF_n} \quad \text{(thermal noise limit)} \tag{10.72}$$

Again substituting for I_p from Eq. (10.63) gives:

$$P_o \simeq \frac{hf}{e\eta m_a^2} \left(\frac{8KTF_n}{R_L}\right)^{\frac{1}{2}} \left(\frac{S}{N}\right)_{rms}^{\frac{1}{2}} B^{\frac{1}{2}} \tag{10.73}$$

Therefore it may be observed from Eq. (10.73) that in the thermal noise limit the average incident optical power is directly proportional to $B^{\frac{1}{2}}$ instead of the direct dependence on B shown in Eq. (10.71) for the quantum noise limit. The dependence expressed in Eq. (10.73) is typical of the *p–i–n* photodiode receiver operating at low optical input power levels. Thus Eq. (10.73) may be used to estimate the required input optical power to achieve a particular SNR for a *p–i–n* photodiode receiver which is dominated by thermal noise.

Example 10.12

An analog optical fiber link employing D–IM has a *p–i–n* photodiode receiver in which thermal noise is dominant. The system components have the following characteristics and operating conditions.

p–i–n photodiode quantum efficiency	60%
effective load impedance for the photodiode	50 kΩ
preamplifier noise figure	6 dB

operating wavelength	1 μm
operating temperature	300 K
receiver post detection bandwidth	10 MHz
modulation index	0.5

Estimate the required average incident optical power at the receiver in order to maintain an SNR, defined in terms of the mean square signal current to mean square noise current, of 45 dB.

Solution: The average incident optical power for a thermal noise limited *p–i–n* photodiode receiver may be estimated using Eq. (10.73) where:

$$P_o \simeq \frac{hf}{e\eta m_a^2}\left(\frac{8KTF_n}{R_L}\right)^{\frac{1}{2}}\left(\frac{S}{N}\right)_{rms}^{\frac{1}{2}} B^{\frac{1}{2}}$$

and

$$\frac{hf}{e\eta m_a^2} = \frac{hc}{e\eta m_a^2\lambda} = \frac{6.626 \times 10^{-34} \times 2.998 \times 10^8}{1.602 \times 10^{-19} \times 0.6 \times 0.25 \times 1 \times 10^{-6}}$$

$$= 8.267$$

$$\left(\frac{8KTF_n}{R_L}\right)^{\frac{1}{2}} = \left(\frac{8 \times 1.381 \times 10^{-23} \times 300 \times 4}{50 \times 10^3}\right)^{\frac{1}{2}}$$

$$= 1.628 \times 10^{-12}$$

$$\left(\frac{S}{N}\right)_{rms}^{\frac{1}{2}} B^{\frac{1}{2}} = (3.162 \times 10^4 \times 10^7)^{\frac{1}{2}}$$

$$= 5.623 \times 10^5$$

Hence,

$$P_o \simeq 8.267 \times 1.628 \times 10^{-12} \times 5.623 \times 10^5$$

$$= 7.57\ \mu W$$

$$= -21.2\ dBm$$

Therefore, as anticipated, the receiver sensitivity in the thermal noise limit is low.

10.7.2 System Planning

Many of the general planning considerations for optical fiber systems outlined in Section 10.4 may be applied to analog transmission. However, extra care must be taken to ensure that the optical source and, to a lesser extent, the detector have linear input–output characteristics, in order to avoid distortion of the transmitted optical signal. Furthermore, careful optical power budgeting is often necessary with analog systems because of the generally high SNRs required at the optical receiver (40–60 dB) in comparison with digital systems (20–25 dB), to obtain a similar fidelity. Therefore, although analog system optical power budgeting may be carried out in a similar manner to digital systems (see Section 10.6.6), it is common for the system margin, or the

difference between the optical power launched into the fiber and the required optical power at the receiver, for analog systems to be quite small (perhaps only 10–20 dB when using an LED source to *p–i–n* photodiode receiver). Consequently analog systems employing direct intensity modulation of the optical source tend to have a limited transmission distance without repeaters which generally prohibits their use for long-haul applications.

Example 10.13

A D–IM analog optical fiber link of length 2 km employs an LED which launches mean optical power of −10 dBm into a multimode optical fiber. The fiber cable exhibits a loss of 3.5 dB km^{-1} with splice losses calculated at 0.7 dB km^{-1}. In addition there is a connector loss at the receiver of 1.6 dB. The *p–i–n* photodiode receiver has a sensitivity of −25 dBm for an SNR ($\overline{i^2_{sig}}/\overline{i^2_N}$) of 50 dB and with a modulation index of 0.5. It is estimated that a safety margin of 4 dB is required. Assuming there is no dispersion–equalization penalty:

(a) Perform an optical power budget for the system operating under the above conditions and ascertain its viability.
(b) Estimate any possible increase in link length which may be achieved using an injection laser source which launches mean optical power of 0 dBm into the fiber cable. In this case the safety margin must be increased to 7 dB.

Solution: (a) Optical power budget:

Mean power launched into the fiber cable from the LED transmitter	−10 dBm
Mean optical power required at the *p–i–n* photodiode receiver for SNR of 50 dB and a modulation index of 0.5	−25 dBm
Total system margin	15 dB
Fiber cable loss (2 × 3.5)	7.0 dB
Splice losses (2 × 0.7)	1.4 dB
Connector loss at the receiver	1.6 dB
Safety margin	4.0 dB
Total system loss	14.0 dB
Excess power margin	1.0 dB

Hence the system is viable, providing a small excess power margin.

(b) In order to calculate any possible increase in link length when using the injection laser source we refer to Eq. (10.53), where

$$P_i - P_0 = (\alpha_{fc} + \alpha_j)L + \alpha_{cr} + M_a \text{ dB}$$

Therefore,

$$0 \text{ dBm} - (-25 \text{ dBm}) = (3.5 + 0.7)L + 1.6 + 7.0$$

and

$$4.2L = 25 - 8.6 = 16.4 \text{ dB}$$

giving

$$L = \frac{16.4}{4.2} = 3.9 \text{ km}$$

Hence the use of the injection laser gives a possible increase in the link length of 1.9 km or almost a factor of 2. It must be noted that in this case the excess power margin has been reduced to zero.

The transmission distance without repeaters for the analog link of example 10.13 could be extended further by utilizing an APD receiver which has increased sensitivity. This could facilitate an increase in the maximum link length to around 7 km, assuming no additional power penalties or excess power margin. Although this is quite a reasonable transmission distance, it must be noted that a comparable digital system could give in the region of 13 km transmission without repeaters.

The temporal response of analog systems may be determined from system rise time calculations in a similar manner to digital systems (see Section 10.6.5). The maximum permitted 3 dB optical bandwidth for analog systems in order to avoid dispersion penalties follows from Eq. (10.49) and is given by:

$$B_{\text{opt}}(\max) = \frac{0.35}{T_{\text{syst}}} \tag{10.74}$$

Hence calculation of the total system 10–90% rise time T_{syst} allows the maximum system bandwidth to be estimated. Often this calculation is performed in order to establish that the desired system bandwidth may be achieved using a particular combination of system components.

Example 10.14

The 10–90% rise times for possible components to be used in a D–IM analog optical fiber link are specified below:

Source (LED)	10 ns
Fiber cable: intermodal	9 ns km^{-1}
intramodal	2 ns km^{-1}
Detector (APD)	3 ns

The desired link length without repeaters is 5 km and the required optical bandwidth is 6 MHz. Determine whether the above combination of components give an adequate temporal response.

Solution: Equation (10.74) may be used to calculate the maximum permitted system rise time which gives the desired bandwidth where:

$$T_{\text{syst}}(\max) = \frac{0.35}{B_{\text{opt}}} = \frac{0.35}{6 \times 10^6} = 58.3 \text{ ns}$$

The total system rise time using the specified components can be estimated using Eq. (10.43) as:

$$\begin{aligned} T_{\text{syst}} &= 1.1(T_S^2 + T_n^2 + T_c^2 + T_D^2)^{\frac{1}{2}} \\ &= 1.1(10^2 + (9 \times 5)^2 + (2 \times 5)^2 + 3^2)^{\frac{1}{2}} \\ &\simeq 52 \text{ ns} \end{aligned}$$

Therefore the specified components give a system rise time which is adequate for the bandwidth and distance requirements of the optical fiber link. However, there is little leeway for upgrading the system in terms of bandwidth or distance without replacing one or more of the system components.

10.7.3 Subcarrier Intensity Modulation

Direct intensity modulation of the optical source is suitable for the transmission of a baseband analog signal. However, if the wideband nature of the optical fiber medium is to be fully utilized it is essential that a number of baseband channels are multiplexed onto a single fiber link. This may be achieved with analog transmission through frequency division multiplexing of the individual baseband channels. Initially, the baseband channels must be translated onto carriers of different frequency by amplitude modulation (AM), frequency modulation (FM) or phase modulation (PM) prior to being simultaneously transmitted as an FDM signal. The frequency translation may be performed in the electrical regime where the baseband analog signals modulate electrical subcarriers and are then frequency division multiplexed to form a composite electrical signal prior to intensity modulation of the optical source.

A block schematic of an analog system employing this technique which is known as subcarrier intensity modulation is shown in Fig. 10.42. The baseband signals are modulated onto radiofrequency (RF) subcarriers by either AM, FM or PM and multiplexed before being applied to the optical source drive circuit. Hence an intensity modulated (IM) optical signal is obtained which may be either AM–IM, FM–IM or PM–IM. In practice, however, system output SNR considerations dictate that generally only the

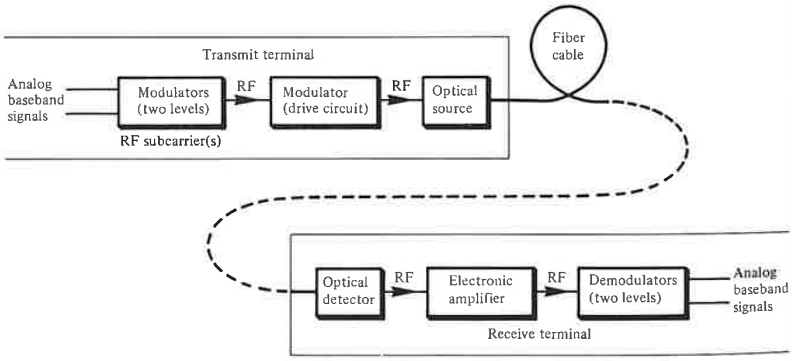

Fig. 10.42 Subcarrier intensity modulation system for analog optical fiber transmission.

latter two modulation formats are used. Nevertheless systems may incorporate two levels of electrical modulation whereby the baseband channels are initially amplitude modulated prior to frequency or phase modulation [Ref. 66]. The FM or PM signal thus obtained is then used to intensity modulate the optical source. At the receive terminal the transmitted optical signal is detected prior to electrical demodulation and demultiplexing (filtering) to obtain the originally transmitted baseband signals.

A further major advantage of subcarrier intensity modulation is the possible improvement in SNR that may be obtained during subcarrier demodulation. In order to investigate this process it is necessary to obtain a general expression for the SNR of the intensity modulated optical carrier which may then be applied to the subcarrier intensity modulation formats. Therefore, as with D–IM, considered in the previous section, an electrical signal $m(t)$ modulates the source intensity. The transmitted optical power waveform is of the same form as Eq. (10.59), where:

$$P_{\text{opt}}(t) = P_{\text{i}}(1 + m(t)) \tag{10.75}$$

Also the secondary photocurrent $I(t)$ generated at an APD receiver following Eq. (10.62) is given by:

$$I(t) = I_{\text{p}}M(1 + m(t)) \tag{10.76}$$

The mean square signal current $\overline{i_{\text{sig}}^2}$ may be written as [Ref. 65]:

$$\overline{i_{\text{sig}}^2} = (I_{\text{p}}M)^2 P_m \tag{10.77}$$

where P_m is the total power of $m(t)$, which can be defined in terms of the spectral density $S_m(\omega)$ of $m(t)$ occupying a one-sided bandwidth B_m Hz as:

$$P_m = \frac{1}{2\pi}\int_{-2\pi B_m}^{2\pi B_m} S_m(\omega)\,\mathrm{d}\omega \tag{10.78}$$

Hence the SNR defined in terms of the mean square signal current to mean square noise current (i.e. rms signal power to rms noise power) using Eqs. (10.77) and (10.66) can now be written as:

$$\left(\frac{\text{S}}{\text{N}}\right)_{\text{rms}} = \frac{\overline{i_{\text{sig}}^2}}{\overline{i_{\text{N}}^2}} = \frac{(I_{\text{p}}M)^2 P_m}{2eB_m(I_{\text{p}} + I_{\text{d}})M^2F(M) + (4KTBF_{\text{n}}/R_{\text{L}})}$$

$$= \frac{I_{\text{p}}^2 P_m}{2B_m e(I_{\text{p}} + I_{\text{d}})F(M) + (4KTBF_{\text{n}}/M^2R_{\text{L}})}$$

$$= \frac{(RP_{\text{o}})^2 P_m}{2B_m N_{\text{o}}} \quad \text{(D–IM)} \tag{10.79}$$

where we substitute for I_p from Eq. (8.4) and for notational simplicity write:

$$N_o = e(I_p + I_d)F(M) + \frac{4KTBF_n}{M^2 R_L} \tag{10.80}$$

The result obtained in Eq. (10.79) gives the SNR for a direct intensity modulated optical source where the total modulating signal power is P_m. In this context Eq. (10.79) is simply a more general form of Eq. (10.67). However, we are now in a position to examine the signal to noise performance of various subcarrier intensity modulation formats.

10.7.4 Subcarrier Double Sideband Modulation (DSB–IM)

A simple way to translate the spectrum of the baseband message signal $a(t)$ is by direct multiplication with the subcarrier waveform $A_c \cos \omega_c t$ giving the modulated waveform $m(t)$ as:

$$m(t) = A_c a(t) \cos \omega_c t \tag{10.81}$$

where A_c is the amplitude, and ω_c the angular frequency of the subcarrier waveform. For a cosinusoidal modulating signal ($\cos \omega_m t$) the subcarrier electric field $E_m(t)$ becomes:

$$E_m(t) = \frac{A_c}{2} \cos(\omega_c + \omega_m)t + \cos(\omega_c - \omega_m)t \tag{10.82}$$

giving the upper and lower sidebands. The time and frequency domain representations of the modulated waveform are shown in Fig. 10.43. It may be

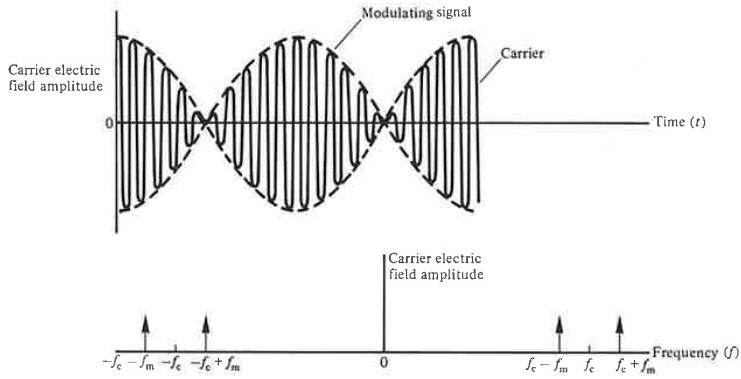

Fig. 10.43 Time and frequency domain representations of double sideband modulation.

observed from the frequency domain representation that only the two sideband components are present as indicated in Eq. (10.82). This modulation technique is known as double sideband modulation (DSB) or double sideband suppressed carrier (DSBSC) amplitude modulation. It provides a more efficient method of translating the spectrum of the baseband message signal than conventional full amplitude modulation where a large carrier component is also present in the modulated waveform.

The DSB signal shown in Fig. 10.43 intensity-modulates the optical source. Therefore the transmitted optical power waveform is obtained by combining Eqs. (10.75) and (10.81) where for simplicity we set the carrier amplitude A_c to unity, giving:

$$P_{opt}(t) = P_i(1 + a(t)\cos\omega_c t) \tag{10.83}$$

Furthermore, in order to prevent overmodulation, the value of the message signal is normalized such that $|a(t) \leqslant 1|$ with power $P_a \leqslant 1$. The DSB modulated electrical subcarrier occupies a bandwidth $B_m = 2B_a$, and with a carrier amplitude of unity, $P_m = P_a/2$. Hence, the ratio of rms signal power to rms noise power obtained within the subcarrier bandwidth at the input to the double sideband demodulator is given by Eq. (10.79), where:

$$\left(\frac{S}{N}\right)_{rms} \text{input DSB} = \frac{(RP_o)^2 P_a/2}{2 \times 2B_a N_o} = \frac{(RP_o)^2 P_a}{8B_a N_o} \tag{10.84}$$

However, an ideal DSB demodulator gives a detection gain of 2 or 3 dB improvement in SNR [Ref. 67]. This yields an output SNR of:

$$\left(\frac{S}{N}\right)_{rms} \text{output DSB} = 2\left(\frac{S}{N}\right)_{rms} \text{input DSB} = \frac{(RP_o)^2 P_a}{4B_a N_o} \tag{10.85}$$

Comparison of the result obtained in Eq. (10.85) to that using direct intensity modulation of the baseband signal given by Eq. (10.79) shows a 3 dB degradation in SNR when employing DSB–IM under the same conditions of bandwidth (i.e. $B_m = B_a$), modulating signal power (i.e. $P_m = P_a$), detector photocurrent and noise. For this reason DSB–IM systems (and also AM–IM systems in general) are usually not considered efficient for optical fiber communications. Therefore far more attention is devoted to both FM–IM and PM–IM systems.

10.7.5 Subcarrier Frequency Modulation (FM–IM)

In this modulation format, the subcarrier is frequency modulated by the message signal. The conventional form for representing the baseband signal

which intensity modulates the optical source is [Ref. 67]:

$$m(t) = A_c \cos\left[\omega_c t + k_f \int_0^t a(\tau)\,d\tau\right] \tag{10.86}$$

where k_f is the angular frequency deviation in radians per second per unit of $a(t)$. To prevent intensity over modulation, the carrier amplitude $A_c \leqslant 1$. The generally accepted expression for the bandwidth which is referred to as Carson's rule is given by:

$$B_m \simeq 2(D_f + 1)B_a \tag{10.87}$$

where D_f is the frequency deviation ratio defined by:

$$D_f = \frac{\text{peak frequency deviation}}{\text{bandwidth of } a(t)} = \frac{f_d}{B_a} \tag{10.88}$$

The peak frequency deviation in the subcarrier FM signal f_d is given by:

$$f_d = k_f \max|a(t)| \tag{10.89}$$

Hence the SNR at the input to the subcarrier FM demodulator is:

$$\left(\frac{S}{N}\right)_{rms} \text{input FM} = \frac{(RP_o)^2(A_c^2/2)}{2B_m N_o} \tag{10.90}$$

The subcarrier demodulator operating above threshold yields an output SNR [Ref. 65]:

$$\left(\frac{S}{N}\right)_{rms} \text{output FM} = 6D_f^2(D_f^2 + 1)\frac{P_a(RP_o)^2(A_c^2/2)}{2B_m N_o} \tag{10.91}$$

Substituting for B_m from Eq. (10.87) gives:

$$\left(\frac{S}{N}\right)_{rms} \text{output FM} = \frac{3D_f^2 P_a(RP_o)^2(A_c^2/2)}{2B_a N_o} \tag{10.92}$$

The result obtained in Eq. (10.92) indicates that a significant improvement in the postdetection SNR may be achieved by using wideband FM–IM as demonstrated in the following example.

Example 10.15

(a) A D–IM and an FM–IM optical fiber communication system are operated under the same conditions of modulating signal power and bandwidth, detector photocurrent and noise. Furthermore, in order to maximize the SNR in the FM–IM system, the amplitude of the subcarrier is set to unity. Derive an expression for the improvement in post detection SNR of the FM–IM system over the D–IM system. It

Ex. 1017.98

may be assumed that the SNR is defined in terms of the rms signal power to rms noise power.

(b) The FM–IM system described in (a) has an 80 MHz subcarrier which is modulated by a baseband signal with a bandwidth of 4 kHz such that the peak frequency deviation is 400 kHz. Use the result obtained in (a) to determine the improvement in post detection SNR (in decibels) over the D–IM system operating under the same conditions. Also estimate the bandwidth of the FM signal.

Solution: (a) The output SNR for the D–IM system is given by Eq. (10.79) where we can write $P_m = P_a$ and $B_m = B_a$. Hence:

$$\left(\frac{S}{N}\right)_{rms} \text{output D–IM} = \frac{(RP_o)^2 P_a}{2B_a N_o}$$

The corresponding output SNR for the FM–IM system is given by Eq. (10.92) where setting A_c to unity gives:

$$\left(\frac{S}{N}\right)_{rms} \text{output FM} = \frac{3D_f^2 P_a (RP_o)^2}{4B_a N_o}$$

Therefore the improvement in SNR of the FM–IM system over the D–IM system is given by:

$$\text{SNR improvement} = \frac{[3D_f^2 P_a (RP_o)^2]/(4B_a N_o)}{[(RP_o)^2 P_a]/(2B_a N_o)}$$

$$= \frac{3D_f^2}{2}$$

and,

$$\text{SNR improvement in decibels} = 10 \log_{10} \frac{3}{2} D_f^2$$

$$= 1.76 + 20 \log_{10} D_f$$

(b) The frequency deviation ratio is given by Eq. (10.88) where:

$$D_f = \frac{f_d}{B_a} = \frac{400 \times 10^3}{4 \times 10^3} = 100$$

Therefore the SNR improvement is:

$$\text{SNR improvement} = 1.76 + 20 \log_{10} 100$$

$$= 41.76 \text{ dB}$$

The bandwidth of the FM–IM signal may be estimated using Eq. (10.87) where:

$$B_m \simeq 2(D_f + 1)B_a = 2(100 + 1)4 \times 10^3$$

$$= 808 \text{ kHz}$$

This result indicates that the system is operating as a wideband FM–IM system.

Example 10.15 illustrates that a substantial improvement in the post detection SNR over D–IM may be obtained using FM–IM. However, it must be noted that this is at the expense of a tremendous increase in the bandwidth required (808 kHz) for transmission of the 4 kHz baseband channel.

10.7.6 Subcarrier Phase Modulation (PM–IM)

With this modulation technique the instantaneous phase of the subcarrier is set proportional to the modulating signal. Hence in a PM–IM system the modulating signal $m(t)$ may be written as [Ref. 67]:

$$m(t) = A_c \cos(\omega_c t + k_p a(t)) \tag{10.93}$$

where k_p is the phase deviation constant in radians per unit of $a(t)$. Again the carrier amplitude $A_c \leqslant 1$ to prevent intensity overmodulation. Moreover, the bandwidth of the PM–IM signal is given by Carson's rule as:

$$B_m \simeq 2(D_p + 1)B_a \tag{10.94}$$

where D_p is the frequency deviation ratio for the PM–IM system. In common with subcarrier frequency modulation the frequency deviation ratio is defined as:

$$D_p = \frac{f_d}{B_a} \tag{10.95}$$

where f_d is the peak frequency deviation of the subcarrier PM signal, which is given by:

$$f_d = k_p \max\left|\frac{da(t)}{dt}\right| \tag{10.96}$$

The SNR at the input to the subcarrier PM demodulator is:

$$\left(\frac{S}{N}\right)_{rms} \text{input PM} = \frac{(RP_o)^2 A_c^2/2}{2B_m N_o} \tag{10.97}$$

The output SNR from an ideal subcarrier PM demodulator operating above threshold is [Ref. 65]:

$$\left(\frac{S}{N}\right)_{rms} \text{output PM} = \frac{D_p^2 P_a (RP_o)^2 A_c^2/2}{2B_a N_o} \tag{10.98}$$

The result given in Eq. (10.98) suggests that an improvement in SNR over D–IM may be obtained using PM–IM, especially when the SNR is maximized with $A_c = 1$. However, comparison of PM–IM with FM–IM indicates that the latter modulation format gives the greatest improvement.

Ex. 1017.100

Example 10.16

A PM–IM and an FM–IM optical fiber communication system are operated under the same conditions of bandwidth, baseband signal power, subcarrier amplitude, frequency deviation, detector photocurrent and noise. Assuming the demodulators for both systems are ideal, determine the ratio (in decibels) of the output SNR from the FM–IM system to the output SNR from the PM–IM system.

Solution: The output SNR from the FM–IM system is given by Eq. (10.92) where:

$$\left(\frac{S}{N}\right)_{rms} \text{output FM} = \frac{3D_f^2 P_a (RP_o)^2 A_c^2/2}{2B_a N_o}$$

Substituting for D_f from Eq. (10.88) gives:

$$\left(\frac{S}{N}\right)_{rms} \text{output FM} = \frac{3f_d^2 P_a (RP_o)^2 A_c^2/2}{2B_a^3 N_o}$$

The output SNR for the PM–IM system is given by Eq. (10.98) where:

$$\left(\frac{S}{N}\right)_{rms} \text{output PM} = \frac{D_p^2 P_a (RP_o)^2 A_c^2/2}{2B_a N_o}$$

Substituting for D_p from Eq. (10.95) gives:

$$\left(\frac{S}{N}\right)_{rms} \text{output PM} = \frac{f_d^2 P_a (RP_o)^2 A_c^2/2}{2B_a^3 N_o}$$

The ratio of the output SNRs from the FM–IM and the PM–IM system is:

$$\text{Ratio} = \frac{[3 f_d^2 P_a (RP_o)^2 A_c^2/2]/(2B_a^3 N_o)}{[f_d P_a (RP_o)^2 A_c^2/2]/(2B_a^3 N_o)}$$

$$= 3$$

$$= 4.77 \text{ dB}$$

Example 10.16 shows that the FM–IM system has a superior output SNR by some 4.77 dB over the corresponding PM–IM system. Nevertheless, this does not prohibit the use of PM–IM systems for analog optical fiber communications as they still exhibit a substantial improvement in output SNR over D–IM systems, as well as allowing frequency division multiplexing. It should be noted, however, that a similar bandwidth penalty to FM–IM is incurred using this modulation format.

10.7.7 Pulse Analog Techniques

Pulse modulation techniques for analog transmission, rather than encoding the analog waveform into PCM, were mentioned within the system design considerations of Section 10.4. The most common techniques are pulse amplitude

modulation (PAM), pulse width modulation (PWM), pulse position modulation (PPM) and pulse frequency modulation (PFM). All the pulse analog techniques employ pulse modulation in the electrical regime prior to intensity modulation of the optical source. However, PAM–IM is affected by source nonlinearities and is less efficient than D–IM, and therefore is usually discounted. PWM–IM is also inefficient since a large part of the transmitted energy conveys no information as only variations of the pulse width about a nominal value are of interest. Alternatively, PPM–IM and PFM–IM offer distinct advantages since the modulation affects the timing of the pulses, thus allowing the transmission of very narrow pulses. Hence, PPM–IM and PFM–IM provide similar signal to noise performance to subcarrier phase and frequency modulation whilst avoiding problems involved with source linearity. These techniques therefore prove advantageous for longer-haul analog fiber links. Although PPM–IM is slightly more efficient it provides less SNR improvement over D–IM, than that gained with PFM–IM, where wideband FM gain may be obtained. Furthermore, the terminal equipment required for PFM–IM is less complex and therefore it is generally the preferred pulse analog technique [Refs. 68 and 72–76]. For these reasons the system aspects of pulse analog transmission will be considered in relation to PFM–IM.

A block schematic of a PFM–IM optical fiber system is shown in Fig. 10.44. Pulse frequency modulation in which the pulse repetition rate is varied in sympathy with the modulating signal is performed in the PFM modulator which consists of a voltage controlled oscillator (VCO). This in turn operates the optical source by means of either a fixed pulse width or a fixed duty cycle (e.g. 50%). Demodulation in the system shown in Fig. 10.44 is by regenerative baseband recovery, whereby the individual pulses are detected in a wideband receiver before they are regenerated with a limiter and monostable. This provides the desired modulating signal as a baseband component which is recovered through a low pass filter.

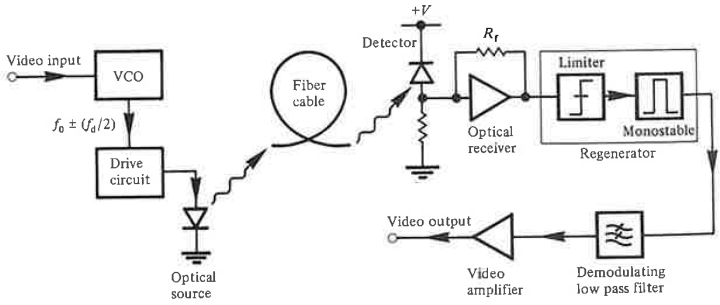

Fig. 10.44 A PFM-IM optical fiber system employing regenerative baseband recovery.

Regenerative baseband recovery gives the best SNR at the system output. A simpler PFM demodulation technique for fixed width pulse transmission is direct baseband recovery. In this case, because a baseband component is generated at the transmit terminal, detection may be performed with a low bandwidth receiver and the modulating signal obtained directly from a low pass filter. However, this technique gives a reduced SNR for a given optical power and therefore does not find wide application.

The SNR in terms of the peak to peak signal power to rms noise power of a PFM–IM system using regenerative baseband recovery is given by [Ref. 68]:

$$\left(\frac{S}{N}\right)_{p-p} = \frac{3(T_0 f_D MRP_{po})^2}{(2\pi T_R B)^2 \overline{i_N^2}} \tag{10.99}$$

where T_0 is the nominal pulse period which is equivalent to the reciprocal of the pulse rate f_0, f_D is the peak to peak frequency deviation, R is the photodiode responsivity, M is the photodiode multiplication factor, P_{po} is the peak received optical power, T_R is the pulse rise time at the regenerator circuit input, B is the post detection or effective baseband noise bandwidth and $\overline{i_N^2}$ is the receiver mean square noise current. It may be noted that improved SNRs are obtained with short rise time detected pulses. Moreover, the pulse rise time at the regenerator circuit input is dictated by the overall 10–90% system rise time T_{syst}, so there is no advantage in using a wideband receiver with a better pulse rise time than this. In fact such a receiver would degrade the system performance by passing increased front end noise. Therefore in an optimized PFM regenerative receiver design, $T_R = T_{syst}$ and following Eq. (10.43):

$$T_R \simeq 1.1\,(T_S^2 + T_n^2 + T_c^2 + T_D^2)^{\frac{1}{2}} \tag{10.100}$$

where T_S, T_n, T_c and T_D are the rise times of the source (or transmitter), the fiber (intermodal and intramodal) and the detector (or receiver) respectively.

Example 10.17

An optical fiber PFM–IM system for video transmission employs regenerative baseband recovery. The system uses graded index fiber and an APD detector and has the following operational parameters:

Nominal pulse rate	20 MHz
Peak to peak frequency deviation	5 MHz
APD responsivity	0.7
APD multiplication factor	60
Total system 10–90% rise time	12 ns
Baseband noise bandwidth	6 MHz
Receiver mean square noise current	1×10^{-17} A^2

Calculate: (a) the optimum receiver bandwidth; (b) the peak to peak signal power to rms noise power ratio obtained when the peak input optical power to the receiver is −40 dBm.

Solution: (a) For an optimized design the pulse rise time at the regenerator circuit

is equal to the total system rise time, hence $T_R = 12$ ns. The optimum receiver bandwidth is simply obtained by taking the reciprocal of T_R.

Solution: (a) For an optimized design the pulse rise time at the regenerator circuit is equal to the total system rise time, hence $T_R = 12$ ns. The optimum receiver bandwidth is simply obtained by taking the reciprocal of T_R giving 83.3 MHz.

(b) The nominal pulse period T_0 ($= 1/f_0$) is 5×10^{-8} s and the peak optical power at the receiver is 1×10^{-7} W. Therefore, the peak to peak signal to rms noise ratio may be obtained using Eq. (10.99), where:

$$\left(\frac{S}{N}\right)_{p-p} = \frac{3(T_0 f_D M R P_{po})^2}{(2\pi T_R B)^2 \overline{i_N^2}}$$

$$= \frac{3(5 \times 10^{-8} \times 5 \times 10^6 \times 60 \times 0.7 \times 10^{-7})^2}{(2\pi \times 12 \times 10^{-9} \times 6 \times 10^6)^2 \times 10^{-17}}$$

$$= 1.62 \times 10^6$$

$$= 62.1 \text{ dB}$$

The result of example 10.17(b) illustrates the possibility of acquiring high SNRs at the output to a PFM–IM system using a regenerative receiver with achievable receiver noise levels and with moderate input optical signal power to the receiver.

10.8 COHERENT SYSTEMS

The detection of an intensity modulated optical carrier is basically a photon counting process where each detected photon is converted into an electron–hole pair (or in the case of the APD a number of pairs due to avalanche gain). It was indicated in Section 7.5 that this process which ignores the phase and polarization of the electromagnetic carrier may be readily implemented with currently available optical components. Thus all the previous discussion in this chapter involving both digital and analog systems has been applied to an intensity modulated optical carrier. However, receivers designed to detect the intensity modulated lightwave are often limited by noise generated in the electronic amplifier, except at very high SNRs. This reduces receiver sensitivity below the quantum noise limited conditions by at least 10–20 dB. It has been demonstrated that improved sensitivity may be obtained using well-known coherent detection techniques for the optical signal (i.e. heterodyne or homodyne detection). These methods have been successfully applied in free space optical communication systems using gas lasers [Ref. 77].

Coherent optical fiber transmission requires the direct modulation of the amplitude (direct AM), frequency (direct FM) or phase (direct PM) of a coherent optical carrier prior to demodulation using coherent detection. In the case of digital transmission this implies amplitude, frequency or phase shift

keying (ASK, FSK or PSK) modulation techniques [Ref. 67]. Coherent detection by heterodyning involves the mixing of the incoming signal with a local optical oscillator to produce an intermediate frequency (IF), which is a difference signal (or difference frequency) carrying the modulating information signal. This signal may then be processed using standard techniques [Ref. 67]. Alternatively, with homodyne detection a local oscillator is set at the same frequency and phase as the coherent carrier, prior to optical mixing, which then translates the required information signal into the baseband.

A principal advantage of coherent detection for optical systems is the fact that the local oscillator power may be set such that the receiver noise is dominated by the shot noise contribution from the local oscillator. Furthermore, the signal power is proportional to the local oscillator power giving, for large local oscillator powers, an SNR which is independent of electronic amplifier noise. This allows a significant improvement in SNR at the receiver. In free space optical communications the SNR at the receiver output when using heterodyne detection may be shown [Ref. 78] to be at least a factor of 8 (or 9 dB) higher than that for subcarrier intensity modulation; the SNR improvement using homodyne in a similar system is at least a factor of 4 (or 6 dB). Conversely, investigation of digital optical modulation formats for coherent transmission [Ref. 79] indicates that PSK homodyne detection gives the best sensitivity by some 16–22 dB over ASK baseband direct detection. PSK heterodyne detection also proves to be the most sensitive heterodyning

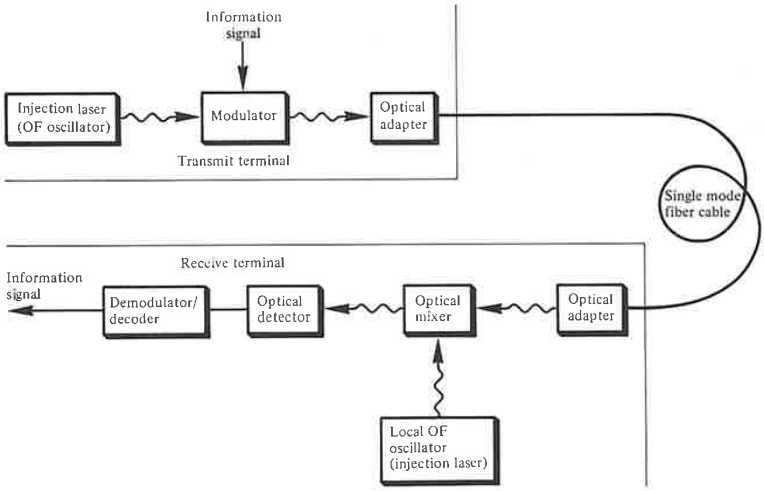

Fig. 10.45 A coherent optical fiber system employing heterodyne detection [Ref. 84].

technique with a minimum detectable power only 3 dB higher than that of PSK homodyne detection. Hence this shot noise limited detection offers to provide a distinct increase in the potential repeater spacing for optical fiber links. Moreover, coherent transmission will allow high capacity information transfer using frequency division multiplexing with fine frequency separation. This in turn will allow full exploitation of the low loss transmission windows in the longer wavelength region (around 1.3 μm and 1.55 μm).

However, there are problems associated with coherent optical fiber transmission which can be observed by considering the block schematic of a possible system employing heterodyne detection shown in Fig. 10.45 [Ref. 80]. The transmitter comprises an injection laser source which acts as an optical frequency oscillator, the output of which is modulated by the information signal using a suitable optical modulator. The directly modulated optical carrier is then launched into a single mode fiber through an optical adapter. The received optical signal is mixed with the output from the local optical oscillator, which is also provided by a suitable injection laser. To permit satisfactory heterodyne detection, the optical mixer must combine the polarized optical signal field with the similarly polarized local optical field in the most efficient manner. Ideally this device would be realized using integrated optical techniques (see Section 11.7). Finally, the signal is demodulated to obtain the originally transmitted information. For such a system to be practical both the source and local oscillator must be spectrally pure and frequency stabilized with respect to each other. Although this has proved possible using gas lasers, suitable semiconductor injection lasers are not easily obtained. The frequency stabilization of good, pure frequency, single mode injection lasers by control of temperature and injection current has received some attention [Refs. 81 and 82], but work is still at a preliminary stage. In this context injection locked semiconductor lasers or optical voltage controlled oscillators operating a very low input level may prove essential [Ref. 83].

In order to achieve coherent transmission a single polarization state of the fundamental HE_{11} mode must be launched into and maintained in the fiber. Therefore a suitable optical adapter (e.g. birefringent plate) is required to adjust the polarization of the input optical wave to one of the orthogonal polarization states of the single mode fiber cable. Such an adapter will also ensure the best possible matching to maximize the launching efficiency into the fiber. Finally, the fiber cable must be capable of maintaining this carrier polarization state over its length for coherent detection to take place at the receiver. This aspect of coherent transmission is also currently under investigation as discussed in Section 3.12.

Therefore the realization of practical coherent optical fiber transmission systems requires further research and development of the optical system components. Nevertheless, the feasibility of coherent transmission has been shown with the successful demonstration of optical FSK heterodyne detection using a

Ex. 1017.106

semiconductor laser source and local oscillator [Ref. 84]. Furthermore the potential benefits of these systems, especially in the area of long-haul, wide-band optical fiber communications ensures that interesting developments may be anticipated in the near future.

PROBLEMS

10.1 Discuss the major considerations in the design of digital drive circuits for:
(a) an LED source;
(b) an injection laser source.
Illustrate your answer with an example of a drive circuit for each source.

10.2 Outline, with the aid of suitable diagrams, possible techniques for:
(a) the linearization of LED transmitters;
(b) the maintenance of constant optical output power from an injection laser transmitter.

10.3 Discuss, with the aid of a block diagram, the function of the major elements of an optical fiber receiver. In addition, describe possible techniques for automatic gain control in APD receivers.

10.4 Equalization within an optical receiver may be provided using the simple frequency 'rollup' circuit shown in Fig. 10.46(a). The normalized frequency response for this circuit is illustrated in Fig. 10.46(b).

The amplifier indicated in Fig. 10.46(a) presents a load of 5 kΩ to the photodetector and together with the photodetector gives a total capacitance of 5 pF. However, the desired response from the amplifier–equalizer configuration has an upper 3 dB point or corner frequency at 30 MHz. Assuming R_2 is fixed at 100 Ω determine the required values for C_1 and R_1 in order to obtain such a response.

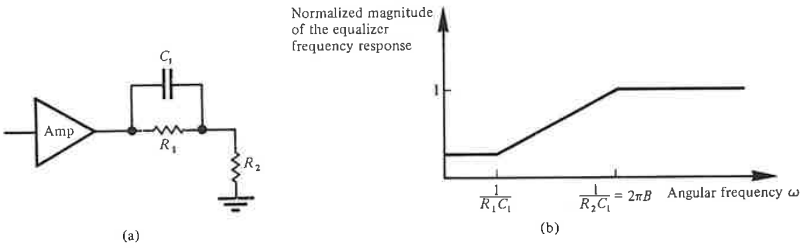

Fig. 10.46 The equalizer of problem 10.4: (a) the frequency 'rollup' circuit; (b) the spectral transfer characteristic for the circuit.

10.5 Describe the conversion of an analog signal into a pulse code modulated waveform for transmission on a digital optical fiber link. Furthermore indicate how several signals may be multiplexed onto a single fiber link.

A speech signal is sampled at 8 kHz and encoded using a 256 level binary code. What is the minimum transmission rate for this single pulse code modulated speech signal? Comment on the result.

10.6 A 1.5 MHz information signal with a dynamic range of 64 mV is sampled, quantized and encoded using a direct binary code. The quantization is linear with 512 levels. Determine:

(a) the maximum possible bit duration;
(b) the amplitude of one quantization level.

10.7 Describe, with the aid of a suitable block diagram, the operation of an optical fiber regenerative repeater. Indicate reasons for the occurrence of bit errors in the regeneration process and outline a technique for establishing the quality of the channel.

10.8 Twenty-four 4 kHz speech channels are sampled, quantized, encoded and then time division multiplexed for transmission as binary PCM on a digital optical fiber link. The quantizer is linear with 0.5 mV steps over a dynamic range of 2.048 V.

Calculate:

(a) the frame length of the PCM transmission, assuming an additional channel time slot is used for signalling and synchronization;
(b) the required channel bandwidth assuming NRZ pulses.

10.9 Develop a relationship between the error probability and the received SNR (peak signal power to rms noise power ratio) for a baseband binary optical fiber system. It may be assumed that the number of ones and zeros are equiprobable and that the decision threshold is set midway between the one and zero level.

The electrical SNR (defined as above) at the digital optical receiver is 20.4 dB. Determine:

(a) the optical SNR;
(b) the BER.

It may be assumed that $\text{erfc}\,(3.71) \simeq 1.7 \times 10^{-7}$.

10.10 The error function (erf) is defined in the text by Eq. (10.16). However an error function also used in communications is defined as:

$$\text{Erf}\,(u) = \frac{1}{\sqrt{(2\pi)}} \int_{-\infty}^{u} \exp\,(-x^2/2)\,\mathrm{d}x$$

where a capital E is used to denote this form of the error function. The corresponding complementary error function is:

$$\text{Erfc}\,(u) = 1 - \text{Erf}\,(u) = \frac{1}{\sqrt{(2\pi)}} \int_{u}^{\infty} \exp\,(-x^2/2)\,\mathrm{d}x$$

This complementary error function is also designated as $Q(u)$ in certain texts. Use of Erfc (u) or $Q(u)$ is sometimes considered more convenient within communication systems.

Develop a relationship for erfc (u) in terms of Erfc (u). Hence obtain an expression for the error probability $P(\text{e})$ as a function of the Erfc for a binary digital optical fiber system where the decision threshold is set midway between the one and zero levels and the number of transmitted ones and zeros are equiprobable. In addition given that $\text{Erfc}\,(4.75) \simeq 1 \times 10^{-6}$ estimate the required peak signal power to rms noise power ratios (both

optical and electrical) at the receiver of such a system in order to maintain a BER of 10^{-6}.

10.11 Show that Eq. (9.27) reduces to Eq. (10.28). Hence determine $F(M)$ when $k = 0.3$ and $M = 20$.

10.12 A silicon APD detector is utilized in a baseband binary PCM receiver where the decision threshold is set midway between the one and zero signal level. The device has a quantum efficiency of 70% and a ratio of carrier ionization rates of 0.05. In operation the APD has a multiplication factor of 65. Assuming a raised cosine signal spectrum and a zero disparity code, and given that erfc (4.47) $\simeq 2 \times 10^{-10}$:

(a) estimate the number of photons required at the receiver to register a binary one with a BER of 10^{-10};
(b) calculate the required incident optical power at the receiver when the system is operating at a wavelength of 0.9 μm and a transmission rate of 34 Mbit s^{-1};
(c) indicate how the value obtained in (b) should be modified to compensate for a $3B4B$ line code.

10.13 A *p–i–n* photodiode receiver requires 2×10^4 incident photons in order to register a binary one with a BER of 10^{-9}. The device has a quantum efficiency of 65%. Estimate in decibels the additional signal level required in excess of the quantum limit for this photodiode to maintain a BER of 10^{-9}.

10.14 An optical fiber system employs an LED transmitter which launches an average of 300 μW of optical power at a wavelength of 0.8 μm into the optical fiber cable. The cable has an overall attenuation (including joints) of 4 dB km^{-1}. The APD receiver requires 1200 incident photons in order to register a binary one with a BER of 10^{-10}. Determine the maximum transmission distance (without repeaters) provided by the system when the transmission rate is 1 Mbit s^{-1} and 1 Gbit s^{-1} such that a BER of 10^{-10} is maintained.

Hence sketch a graph showing the attenuation limit on transmission distance against the transmission rate for the system.

10.15 An optical fiber system uses fiber cable which exhibits a loss of 7 dB km^{-1}. Average splice losses for the system are 1.5 dB km^{-1}, and connector losses at the source and detector are 4 dB each. After safety margins have been allowed, the total permitted channel loss is 37 dB. Assuming the link to be attenuation limited, determine the maximum possible transmission distance without a repeater.

10.16 Assuming a linear increase in pulse broadening with fiber length, show that the transmission rate $B_T(\mathrm{DL})$ at which a digital optical fiber system becomes dispersion limited is given by:

$$B_T(\mathrm{DL}) \simeq \frac{(\alpha_{dB} + \alpha_j)}{5\sigma_T(\mathrm{km})} \frac{1}{10 \log_{10} (P_i/P_o)}$$

where $\sigma_T(\mathrm{km})$ is the total rms pulse broadening per kilometer on the link (hint: refer to Eqs. (3.3) and (3.10)).

(a) A digital optical fiber system using an injection laser source displays rms pulse broadening of 1 ns km^{-1}. The fiber cable has an attenuation of 3.5 dB km^{-1} and joint losses average out to 1 dB km^{-1}. Estimate the transmission rate at the dispersion limit when the difference in optical power levels between the input and output is 40 dB.

(b) Calculate the dispersion limited transmission distance for the system described in (b) when the transmission rates are 1 Mbit s^{-1} and 1 Gbit s^{-1}. Hence sketch a graph showing the dispersion limit on transmission distance against the transmission rate for the system.

10.17 The digital optical fiber system described in problem 10.16(a) has a transmission rate of 50 Mbit s^{-1} and operates over a distance of 12 km without repeaters. Assuming Gaussian shaped pulses, calculate the dispersion–equalization penalty exhibited by the system for the cases when:

(a) there is no mode coupling; and

(b) there is mode coupling.

10.18 A digital optical fiber system uses an RZ pulse format. Show that the maximum bit rate for the system $B_T(\max)$ may be estimated using the expression:

$$B_T(\max) = \frac{0.35}{T_{syst}}$$

where T_{syst} is the total system rise time. Comment on the possible use of the factor 0.44 in place of 0.35 in the above relationship.

An optical fiber link is required to operate over a distance of 10 km without repeaters. The fiber available exhibits a rise time due to intermodal dispersion of 0.7 ns km^{-1}, and a rise time due to intramodal dispersion of 0.2 ns km^{-1}. In addition the APD detector has a rise time of 1 ns. Estimate the maximum rise time allowable for the source in order for the link to be successfully operated at a transmission rate of 40 Mbit s^{-1} using an RZ pulse format.

10.19 A digital single mode optical fiber system is designed for operation at a wavelength of 1.5 μm and a transmission rate of 560 Mbit s^{-1} over a distance of 50 km without repeaters. The single mode injection laser is capable of launching a mean optical power of −13 dBm into the fiber cable which exhibits a loss of 0.35 dB km^{-1}. In addition splice losses are 0.1 dB km^{-1}. The connector loss at the receiver is 0.5 dB and the receiver sensitivity is −39 dBm. Finally an extinction ratio penalty of 1 dB is predicted for the system. Perform an optical power budget for the system and determine the safety margin.

10.20 Briefly discuss the reasons for the use of block codes in digital optical fiber transmission. Indicate the advantages and drawbacks when a *5B6B* code is employed.

10.21 A D–IM analog optical fiber system utilizes a *p–i–n* photodiode receiver. Derive an expression for the rms signal power to rms noise power ratio in the quantum limit for this system.

The *p–i–n* photodiode in the above system has a responsivity of 0.5 at the operating wavelength of 0.85 μm. Furthermore the system has a modulation

index of 0.4 and transmits over a bandwidth of 5 MHz. Sketch a graph of the quantum limited receiver sensitivity against the received SNR (rms signal power to rms noise power) for the system over the range 30–60 dB. It may be assumed that the photodiode dark current is negligible.

10.22 In practice the analog optical fiber receiver of problem 10.21 is found to be thermal noise limited. The mean square thermal noise current for the receiver is 2×10^{-23} A^2 Hz^{-1}. Determine the peak to peak signal power to rms noise power ratio at the receiver when the average incident optical power is −17.5 dBm.

10.23 An analog optical fiber system has a modulation bandwidth of 40 MHz and a modulation index of 0.6. The system utilizes an APD receiver with a responsivity of 0.7 and is quantum noise limited. An SNR (rms signal power to rms noise power) of 35 dB is obtained when the incident optical power at the receiver is −30 dBm. Assuming the detector dark current may be neglected, determine the excess avalanche noise factor at the receiver.

10.24 A simple analog optical fiber link operates over a distance of 15 m. The transmitter comprises an LED source which emits an average of 1 mW of optical power into air when the drive current is 40 mA. Plastic fiber cable with an attenuation of 500 dB km^{-1} at the transmission wavelength is utilized. The minimum optical power level required at the receiver for satisfactory operation of the system is 5 μW. The coupling losses at the transmitter and receiver are 8 and 2 dB respectively. In addition a safety margin of 4 dB is necessary. Calculate the minimum LED drive current required to maintain satisfactory system operation.

10.25 An analog optical fiber system employs an LED which emits 3 dBm mean optical power into air. However, a coupling loss of 17.5 dB is encountered when launching into a fiber cable. The fiber cable which extends for 6 km without repeaters exhibits a loss of 5 dB km^{-1}. It is spliced every 1.5 km with an average loss of 1.1 dB per splice. In addition there is a connector loss at the receiver of 0.8 dB. The PIN–FET receiver has a sensitivity of −54 dBm at the operating bandwidth of the system. Assuming there is no dispersion–equalization penalty, perform an optical power budget for the system and establish a safety margin.

10.26 Indicate the techniques which may be used for analog optical fiber transmission where an electrical subcarrier is employed. Illustrate your answer with a system block diagram showing the multiplexing of several signals onto a single analog optical fiber link.

10.27 A narrowband FM–IM optical signal has a maximum frequency deviation of 120 kHz when the frequency deviation ratio is 0.2. Compare the post detection SNR of this signal with that of a DSB–IM optical signal having the same modulating signal power, bandwidth, detector photocurrent and noise. Also estimate the bandwidth of the FM–IM signal. Comment on both results.

10.28 A frequency division multiplexed optical fiber system uses FM–IM. It has 50 equal amplitude voice channels each bandlimited to 3.5 kHz. A 1 kHz guard band is provided between the channels and below the first channel. The peak frequency deviation for the system is 1.35 MHz. Determine the transmission bandwidth for this FDM system.

10.29 An FM–IM system utilizes pre-emphasis and de-emphasis to enhance its performance in noise [Ref. 65]. The de-emphasis filter is a first order RC low pass filter placed at the demodulator to reduce the total noise power. This filter may be assumed to have an amplitude response $H_{de}(\omega)$ given by:

$$|H_{de}(\omega)| = \frac{1}{1 + (\omega/\omega_c)^2}$$

where $\omega_c = 2\pi f_c = 1/RC$.

The SNR improvement over FM–IM without pre-emphasis and de-emphasis is given by:

$$\text{SNR}_{de} \text{ improvement} = \frac{1}{3}\left(\frac{B_a}{f_c}\right)^2$$

where B_a is the bandwidth of the baseband signal and $f_c \ll B_a$.

(a) Write down an expression for the amplitude response of the pre-emphasis filter so that there is no overall signal distortion.

(b) Deduce an expression for the post detection SNR improvement in decibels for the FM–IM system with pre-emphasis and de-emphasis over a D–IM system operating under the same conditions of modulating signal power and bandwidth, photocurrent and noise. It may be assumed that $f_c \ll B_a$.

(c) A baseband signal with a bandwidth of 300 kHz is transmitted using the FM–IM system with pre-emphasis and de-emphasis. The maximum frequency deviation for the system is 4 MHz. In addition the de-emphasis filter comprises a 500 Ω resistor and a 0.1 μF capacitor. Determine the post detection SNR improvement for this system over a D–IM system operating under the same conditions of modulating signal power and bandwidth, photocurrent and noise.

10.30 A PM–IM optical fiber system operating above threshold has a frequency deviation ratio of 15 and a transmission bandwidth of 640 kHz.

(a) Estimate the bandwidth of the baseband message signal.

(b) Compute the post detection SNR improvement for the system over a D–IM system operating with the same modulating signal power and bandwidth, detector photocurrent and noise.

10.31 Discuss the advantages and drawbacks of the various pulse analog techniques for optical fiber transmission. Describe the operation of a PFM–IM optical fiber system employing regenerative baseband recovery.

10.32 An optical fiber PFM–IM system uses regenerative baseband recovery. The optical receiver which incorporates a *p–i–n* photodiode has an optimized bandwidth of 125 MHz. The other system parameters are:

Nominal pulse rate	35 MHz
Peak to peak frequency deviation	8 MHz
p–i–n photodiode responsivity	0.6 A W^{-1}
Baseband noise bandwidth	10 MHz
Receiver mean square noise current	3×10^{-25} A^2 Hz^{-1}

(a) Calculate the peak level of incident optical power necessary at the receiver to maintain a peak to peak signal power to rms noise power ratio of 60 dB.
(b) The source and detector have rise times of 3.5 and 5.0 ns respectively. Estimate the maximum permissible total rise time for the fiber cable utilized in the system such that satisfactory operation is maintained. Comment on the value obtained.

10.33 Discuss, with the aid of a suitable system block diagram, coherent optical fiber transmission. Indicate the system component requirements necessary to achieve successful coherent operation.

Answers to Numerical Problems

10.4 53.0 pF, 472 Ω
10.5 64 kbit s^{-1}
10.6 (a) 37 ns; (b) 125 μV
10.8 (a) 300 bits; (b) 1.2 MHz
10.9 (a) 10.2 dB; (b) 3.4×10^{-7}
10.10 $P(e) = \text{Erfc}\,((S/N)^{\frac{1}{2}}/2)$, 19.6 dB
10.11 7.4
10.12 (a) 1400; (b) −52.8 dBm; (c) −51.8 dBm
10.13 27.9 dB
10.14 15.76 km, 8.26 km
10.15 3.41 km
10.16 (a) 22.5 Mbit s^{-1}; (b) 200 km, 0.2 km
10.17 (a) 16.6 dB; (b) 0.1 dB
10.18 3.04 ns
10.19 2.1 dB
10.21 40 nW, 40 μW
10.22 49.0 dB
10.23 3.1
10.24 35.5 mA
10.25 5.4 dB
10.27 Ratio of output SNRs (rms signal power to rms noise power) for FM–IM to DSB–IM is −9.21 dB, 1200 kHz
10.28 3.15 MHz
10.29 (a) $1 + (\omega/\omega_c)^2$; (b) $-3 + 20 \log_{10} (D_f B_a/f_c)$; (c) 59.0 dB
10.30 (a) 20 kHz; (b) 20.5 dB
10.32 (a) −24.4 dBm; (b) 4.6 ns

REFERENCES

1 C. C. Timmermann, 'Highly efficient light coupling from GaAlAs lasers into optical fibers', *Appl. Opt.*, **15**(10), pp. 2432–2433, 1976.
2 M. Maeda, I. Ikushima, K. Nagano, M. Tanaka, H. Naskshima, R. Itoh, 'Hybrid laser to fiber coupler with a cylindrical lens', *Appl. Opt.*, **16**(7), pp. 1966–1970, 1977.
3 R. W. Dawson, 'Frequency and bias dependence of video distortion in Burrus-type homostructure and heterostructure LED's', *IEEE Trans. Electron. Devices*, **ED-25**(5), pp. 550–553, 1978.
4 J. Strauss, 'The nonlinearity of high-radiance light-emitting diodes', *IEEE J. Quantum Electron.*, **QE-14**(11), pp. 813–819, 1978.
5 K. Asatani and T. Kimura, 'Non-linear phase distortion and its compensation in LED direct modulation', *Electron. Lett.*, **13**(6), pp. 162–163, 1977.
6 G. White and C. A. Burrus, 'Efficient 100 Mb/s driver for electroluminescent diodes', *Int. J. Electron.*, **35**(6), pp. 751–754, 1973.
7 P. W. Shumate Jr and M. DiDomenico Jr, 'Lightwave transmitter', in H. Kressel (Ed.), *Semiconductor Devices for Optical Communications, Topics in Applied Physics,* Volume 39, pp. 161–200, Springer-Verlag, 1982.

8 L. Foltzer, 'Low-cost transmitters, receivers serve well in fibre-optic links', *EDN*, pp. 141–146, 20 October 1980.

9 A. Albanese and H. F. Lenzing, 'Video transmission tests, performed on intermediate-frequency light wave entrance links', *J. SMPTE (USA)*, **87**(12), pp. 821–824, 1978.

10 J. Strauss, 'Linearized transmitters for analog fiber links', *Laser Focus (USA)*, **14**(10), pp. 54–61, 1978.

11 A. Prochazka, P. Lancaster, R. Neumann, 'Amplifier linearization by complementary pre or post distortion', *IEEE Trans. Cable Telev.*, **CATV-1**(1), pp. 31–39, 1976.

12 K. Asatani and T. Kimura, 'Nonlinear distortions and their compensations in light emitting diodes', *Proceedings of International Conference on Integrated Optics and Optical Fiber Communications*, p. 105, 1977.

13 K. Asatani and T. Kimura, 'Linearization of LED nonlinearity by predistortions', *IEEE J. Solid State Circuits*, **SC-13**(1), pp. 133–138, 1978.

14 J. Strauss, A. J. Springthorpe and O. I. Szentesi, 'Phase shift modulation technique for the linearisation of analogue optical transmitters', *Electron. Lett.*, **13**(5), pp. 149–151, 1977.

15 J. Strauss and D. Frank, 'Linearisation of a cascaded system of analogue optical links', *Electron. Lett.*, **14**(14), 436–437, 1978.

16 H. S. Black, US Patent 1686792, issued Oct 9, 1929.

17 B. S. Kawasaki ands K. O. Hill, 'Low-loss access coupler for multimode optical fiber distribution network', *Appl. Opt.*, **16**(7) p. 1794, 1977.

18 J. Strauss and O. I. Szentesi, 'Linearisation of optical transmitters by a quasifeedforward compensation technique', *Electron. Lett.*, **13**(6), pp. 158–159, 1977.

19 S. M. Abbott, W. M. Muska, T. P. Lee, A. G. Dentai ands C. A. Burrus, '1.1 Gb/s pseudorandsom pulse-code modulation of 1.27 μm wavelength CW InGaAsP/InP DH lasers', *Electron. Lett.*, **14**(11), pp. 349–350, 1978.

20 J. Gruber, P. Marten, R. Petschacher and P. Russer, 'Electronic circuits for high bit rate digital fiber optic communication systems', *IEEE Trans. Commun.*, **COM-26**(7), pp. 1088–1098, 1978.

21 P. K. Runge, 'An experimental 50 Mb/s fiber optic PCM repeater', *IEEE Trans. Commun.*, **COM-24**(4), pp. 413–418, 1976.

22 U. Wellens, 'High-bit-rate pulse regeneration and injection laser modulation using a diode circuit', *Electron. Lett.*, **13**(18), pp. 529–530, 1977.

23 A. Chappell (Ed.), *Optoelectronics: Theory and Practice*, McGraw-Hill, 1978.

24 S. R. Salter, D. R. Smith, B. R. White and R. P. Webb, 'Laser automatic level control for optical communications systems', Third European Conf. on Optical Communications, Munich, September 1977, VDE-Verlag GmbH, Berlin, 1977.

25 A. Fausone, 'Circuit considerations', *Optical Fibre Communication*, by Tech. Staff of CSELT, pp. 777–800, McGraw-Hill, 1981.

26 A. Moncalvo and R. Pietroiusti, 'Transmission systems using optical fibres', *Telecommunication J. (Switzerland)*, **49**, pp. 84–92, 1982.

27 S. D. Personick, 'Design of receivers and transmitters for fiber systems', in M. K. Barnoski (Ed.), *Fundamentals of Optical Fiber Communications* (2nd Ed.), pp. 295–328. Academic Press, 1981.

28 T. L. Maione and D. D. Sell, 'Experimental fiber-optic transmission system for interoffice trunks', *IEEE Trans. Commun.*, **COM-25**(5), pp. 517–522, 1977.

29 R. G. Smith and S. D. Personick, 'Receiver design for optical fibre communication systems', in H. Kressel (Ed.), *Semiconductor Devices for Optical Communications*, Topics in Advanced Physics, Vol. 39, pp. 88–160, Springer-Verlag, 1982.

30 R. G. Smith, C. A. Brackett and H. W. Reinbold, 'Atlanta fiber system experiment, optical detector package', *Bell Syst. Tech. J.*, **57**(6), pp. 1809–1822, 1978.
31 J. L. Hullett and T. V. Muoi, 'A feedback amplifier for optical transmission systems', *IEEE Trans. Commun.*, **COM-24**, pp. 1180–1185, 1976.
32 J. L. Hullett, 'Optical communication receivers', *Proc. IREE Australia*, pp. 127–134, September 1979.
33 N. J. Bradley, 'Fibre optic systems design', *Electronic Eng.*, pp. 98–101, mid April 1980.
34 T. L. Maione, D. D. Sell and D. H. Wolaver, 'Practical 45 Mb/s regenerator for lightwave transmission', *Bell Syst. Tech. J.*, **57**(6), pp. 1837–1856, 1978.
35 S. D. Personick, 'Receiver design for optical systems', *Proc. IEEE*, **65**(12), pp. 1670–1678, 1977.
36 J. E. Goell, 'Input amplifiers for optical PCM receivers', *Bell Syst. Tech. J.*, **53**(9), pp. 1771–1793, 1974.
37 S. D. Personick, 'Time dispersion in dielectric waveguides', *Bell Syst. Tech. J.*, **50**(3), pp. 843–859, 1971.
38 I. Garrett, 'Receivers for optical fibre communications', *Radio Electron. Eng. J. IERE*, **51**(7/8), pp. 349–361, 1981.
39 S. D. Personick, 'Receiver design', in S. E. Miller and A. G. Chynoweth (Eds.), *Optical Fiber Telecommunications*, pp. 627–651, Academic Press Inc., 1979.
40 A. Moncalvo and L. Sacchi, 'System considerations', *Optical Fibre Communication*, by Tech. Staff of CSELT, pp. 723–776, McGraw-Hill, 1981.
41 M. Rocks and R. Kerstein, 'Increase in fiber bandwidth for digital systems by means of multiplexing', ICC 80 1980 International Conf. on Commun., Seattle, WA, USA, Part 28 5/1–5, June 1980.
42 W. Koester and F. Mohr, 'Bidirectional optical link', *Electrical Commun.*, **55**(4), pp. 342–349, 1980.
43 H. Taub and D. L. Schilling, *Principles of Communication System*, McGraw-Hill, 1971.
44 P. Hensel and R. C. Hooper, 'The development of high performance optical fibre data links', *IERE Conference Proceedings Fibre Optics*, 1–2 March 1982 (London), pp. 91–98, 1982.
45 D. C. Gloge and T. Li, 'Multimode-fiber technology for digital transmission', *Proc. IEEE*, **68**(10), pp. 1269–1275, 1980.
46 G. E. Stillman, 'Design considerations for fibre optic detectors', *Proc. Soc. Photo-opt. Instrum. Eng.*, **239**, pp. 42–52, 1980.
47 P. P. Webb, R. J. McIntyre and J. Conradi, 'Properties of avalanche photodiodes', *RCA Rev.*, **35**, pp. 234–278, 1974.
48 J. E. Midwinter, *Optical Fibers for Transmission*, John Wiley, 1979.
49 I. Garrett and J. E. Midwinter, 'Optical communication systems', in M. J. Howes and D. V. Morgan (Eds.), *Optical Fibre Communications: Devices, Circuits, and Systems*, pp. 251–300, John Wiley, 1980.
50 R. J. McIntyre and J. Conradi, 'The distribution of gains in uniformly multiplying avalanche photodiodes', *IEEE Trans. Electron. Devices*, **ED-19**, pp. 713–718, 1972.
51 K. Mouthaan, 'Telecommunications via glass–fibre cables', *Philips Telecommun. Rev.*, **37**(4), pp. 201–214, 1979.
52 H. F. Wolf, 'System aspects', in H. F. Wolf (Ed.), *Handbook of Fiber Optics: Theory and Applications*, pp. 377–427, Granada, 1979.
53 S. D. Personick, N. L. Rhodes, D. C. Hanson and K. H. Chan, 'Contrasting fiber-optic-component-design requirements in telecommunications, analog, and local data communications applications', *Proc. IEEE*, **68**(10), pp. 1254–1262, 1980.

54 S. E. Miller, 'Transmission system design', in S. E. Miller and A. G. Chynoweth (Eds.), *Optical Fiber Telecommunications*, pp. 653–683, Academic Press, 1979.
55 C. K. Koa, *Optical Fiber Systems: Technology, Design and Applications*, McGraw-Hill, 1982.
56 C. Kleekamp and B. Metcalf, *Designer's Guide to Fiber Optics*, Cahners Publishing Company, 1978.
57 G. R. Elion and H. A. Elion, *Fiber Optics in Communications Systems*, Marcel Dekker, 1978.
58 S. Shimada, 'Systems engineering for long-haul optical-fiber transmission', *Proc. IEEE*, **68**(10), pp. 1304–1309, 1980.
59 J. H. C. Van Heuven, 'Techniques for optical transmission', in *Proceedings of 11th European Microwave Conference*, Amsterdam, Netherlands, pp. 3–10, 1981.
60 R. Tell and S. T. Eng, 'Optical fiber communication at 5 Gbit/sec', *Appl. Opt.*, **20**(22), pp. 3853–3858, 1981.
61 P. Wells, 'Optical-fibre systems for telecommunications', *GEC J. Sci. Tech.*, **46**(2), pp. 51–60, 1980.
62 M. Chown and K. C. Koa, 'Some broadband fiber system design considerations', in *Proceedings of IEEE International Conference on Communications*, Philadelphia PA, 1972, pp. 12/1–5, IEEE, 1972.
63 I. Garrett and C. J. Todd, 'Optical fiber transmission systems at 1.3 and 1.5 μm wavelength', in *Proceedings of IEEE 1981 International Conference on Communications*, New York, Vol. 1, Pt. 16.2/1–5, IEEE, 1981.
64 J. L. Hullett and T. V. Muoi, 'Optical fiber systems analysis', *Proc. IREE Australia*, **38**(1–2), pp. 390–397, 1977.
65 A. Luvison, 'Topics in optical fibre communication theory', *Optical Fibre Communications*, by Technical Staff of CSELT, pp. 647–721, McGraw-Hill, 1981.
66 M. Chown, A. W. Davis, R. E. Epworth and J. G. Farrington, 'System design', in C. P. Sandbank (Ed.), *Optical Fibre Communication Systems*, pp. 206–283, John Wiley, 1980.
67 K. Sam Shanmugan, *Digital and Analog Communication Systems*, John Wiley, 1979.
68 G. G. Windus, 'Fibre optic systems for analogue transmission', *Marconi Rev.*, **XLIV**(221), pp. 78–100, 1981.
69 W. Horak, 'Analog TV signal transmission over multimode optical waveguides', *Siemens Research and Development Reports*, **5**(4), pp. 192–202, 1976.
70 K. Sato and K. Asatani, 'Analogue baseband TV transmission experiments using semiconductor laser diodes', *Electron. Lett.*, **15**(24), pp. 794–795, 1979.
71 R. M. Gagliadi and S. Karp, *Optical Communications*, John Wiley, 1976.
72 C. C. Timmerman, 'Signal to noise ratio of a video signal transmitted by a fiber-optic system using pulse-frequency modulation', *IEEE Trans. Broadcasting*, **BC-23**(1), pp. 12–16, 1976.
73 C. C. Timmerman, 'A fiber optical system using pulse frequency modulation', *NTZ*, **30**(6), pp. 507–508, 1977.
74 D. J. Brace and D. J. Heatley, 'The application of pulse modulation schemes for wideband distribution to customers (integrated optical fibre systems)', in *Sixth European Conference on Optical Communication*, York, UK, 16–19 Sept. 1980, pp. 446–449, 1980.
75 E. Yoneda, T. Kanada and K. Hakoda, 'Design and performance of optical fibre transmission systems for color television signals', *Rev. Elect. Commun. Lab.*, **29**(11–12), pp. 1107–1117, 1981.

76 T. Kanada, K. Hakoda and E. Yoneda, 'SNR fluctuation and nonlinear distortion in PFM optical NTSC video transmission systems', *IEEE Trans. Commun.*, **COM-30**(8), pp. 1868–1875, 1982.

77 M. C. Teich, 'Homodyne detection of infrared radiation from a moving diffuse target', *Proc. IEEE*, **57**(5), pp. 789–792, 1969.

78 W. K. Pratt, *Laser Communication Systems*, John Wiley, 1969.

79 Y. Yamamoto, 'Receiver performance evaluation of various digital optical modulation–demodulation systems in the 0.5–10 μm wavelength region', *IEEE J. Quantum Electron.*, **QE-16**(11), pp. 1251–1259, 1980.

80 F. Favre, L. Jeunhomme, I. Joindot, M. Monerie and J. C. Simon, 'Progress towards heterodyne-type single-mode fibre communication systems', *IEEE J. Quantum Electron.*, **QE-17**(6), pp. 897–905, 1981.

81 T. Okoshi and K. Kikuchi, 'Frequency stabilisation of semiconductor lasers for heterodyne type optical communication systems', *Electron. Lett.*, **16**(5), pp. 179–181, 1980.

82 F. Favre and D. Le Guen, 'High frequency stability of laser diode for heterodyne communication systems', *Electron. Lett.*, **16**, pp. 709–710, 1980.

83 R. Lang, 'Injection locking properties of a semiconductor laser', *IEEE J. Quantum Electron.*, **QE-18**(6), pp. 976–983, 1982.

84 S. Saito, Y. Yamamoto and T. Kimura, 'Optical FSK heterodyne detection experiments using semiconductor laser transmitter and local oscillator', *IEEE J. Quantum Electron.*, **QE-17**(6), pp. 935–941, 1981.

85 Y. Yamamoto and T. Kimura, Coherent optical fiber transmission systems', *IEEE J. Quantum Electron.*, **QE-17**(6), pp. 919–934, 1982.

86 B. E. A. Saleh and M. I. Irshid, 'Coherence and intersymbol interference in digital fiber optic communication systems', *IEEE J. Quantum Electron.*, **QE-18**(6), pp. 944–951, 1982.

87 T. Kimura and Y. Yamamoto, 'Progress of coherent optical fibre communication systems', *Opt. Quantum Electron.*, **15**, pp. 1–39, 1983.